Differentiation of encapsulated human pluripotent stem cells into insulin-producing cells.

Luke M. Carroll

A thesis submitted in fulfilment of the requirements for the degree of

Doctor of Philosophy

Faculty of Medicine and Health

The University of Sydney

June 2019

Contents

Abstract

Human islet transplantation can provide glycaemic control in diabetic recipients without the need for exogenous insulin. However, there are two major factors limiting its application. Firstly, there is the recipient's need to adhere to life-long immunosuppression, something that carries serious side effects. Secondly, the limited availability of donor tissue restricts the option to individuals most in need. Differentiating human pluripotent stem cells offers a potentially limitless supply of transplantable material. This tissue would still be rejected by the host's immune system without the use of immunosuppression. Isolating the tissue from the host's immune system is a technique which has been trialled to overcome the need for immunosuppression. The varying methods many researchers are approaching this challenge are outlined in Chapter 1 and include alginate microspheres, alginate-nylon threads and silicone membranes. The disadvantages and strategies to overcome these barriers are discussed.

Limited islet availability can be overcome by differentiating human pluripotent stem cells into insulin-producing cells. Chapter 3 details the differentiation of human embryonic stem cells differentiated while encapsulated in alginate microspheres. The gene profiles of the cells differentiated while encapsulated were not statistically different from the cells differentiated on a 2D matrix. These cells were differentiated for 9 days, at which point they expressed the key pancreatic marker PDX1.

In chapter 4 the encapsulated cells which had been put through the 9 day differentiation protocol were then transplanted into STZ (Streptozotocin) treated NOD SCID mice. The weight, BGL (Blood Glucose Level) and serum c-peptide level were checked regularly for 3 months. At the three month time point, there were detectable levels of human C-peptide in the serum of the mouse. However, there was no correction of hyperglycaemia.

Finally, induced pluripotent stem cells from a person with Type 1 diabetes were encapsulated and differentiated. These cells showed the same gene profiles as the encapsulated human embryonic stem cells differentiated over 9 days.

Acknowledgements

I would like to thank the following people for their support and encouragement throughout the course of my PhD;

My primary supervisor Professor Bernard Tuch for enabling me to undertake this project and supporting me through the Australian Foundation for Diabetes Research with the Alginate Encapsulated Stem Cell Scholarship. I am grateful for his enthusiasm, mentorship and the opportunities he has given me. His drive for me to produce the best work possible has been what has enabled this project to be completed.

My co-supervisor Assoc. Prof. Anandwardhan A. Hardikar for his support, advice, equipment and molecular biological expertise during this project. The critical developmental stage molecular analysis would not have been possible without him.

My co-supervisor Dr Michael Morris for his guidance, support, laboratory space and cell culture expertise. Without his calm guidance and tolerance, this journey would not have been possible.

Dr Auvro Mridha for his help in the laboratory and expertise in animal work. As my first port of call for assistance, he bore the brunt of my everyday requests for assistance. His excellent advice for everything career and scientific related greatly helped throughout my PhD. I would like to especially thank him for the help preparing this thesis which would not have been possible without him.

The CSIRO, Penny Bean and Dr Meg Evans, for getting my project going on the right foot and help during the critical first year, as well as for providing funding for the consumables used during the first 3 years of experiments.

Prof. Paul Verma and Dr Jun Liu for providing the iPSC which enabled the final chapter of this project to be possible.

The University of Sydney and the Bosch Institute, in particular, the Bosch Young Investigators group for the social and career development opportunities.

Publications, Abstracts and awards arising from this thesis

Publications

1. Carroll, L. M., Michael B. Morris, Anandwardhan Hardikar, Bernard E. Tuch. 2019. "Encapsulation and Transplantation of Pancreatic Progenitor Cells." M. V. Joglekar. (Ed.), *Progenitor Cells: Methods and Protocols*. New York City, New York. (Accepted, December 2018) – *This publication was adapted from my methods section, I wrote the drafts and co-authors edited.*
2. Carroll, L. M., Auvro R. Mridha, Michael B. Morris, Anandwardhan Hardikar, Bernard E. Tuch. "Devices for the management of type 1 diabetes: Current and future." (In preparation) – *This manuscript was adapted from my introduction section p25-28, I wrote the drafts and co-authors edited.*
3. Carroll, L. M., Auvro R. Mridha, Michael B. Morris, Anandwardhan Hardikar, Bernard E. Tuch. "Differentiation of alginate encapsulated human embryonic stem cells to primitive foregut and in vivo conversion to insulin producing cells" (In preparation) – *This manuscript was adapted from my results sections, all experiments and analysis was conducted by me unless otherwise stated, co-authors reviewed drafts.*

Authorship attribution statement

In addition to the statements above, in cases where I am not the corresponding author of a published item, permission to include the published material has been granted by the corresponding author.

Luke Carroll 12/6/2019

As supervisor for the candidature upon which this thesis is based, I can confirm that the authorship attribution statements above are correct.

Bernard Tuch 12/6/2019

Poster Presentations

1. Luke Carroll, Michael B. Morris, Anandwardhan Hardikar, Bernard E. Tuch. Differentiation of Human Embryonic Stem Cells into Insulin-producing Precursors while Encapsulated in Immune-Protective Alginate. 8th Islet Society Meeting, June 2015.
2. Luke Carroll, Michael B. Morris, Anandwardhan Hardikar, Bernard E. Tuch. Differentiation of Human Differentiation of Human Embryonic Stem Cells into Insulin-producing Precursors while Encapsulated in Immune-Protective Alginate. Australasian Society for Stem Cell Research, November 2015.
3. Luke Carroll, Auvro R. Mridha, Michael B. Morris, Anandwardhan Hardikar, and Bernard E. Tuch. Encapsulated human embryonic stem cells partially differentiated *in vitro*, express insulin mRNA and C-peptide when transplanted into diabetic mice. 4th Annual German Stem Cell Network conference, Hannover, September 2016.
4. Luke Carroll, Auvro R. Mridha, Michael B. Morris, Anandwardhan Hardikar, and Bernard E. Tuch. Encapsulated pluripotent stem cells differentiated *in vitro*, express insulin mRNA and C-peptide e*x vivo* after 3 month transplantation in diabetic mice. Australasian Society for Stem Cell Research, December 2016.
5. Luke Carroll, Jun Liu, Auvro R. Mridha, Michael B. Morris, Anandwardhan Hardikar, Bernard E. Tuch. Induced pluripotent stem cells when encapsulated in alginate can be differentiated into pancreatic progenitors: implications in personalised cell based therapy for type 1 diabetes. Bosch Institute Annual Scientific Meeting, July 2017.
6. Luke Carroll, Auvro R. Mridha, Michael B. Morris, Anandwardhan A. Hardikar, Bernard E. Tuch. Encapsulated human embryonic stem cells differentiate while encapsulated, express insulin mRNA, and C-peptide when transplanted into diabetic mice. 27th NSW Stem Cell Network Workshop: Stem Cells and Diabetes Therapies, 2018.

7. Luke Carroll, Auvro R. Mridha, Michael B. Morris, Anandwardhan A. Hardikar, Bernard E. Tuch. Encapsulated human embryonic stem cells differentiate while encapsulated, express insulin mRNA, and C-peptide when transplanted into diabetic mice. International Society for Stem Cell Research Annual Conference, Melbourne, 2018.

Awards

1. Australian Foundation for Diabetes Research Scholarship for 3 years
2. Juvenile Diabetes Research Fund Top Up Scholarship for 3 years
3. Australasian Society for Stem Cell Research travel grant (2016, 2017)
4. Postgraduate Research Support Scheme (PRSS) award administered by The University of Sydney to attend the Australasian Society for Stem Cell Research conference 2016, German Stem Cell Network conference 2017 and International Society for Stem Cell Research conference 2017
5. Runner up Poster award at the 27th NSW Stem Cell Network Workshop: Stem Cells and Diabetes Therapies

List of figures

List of tables

List of abbreviations

6-CFDA	6-carboxyfluorescein diacetate
bFGF	Basic fibroblast growth factor
BGL	Blood glucose levels
BSA	Bovine serum albumin
CHIR	CHIR 99021
CMRL	CMRL-1066 media
CYC	KAAD-cyclopamine
DMEM	Dulbecco's modified Eagle medium
EDTA	Ethylenediaminetetraacetic acid
ELISA	Enzyme-linked immunosorbent assay
ESC	Embryonic stem cells
FBS	Foetal bovine serum
GSIS	Glucose stimulated insulin secretion
H&E	Haematoxylin and Eosin
hESC	Human embryonic stem cells
iPSC	Induced pluripotent stem cells
ITS	Insulin transferrin selenium
KGF	Keratinocyte growth factor
KOSR	KnockOut Serum Replacement
LDN	LDN193189
MPS	Multipotent Stem Cells
NEAA	Non–essential amino acids solution
NOD/SCID	Non-obese diabetic/severe combined immunodeficiency
OCT	Optimal cutting temperature compound
PBS	Phosphate–buffered saline
PBST	Phosphate Buffered Saline with Tween
PdbU	Phorbol 12,13-dibutyrate
PFA	Paraformaldehyde
PI	Propidium iodide
POCD	Point of Care Diagnostics
RA	Retinoic acid
ROCK	Rho-associated, coiled-coil containing protein kinase
RPMI	Roswell Park Memorial Institute
SANT-1	Smoothened and hedgehog signalling antagonist
SCID	Severe combined immune deficiency
SPF	Specific-pathogen-free
STZ	Streptozotocin
T1D	Type 1 diabetes
T3	Triiodothyronine
TBS	Tris-Buffered Saline

TBST	Tris-Buffered Saline with Tween
XXI	XXI γ-secretase inhibitor

Chapter 1

Introduction

1. Introduction to Stem cells

Stem cell therapy remains at the cutting edge of medical science; however, it is yet to be widely adopted into the clinic. This lack of translation from experimentation to application is due to the complex nature of perfecting stem cell treatments regardless of their apparent potential. This potential is based on two key properties of Pluripotent stem cells, their ability for long-term self-renewal without senescence and pluripotency, the ability to differentiate into specialized cell types (1). It is these properties which show the potential for a dynamic shift in the way some disorders might be treated.

1.1 Types of stem cells

Mammalian stem cells can be classified into two broad types based on their origin. These are well known as embryonic stem (ES) cells and adult stem cells. ES cells are localized to the inner cell mass of blastocysts whilst adult stem cells are found localized to various tissues. Based on the potential of these stem cells, they are classified into multiple types that are described below.

1.1.1 Multipotent stem cells

Adult stem cells are often described as multipotent. These cells undergo long term self-renewal but their capacity to differentiate into diverse types of specialized cells is limited(2). An example of multipotent stem cells (MPS) is the mesenchymal stem cell, which can be differentiated into cartilage, bone, fat and other mesodermal cell types, but generally not into endo or ectodermal cells. An advantage of autologous MPS is that they can be sourced from a person to use as a treatment in that person, thereby negating the requirement for immune inhibition. Unlike pluripotent stem cells, MPS do not have the potential to develop into teratomas when transplanted.

MPS can be found in many adult tissues including the amniotic fluid of pregnant women and in the cord blood. While these are not pure MPS populations the collection and storage of cord blood at birth is a growing practice in Australia, both in the private and public sectors. MPS express specific surface antigens, which enables both their identification and isolation. For example cord blood MPS express CD34 and

CD133, and therefore can be isolated using monoclonal antibodies bound to paramagnetic microbeads(3). These isolated cells then can be used as treatments for a wide range of blood disorders, as well as possible novel treatments for other chronic diseases including cerebral palsy and Type 1 Diabetes (T1D)(4). Cord blood cells have an advantage over adult blood stem cells as they have a reduced immune reaction, thereby requiring less stringent tissue matching between donor and recipient with up to 50% mismatch at the major HLA loci being tolerated(5).

Amniotic fluid cells have also been shown to be CD34+ by De Coppi (6). As with cord blood, cells in amniotic fluid are a mixture of cells, only some of which are stem cells. Similar to cord blood, amniotic stem cells have begun to be used in clinical trials (7, 8), the commercialization and storage of amniotic fluid cells are likely to mirror that of cord blood cells.

1.1.2 Totipotent stem cells

Totipotent cells which can later develop into any of the three germ layers of a human (endoderm, mesoderm, or ectoderm), as well as the different layers of the placenta, are found in the initial stages of zygote formation (9). After reaching a 16-cell stage (the morula), the totipotent cells differentiate into cells that will eventually become either the blastocyst's Inner cell mass or the outer trophoblasts. After this specialization, the cells located in the inner cell mass (the source of embryonic stem cells) are classed as pluripotent.

1.1.3 Pluripotent stem cells

Pluripotent stem cells have the potential to turn into cell types of all three germ layers, ecto-, endo- and mesoderm. There are different intracellular signals which induce differentiation along the cell pathways, and attempts are being made to simulate these *in vitro*.

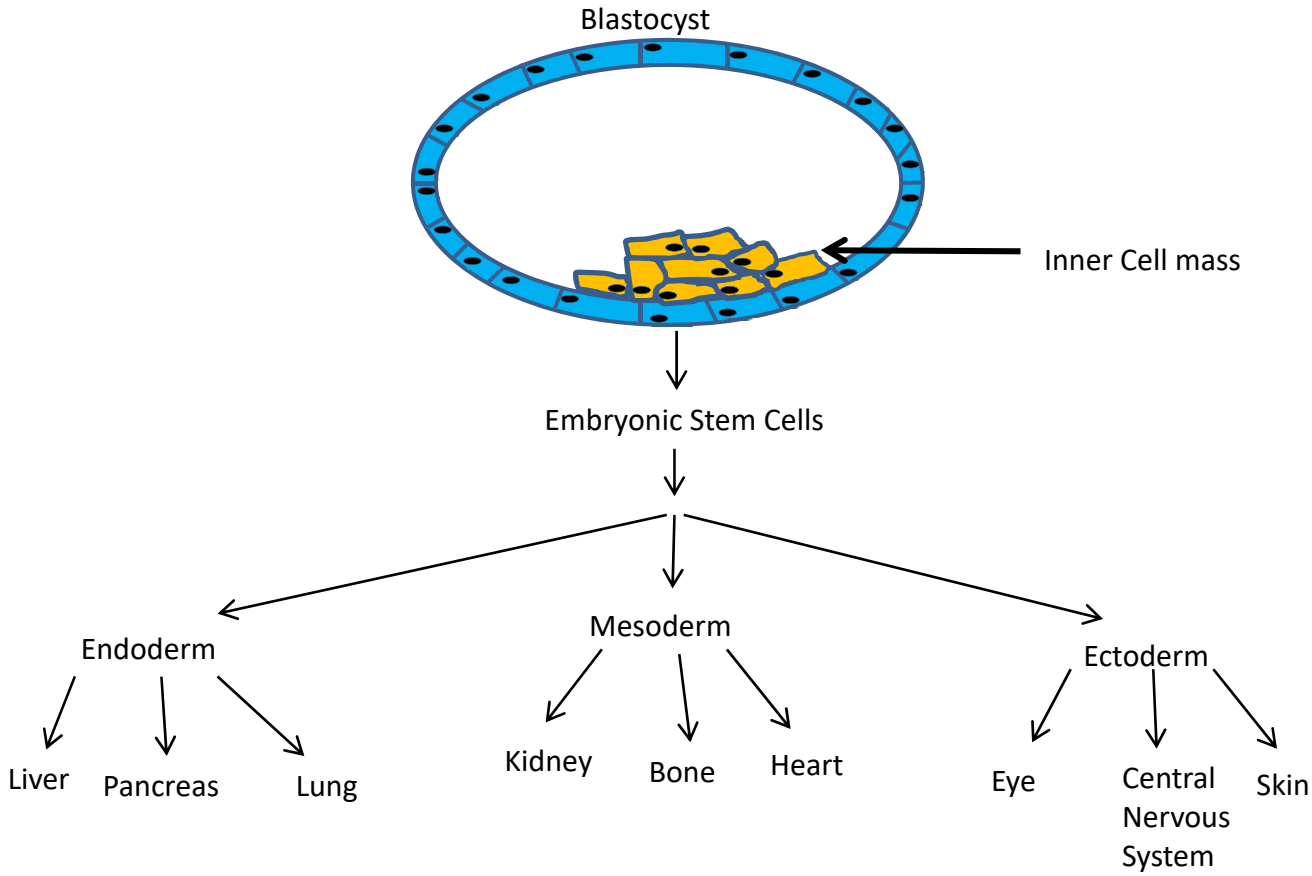

Figure 1.1: Possible developmental pathways of embryonic stem cells

1.1.3.1 Sources of pluripotent stem cells are:

1. Embryos.

Embryonic stem cells (ESC) are derived from the inner cell mass of a developing embryo called the blastocyst, which contains ~128 cells. It takes five days post fertilization to reach this stage of development (10). ESC were first isolated from mice in 1981(5), but it took a further 17 years before human embryonic stem cells (hESC) were isolated and maintained in culture(11). These hESC lines were derived from excess embryos generated by *in vitro* fertilization as part of Assisted Reproductive Technology, with the informed

consent of the donors(4). Whilst fertilized eggs are the usual source for the development of embryos, from which ESC are derived, it is possible for embryos to be created in two other ways, parthenogenesis and somatic cell nuclear transfer (SCNT). Parthenogenesis is the process whereby a mature egg is induced to become an embryo in the absence of sperm. The pores on the surface of the egg are open, for example, by a brief electrical impulse or with a calcium ionophore, and this causes changes in the cytoplasm of the egg that result in the formation of a diploid embryo. hESC lines have been produced from the inner cell mass of these(12).

The generation of hESC through SCNT involves fusing the nucleus of a somatic cell with a mature egg from which the nucleus has been removed. In this situation, the somatic cell nucleus is reprogrammed by the stored mRNAs in the cytoplasm of the egg. An embryo is subsequently formed and from these ESC lines are derived. The technique was first described with mouse eggs in 2000(13) but was only in 2013 that hESC lines were first derived in this manner(14). The production of hESC lines bearing the DNA of the somatic cell donor is called therapeutic cloning. Carrying out this technique is permissible in Australia and at least 10 other countries(15).

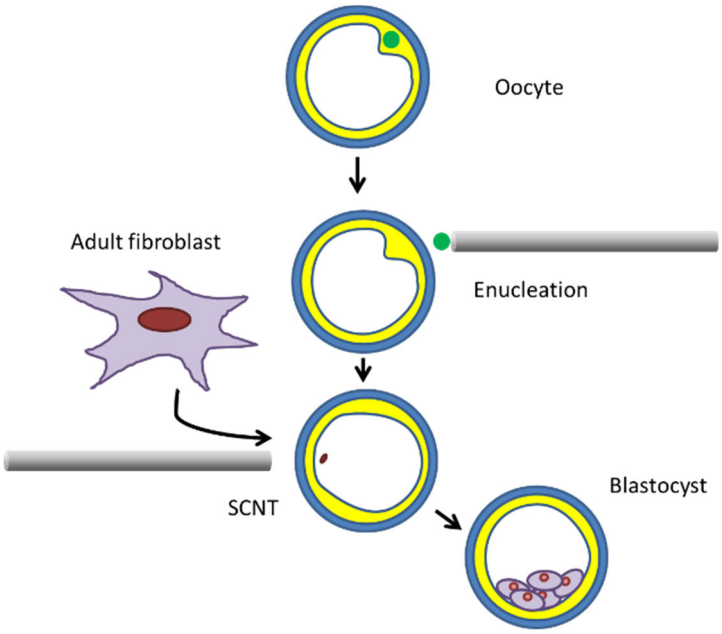

Figure 1.2: Process of SCNT adapted from(16)

Human reproductive cloning is not permissible in any country. This is the implantation of blastocyst-derived by SCNT into the uterus for the purpose of producing progeny. In Australia, this is legislated for in the "Prohibition of Human Cloning for Reproduction and Regulation of Human Embryo Research Amendment Act, 2002". However, the technique has been used in a wide array of species, such as mouse, pig, cows, and horses(17), which often have birthing and developmental problems if implanted and taken to term (18). The technique was introduced to the public by the creation of Dolly the sheep.

2. Somatic Cells

The technique to convert an adult somatic cell into a pluripotent stem cell was first described in 2006 by Yamanaka (19), who subsequently received the Nobel Prize in Medicine and Physiology for the discovery. The reprogramming of somatic cells was achieved by retroviral infection of mouse skin cells using 4 transcription factors - *Oct4, Sox2, KLF4* and *c-Myc*. A year later, it was human somatic cells that were induced to become pluripotent; hence the term induced pluripotent stem cells (iPSC).

Since then, other techniques of reprogramming have been described, including adenoviral gene delivery, micro RNA induction, and the use of recombinant proteins, which offer the advantage of not modifying the endogenous genetic background. The reprogramming technique is important in obtaining regulatory approval for human use, with genetic manipulation likely to be more problematic as it carries greater risks.

1.2 Uses of stem cells

1.2.1 Therapeutic opportunities

Both multi and pluripotent stem cells have great potential and have shown success in the treatment of some diseases. While it is possible to build machinery that replicates the simple function of organs; there are still many misunderstood or missing pieces of how cells all work together. With this in mind, the aims of stem cell research are focussed around the artificial production of tissues and organs for the treatment of disease.

An alternative mechanism for treatment is the use of mesenchymal stem cells to alter microenvironments at the site of injuries. Mesenchymal stem cells have been shown to serve a protective and regenerative function by mediating inflammation. As this is simpler to apply, it is the focal point of several products currently being commercialised (20). The following sections will cover the different areas of opportunity for the use of stem cells.

1.2.1.1 Replacement

Replacement of cells damaged or lost due to disease or injury is the most obvious potential therapeutic pathway for stem cells. However, this goal has proven much more elusive than simply generating the required cell types in the laboratory and transplanting them into patients. Factors which complicate this practise include the immune response of the recipient, the long-term viability of the transplanted cells, the capacity of pluripotent but not multipotent cells to develop teratomas, site of transplantation and the efficacy of the cells. Examples of areas being investigated for replacement opportunities are the generation of pancreatic progenitors for T1D (21), the generation of retinal pigment epithelial cells for dry macular degeneration (22) and cardiomyocytes for the treatment of heart disease (23). These factors have become more evident as successful differentiation protocols are developed but treatment options remain limited.

1.2.1.2 Regeneration

Stem cells can be used to stimulate the microenvironment in which they are transplanted to induce regeneration of the recipient's cells. Specialised cells are extremely sensitive to paracrine signals, and during homeostasis, this helps modulate cellular products and metabolism. The chemical signals released by stem cells can induce migration of endogenous multipotent stem cells that differentiate to regenerate the host tissue (24).

The process of using multipotent and pluripotent cells to regenerate damaged areas has been effective in a variety of tissues. Most notably stem cells have repaired the function of cardiac (25), spinal cord (26) and even ophthalmic (22) tissue. While promising, this mode of treatment is not possible for diseases in which the original tissue lacks regenerative capacity such as kidney or brain tissue. Specifically, this function of

MSC's is to enhance the self-repairing capacity of the damaged tissue through both direct action and immunomodulatory (24).

1.2.1.3 Anti-inflammation

Mesenchymal stem cells have potent immunomodulatory properties, which act to suppress inflammation locally. These properties are under investigation by a number of companies worldwide, an example of which is Mesoblast, who are in phase III clinical trials for their Refractory Crohn's disease product (27). When co-implanted with a hematopoietic stem cell transplantation, mesenchymal stem cells have increased the survival of implanted cells (28). Mesenchymal stem cells exert their effect by downregulating B-Cell antibody production and chemokine receptors (29), inhibiting cytokine production and preventing differentiation of monocytes to dendritic cells (30). With such strong immunomodulatory properties, it is not surprising that patient-derived mesenchymal stem cells offer tremendous therapeutic potential in various areas of human disease.

1.2.2 Pathogenesis of disease

Stem cells provide a powerful tool to examine the pathogenesis of a number of diseases, especially those with a genetic basis. Established pluripotent stem cells lines can be modified through chemical or genetic manipulation such as the polymerase gamma (*POLG*) mutation which induces mitochondrial disease, these cells can then be examined, experimented on and differentiate towards mature cells, such as neurons and muscle cells. Alternatively, iPSC can be derived from somatic cells of people with the disorder, and the reprogrammed cells studied as they differentiate *in vitro*. Another source of pluripotent stem cells affected with the genetic disorder is ESC derived from blastocyst of donors affected with the disorder. The company Genea specializes in the creation of such hESC lines for this purpose (31).

1.2.3 Drug toxicity testing

The possibility of screening the toxicity of drugs against multiple cell types has led to the use of stem cells in drug testing. These tests are highly beneficial to the pharmaceutical industry as they are technically easier and faster to conduct than injecting the drugs into laboratory animals, which is the current industry

standard. Those wishing to minimize the use of animals in laboratory research are likely to support this initiative, further the Federal Drug Administration of the USA has implemented mandatory testing of drugs on ESC derived cardiomyocytes as part of preclinical development (32).

1.2.4 Drug development

Stem cells also are used to evaluate the efficacy of drugs being tested for the treatment of certain conditions, for example, Type 2 Diabetes. The ability of the drugs to increase the production of insulin or increase the uptake of glucose is tested. Additionally, tumour-derived or engineered immortalized cells, which contain abnormal genotypes, can be used, as are primary cells, such as human islets, if they can be obtained. Access to primary human cells derived from pluripotent stem cells, which can be produced in relatively large numbers, saves on cost, time and ethical issues associated with *in vivo* studies—as well as the uncertainty of translatability to humans. Also, by using differentiated disease-specific stem cells *in vitro* it is possible to understand and demonstrate how compounds are absorbed, distributed, metabolised and excreted (5).

1.2.5 Potential drawbacks of using iPSC

There are several drawbacks to iPSC depending on their intended use. The economic case is one of the biggest hurdles to new drug development if there is a cost-effective treatment available it is unlikely there will be demand for a new more expensive treatment. The induction and characterisation of a new iPSC line is costly in time and resources, especially for non-integration iPSC. While methods of retroviral gene delivery are advancing rapidly, specifically non-integration methods which greatly reduce oncogene activation risk and mutagenesis. These are slow, inefficient and require multiple transfections (33).

iPSC exhibit increase genetic instability compared to hESC, this is the result induction method and the reprogramming process rather than cell source (34). There is evidence that during iPSC *in vitro* culturing, adaptation to culture conditions and clonal selection during passaging are probably the main causes of accumulation of genomic instability in iPSCs (35). As seen in hESC *in vitro* culturing decreases DNA damage

repair efficiency and contributes to iPSC genomic instability (36). Continued optimization of reprogramming and culture conditions hope to improve the genetic stability of iPSCs and their safety for clinical cell therapy.

1.3 The Pancreas

1.3.1 Anatomy

The pancreas is an organ situated in the posterior part of the peritoneal cavity, with its head nested in the first 3 parts of the duodenum, and its tail adjacent to the spleen. It has two roles, its exocrine role is to produce enzymes for digestion of food, and its endocrine role is to produce hormones for control of metabolism. The position of the pancreas facilitates the passage of the digestive enzymes it produces, amylase, lipase, chymotrypsin and trypsinogen through the pancreatic duct into the small intestine.

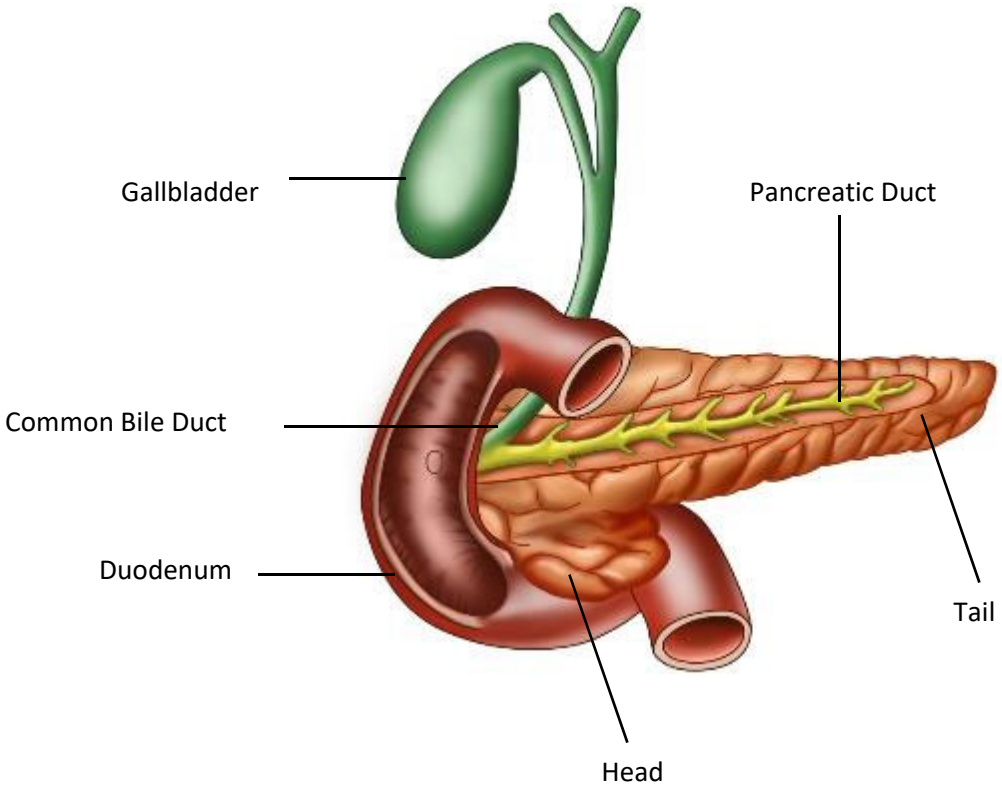

Figure 1.3: The anatomical depiction of the pancreas adapted from(37)

Endocrine hormones are produced in the Islets of Langerhans, which are scattered throughout the pancreas and constitute 1% of its volume. These hormones are secreted into islet capillaries, which eventually drain into the portal vein of the liver and subsequently into the systemic circulation. There are 5 hormones produced by endocrine cells in an islet. The cells are the β, α, δ, PP and ε cells that produce respectively insulin, glucagon, somatostatin, pancreatic polypeptide and ghrelin. The function of these hormones is as follows. Insulin and glucagon are responsible for glucose homeostasis with Insulin inducing the uptake of

glucose into muscle and fat cells while glucagon induces the breakdown of glycogen stores in the liver. In the stomach, somatostatin acts on the acid-producing parietal cells to reduce secretion as well as indirectly decreases stomach acid production by preventing the release of other hormones. Pancreatic Polypeptide primarily acts to self-regulate pancreatic secretion activities both endocrine and exocrine while also having effects on hepatic glycogen levels and gastrointestinal secretions. Ghrelin promotes hunger and restricts insulin release from the pancreas (38). Disorder of the β cells and resistance to its secreted product, insulin, resulting in diabetes mellitus.

1.4 Diabetes

There are two main types of diabetes, Type 1 and Type 2.

1.4.1 Type 1 Diabetes

Type 1 Diabetes (T1D), previously called insulin-dependent diabetes, is an autoimmune disease in which the beta-cells of the pancreas are destroyed. Their destruction is a gradual process with the affected person not displaying symptoms until fewer than 20% of their beta-cells remain (39). Typical symptoms are polyuria, polydipsia, blurred vision, and weight loss, as the muscles and tissues of the body are catabolized (40). Currently, there is no way of slowing disease progression even if detected before symptoms presents, although several strategies are being attempted. Markers of autoimmunity are antibodies to glutamic acid decarboxylase, an antigen on the surface of β cells called IA2, and zinc transporter 8 (41). Once T1D is diagnosed, exogenous insulin administration is required. Without this, the affected person continues to lose weight and dies. While insufficient insulin administration can lead to prolonged hyper-glycaemia which may cause neuropathy, nephropathy, cardiovascular problems and a variety of circulatory problems (42).

1.4.2 Type 2 Diabetes

Type2 Diabetes (T2D) accounts for 90% of all forms of diabetes (43), with 382 million people affected globally T2D is a growing problem in both the developing and developed world (44). It is characterized by a deficiency in the ability of the pancreatic β cell to produce insulin, as well as resistance to the insulin that is produced. It is a progressive disorder, with ~20% of affected people eventually requiring treatment with

exogenous insulin. During the early stages, blood glucose levels are controlled by diet and exercise. As the disorder progresses, medications that stimulate insulin production and/or enhance insulin sensitivity are often required.

1.4.3 Complications from diabetes

Imperfect control of blood glucose levels results in the development of microvascular complications. These include retinopathy, which may result in loss of vision; nephropathy, which may progress to renal failure; and peripheral neuropathy, with loss of feeling especially in the lower limbs. Macrovascular disease is exacerbated in people with diabetes, and this will lead to an increased risk of heart attacks, strokes and gangrene of the feet. There are several strategies that will reduce the risk of the development of these complications. These include good control of blood glucose levels, as well as blood pressure.

1.4.4 Current treatments for Type 1 Diabetes

1.4.4.1 Exogenous insulin

Insulin therapy has come a long way since the first use of bovine insulin in humans in 1922 (45). Currently, most insulin-dependent individuals in the developed world use recombinant human insulin produced in either *E. Coli* or yeast (46). As well as homologous human insulin there are a number of different types of human insulin analogues with different periods of onset and duration of action. These variations allow people who are insulin-dependent to better regulate their blood glucose levels. Insulin analogues are divided into three categories: short-acting, intermediate-acting, and long-acting. Short-acting insulin is administered subcutaneously with or shortly before meals as a bolus, while intermediate and long-acting insulin are administered, also subcutaneously, once or twice a day to maintain a basal level of the hormone.

Compliance with Insulin therapy is a time-consuming practice as it requires recipients to monitor their blood glucose levels and adjust insulin dosages throughout the day. People with insulin-dependent diabetes are advised to check their blood glucose levels at least three times a day (47), before or 2 hours after a meal, or before bed. Hypoglycaemic events, as defined by blood glucose levels < 4 mmol/L, can occur, especially if tight glycaemic control is sought by intensive insulin administration. Reasons for their

occurrence include alteration of mealtimes, decreased carbohydrate intake, increased physical activity, or increased insulin absorption rates (47). Generally, affected people experience symptoms of sweating, shaking, and a reduction in the ability to concentrate. These symptoms are overcome by eating glucose-rich food or a glucose-containing drink. If no action is taken, or in subjects with hypoglycaemic unawareness, the blood glucose level may continue to fall and the person loses consciousness, or exhibits extremely bizarre behaviour. These are called severe hypoglycaemic events, as they require the assistance of another person to overcome them. The remedy required is usually in the form of an intramuscular injection of glucagon, or intravenous administration of glucose. These events are life-threatening. However, the greatest risk of fatality from hypoglycemia is during sleep when patients are unable to notice the onset of symptoms and take corrective action by the consumption of carbohydrates.

1.4.4.2 Tissue therapies

1.4.4.2.1 Whole pancreas transplant

The first whole pancreas transplant was performed in 1966 in combination with a kidney and the duodenum. The recipient experienced a decrease in blood glucose levels but unfortunately succumbed to surgery-related sepsis 2 months post-transplantation (48). By the late 1980's advancements in immunosuppression and improvements in surgical techniques resulted in a one-year survival rate for pancreas transplants of 75%. The graft success rate improved in the following two decades, with an 85% 1-year graft survival rate in 2002/2003, even in high-risk recipients (49). In Australia, the number of whole pancreas transplants is limited to 55 per year largely due to the low supply of deceased donor pancreases (50, 51). Transplantation of a pancreas is considered only when the benefit of the transplant is likely to exceed the risk of immunosuppression (increased chance of infection and tumour formation). Most recipients also receive a kidney transplant due to the need for immunosuppression and the prominence of renal failure.

1.4.4.2.2 Human islet transplant

The morbidity associated with whole pancreas transplants was a stimulus for trying a simpler approach, namely the extraction and implantation of the Islets of Langerhans, which constitute 1% of the human pancreas. Normalization of blood glucose levels with this therapy was first achieved in mice in the 1960s, but it was not until 1989 that the first human recipient was transplanted. The ability to achieve normoglycemia was limited between then and 2000, with only 20% of recipients still being insulin-independent a year after the transplant. The success rate improved in 2000, with a group based in Edmonton, Canada, using a steroid-free form of immunosuppression, subsequently called the "Edmonton Protocol"(52). When this Protocol was applied to 7 consecutive islet recipients with T1D, they all became insulin-independent for one year. This practice was then extended to 9 other institutions and a further 36 patients, 44% of whom achieved insulin independence, 28% had partial function and 28% had total graft dysfunction after one year (53). The 2016 Collaborative Islet Transplant Registry report notes that insulin independence post islet transplantation has been improving and the length of graft function has also increased from 2007 (54). In Australia, the number of recipients of islet transplants is limited, only 12 in 2017 (55). While this Protocol is successful in providing insulin independence, it has similar drawbacks to whole pancreas transplants, namely requiring the use of immunosuppressive drugs. Due to this need for lifelong immunosuppression, only people with T1D who are experiencing unrecognized hypoglycaemic events or recurrent severe hypoglycaemia are recommended for the procedure.

1.4.4.2.3 Islets from animals (Xenotransplant)

A potential source of donor tissue which can be sourced in mass is that from large animals. There are several variables to consider when selecting a suitable donor species. These include similarity of genetics, physiology, the homology of insulin and production. With these factors in mind, non-human primates would be the best organ donors; however, as close relatives to humans, it increases the risk of pathogen exposure (56). Culturally most people in the West, where non-human primates are uncommon, would have difficulty in accepting tissue obtained from such creatures.

One animal that has similar advantages to non-human primates is the pig. Insulin released by pig islets is an effective substitute for human insulin as they differ by only one amino acid. Unlike rodent islets, porcine islets regulate glucose levels in the same physiologic range as humans. Finally, there is a variety of genetic modifications which can make pig islets more suitable for humans (57).

The company Living Cell Technologies Ltd. has completed a phase IIa using porcine neonatal islets clinical trial for the treatment of hypoglycaemic unawareness in humans. These islets are isolated and encapsulated in alginate before being transplanted into people with T1D. Initial results showed some success, but blood glucose levels have yet to be consistently normalized by this procedure (58); the transplant was shown to be safe from zoonosis (59) and Diatranz Otsuka Limited is taking the product to a phase III clinical trial in the US.

1.4.5 Stem cell-derived islet progenitors

Having a relatively unlimited source of insulin-producing cells is a factor driving the possible use of pancreatic progenitors derived *in vitro* from human embryonic stem cells (hESC). The starting pluripotent stem cell is derived from the inner cell mass of spare fertilized embryos obtained by Assisted Reproductive Technology from couples trying to have children. There are various protocols described to differentiate pancreatic progenitors from hESC, but all take 2-3 weeks and progress through the following ontological phases – definitive endoderm, posterior foregut, before reaching pancreatic progenitors (60-62). These are described in more detail below. Several groups have tried to produce glucose-responsive insulin-producing cells by this method (21, 63) but new methods have yielded glucose-sensitive insulin-producing cells (64, 65). Most research groups have differentiated hESC into pancreatic progenitors *in vitro* and allowed the progenitors to mature *in vivo*. This method of beta-cell maturation *in vivo* was first described in the 1980s when human foetal pancreatic tissue was transplanted into diabetic immunodeficient mice and the grafted glucose-unresponsive insulin-producing cells matured (66). The period of time after grafting required to achieve maturation is 3-5 months (67). Mature insulin-producing cells derived from hESC *in vitro* have been transplanted into a mouse that spontaneously develops diabetes, with blood glucose levels maintained within the normal range (64). These cells have been shown to achieve long term glycaemic control in a streptozotocin diabetic immunocompetent mouse (65).

Regardless, a clinical trial with pancreatic progenitors derived from hESC commenced in October 2014, with the company ViaCyte having obtained FDA approval for this in August earlier that year (68). To protect the cells from immune destruction by the recipients, who have T1D, the cells were placed in an immunoprotective device. I will discuss the concept of encapsulation to overcome the need for anti-rejection drugs later in the Chapter.

1.4.5.1 Development of the pancreas and *in vitro* replication

As the pancreas develops it passes through increasingly specialised tissue categories before maturing to the fully developed organ. The current theme in stem cell research is to coax the stem cells *in vitro* down

this same path passing through each category as hurdles to the goal. Currently, there are five major stages of differentiation from pluripotent embryonic stem cells in culture to function β Islet cells; these are definitive endoderm, primitive gut tube, posterior foregut, endocrine progenitors and finally insulin-producing cells. Definitive endoderm is defined by the up-regulation of mRNA transcripts *SOX17*, *FOXA2* and *BMP2* (Fig 1.4). In mouse embryogenesis, it participates in the morphogenesis of the gut tube and the associated visceral organs which include the liver and pancreas (69).

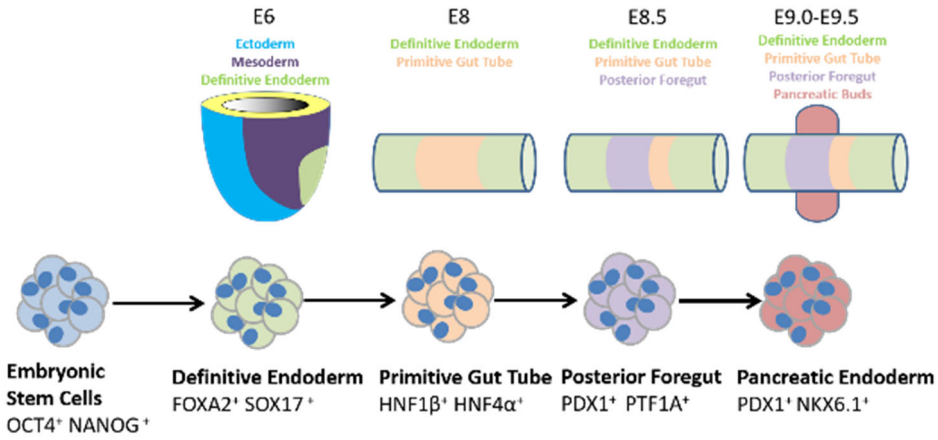

Figure 1.4: Development of the mouse pancreas, adapted from(69)

1.4.5.2 Differentiation of pluripotent stem cells to pancreatic progenitors

To overcome the lack of donor cadaver tissue for islet transplantations several sources have been proposed. The use of induced pluripotent stem cells, human embryonic stem cells and even gut endocrine progenitor cells of mice have been coaxed into insulin-producing cells (70). While these cells produce insulin the *in vitro* secretion of insulin in response to glucose stimulus is missing (71, 72). However once transplanted *in vivo* the cells have been shown to normalize blood glucose levels either implanted before exposure to STZ (73) or after STZ exposure and allowed to mature over several months (67). The same research group has recently applied several refinements of their original protocol to show for the first time that fully functional, beta-like cells could be generated *in vitro*. These cells were able to permanently reverse hyperglycaemia 40 days post-transplantation into diabetic mice (21).

While the focus of differentiating pluripotent stem cells has been on ESC, several strategies to differentiate iPSC into cells capable of producing insulin have been tested. The first paper that reported successful differentiation of human iPSC into insulin-secreting cells dates back to 2008, the group of Zhang adapted the four-step differentiation protocol developed for ESC from Jiang et al (60). This protocol was carried out on a 2D substrate called Matrigel, made from a gelatinous protein mixture secreted by Engelbreth-Holm-Swarm (EHS) mouse sarcoma cells (74). Differentiation protocols would be conducted on monolayer cells on Matrigel or an equivalent competing product (Cultrex® or Geltrex®). The reprogrammed human fibroblasts were differentiated *in vitro*, but the efficiency of differentiation process was very low and the cells were classed as "β cell-like" as the total C-peptide content was diminished when compared to mature β cells (75). Melton's group has described a 4- to 5-week *in vitro* differentiation protocol producing roughly 50 % of C-peptide and Nkx6.1 double-positive cells from both ESC and iPSC (64). While this is promising for an autologous treatment for T1D, there are still several hurdles which need to be overcome. The use of integrating virus-like retroviruses for pluripotency induction may cause insertional mutagenesis and induce tumour formation. Also, the recurrence of autoimmunity which leads to the initial β cell destruction may also trigger the destruction of an autologous transplant. It is very likely that an encapsulation device will be required for the immunoprotection of the cells whether they are autologous or not.

Recently the final stage in the maturation of pancreatic beta-cells has been greatly advanced. The extended use of select epidermal growth factors for up to 34 days has produced glucose-sensitive insulin-producing cells that correct induced diabetes in mice (64). While these cells are insulin-producing they are not as efficient as endogenous cells needing five times more generated cells than human islet cells to normalise blood glucose. With these advancements the differentiation process now has the potential for producing insulin-producing cells on a commercial scale.

Table 1.1: protocols and the additives and media each use.

Method		Stage 1 Definitive endoderm		Stage 2 Primitive gut tube	Stage 3 Posterior forgut	Stage 4 Pancreatic progenitor and endocrine precursor		Stage 5 Hormone expressing endocrine cell
Pagliuca 2014	**Additives**	Activin + CHIR		KGF	KGF RA SANT1 LDN PdbU	KGF RA SANT1	SANT1 Heparin Betacellulin RA T3 XXI Alk5i	T3 Alk5i CMRL supplemented
	Media	RPMI + 0.2% FBS + ITS			DMEM + 1% B27			
	Days	3		3	2	5	7	7-14
Schulz 2012	**Additives**	Activin + Wnt 3a	Activin	KGF+TBI	TT + CYC + Noggin	Noggin+KGF+EGF		
	Media	RPMI + 0.2% FBS + ITS			DMEM + 1% B27			
	Days	1	1	3	3	4+		
Kroon 2008, Kelly 2011	**Additives**	Activin + Wnt 3a	Activin	KGF+TBI	RA + CYC + Noggin	None		
	Media	RPMI + 0.2% FBS			DMEM + 1% B27			
	Days	1	2	3	3	3 to 8		
Rezania 2012	**Additives**	Wnt 3a + Activin	Activin	FGF7	Noggin + RA + SANT-1	Noggin + Alk5 inhibitor + TBP		
	Media	RPMI + 0.2% FBS	RPMI + 0.5 % FBS	DMEM F12 + 2% FBS	DMEM (High Glucose) + 1% B27			
	Days	1	2	3	4	3		
Rezania 2006	**Additives**	Activin + Wnt 3a	Activin	FGF10 + CYC	RA + CYC + FGF10	DAPT: Ex4		EX4 +IGF1 + HGF
	Media	RPMI 0% FBS	RPMI + 0.2 % FBS	RPMI + 2% FBS	DMEM + 1% B27			CMRL + 1% B27
	Days	2	2	4	3	3		3

1.4.5.3 Small Molecules

The investigation into the differentiation pathway which leads to pancreatic islets has been extensively undertaken in mice. It has been shown that inducing high levels of activin signalling will efficiently induce definitive endoderm in mouse ESC cultures (76, 77). These activin-induced populations are identified by the expression of *Foxa2* (78). Once induced, endoderm forms an epithelial sheet which is defined into three distinct regions known as the foregut, midgut, and hindgut (79). As the pancreas forms from the foregut region, retinoic acid combined with the inhibition of sonic hedgehog (SHH) results in a pancreatic progenitor lineage (72). Molecular analysis showed that human embryonic stem cells pass through to definitive endoderm in a time frame similar to that observed in the mouse embryonic cultures (80). Cells implanted at the pancreatic endoderm stage have been shown to continue differentiation *in vivo* (61). While there is the possibility of implantation at this stage the cells can be matured *in vitro* as previously mentioned.

There is a trade-off between these two options as the stem cells can take up to 150 days to mature *in vivo*. The more recently developed *in vitro* protocol requires an additional 34 days of maturation involving many more compounds to produce glucose-sensitive β-cells (64, 81). This protocol is still under review and is being tested in other models of diabetes, there is a great deal of optimism around its potential.

1.4.5.4 Transdifferentiation to beta-cells

Transdifferentiation is the process which a differentiated cell is able to differentiate into another cell type. Acinar cells in the pancreas have been shown to differentiate into duct cells in a process termed ductal metaplasia. In addition, acinar cells differentiate into hepatocyte-like cells and adipocytes, depending on the microenvironment (82, 83). Most relevant to diabetes, glucagon-secreting α-cells are able to differentiate into β-cells (84, 85). Transdifferentiation is thought to be behind spontaneous pancreas regeneration reported in T1D patients, despite continuous β-cell destruction through autoimmunity and glucotoxicity (86). Gene induced transdifferentiation has been induced by transfection of PDX-1 into adipose tissue-derived stem cells. These differentiated cells then reduced hyperglycaemia in diabetic

animals (87). Similar approaches have been applied to converted human skin fibroblasts into pancreatic cells by exposure to 5-azacytidine (AZA) followed by a three-step protocol (36days) for the induction of endocrine pancreatic differentiation (88). Insulin expressing cells have also been generated from skin fibroblasts from type 1 diabetes patients exposed to nicotinamide and exedin-4 (89). This in conjunction with iPSC generated from a person with T1D as well. Nonintegrative approaches carry the least risk in a clinical setting. It has been shown that β-cell transdifferentiation can be achieved through transfection of synthetic mRNAs coding for the three key transcription factors Neurog3, Pdx1, and Mafa (90). Although the cells secreted insulin they were still immature and did not respond natively to glucose stimulation. Transdifferentiation has come a long way and holds promise as a technique, it faces a lot of the same hurdles as modern pluripotent differentiation.

1.5 Encapsulation

The need for recipients of engrafted tissues/organs to take immunosuppressive drugs as a means of preventing rejection of the grafts severely limits the number of potential recipients. For all recipients, the benefit of the therapy given must be greater than the risks of the immunosuppression administered, which include increased risk of infection and neoplasia. Placing cells inside an immunoisolation device prior to transplantation is one means of trying to overcome the need for anti-rejection drugs. Organs cannot be placed inside such a device as they require a blood supply to connect the organs to the recipient.

There are two major types of immunoisolation devices, macro- and microcapsules. The idea of macroencapsulation is there are many insulin-secreting cells encased in one immunoisolating device often bigger than several centimetres. Microencapsulation has fewer cells encased in each individual unit of material, with thousands of individual capsules working together. Each method has advantages and disadvantages; however, the aim is similar, to enable immunoisolated cells to function *in vivo*.

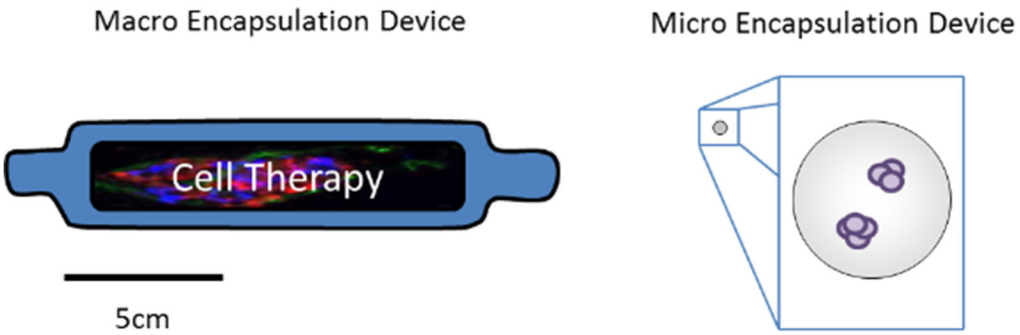

Figure 1.5: Visualisation of macro vs micro encapsulation.

1.5.1 Macroencapsulation

Macroencapuslation devices are of two major groups; intra- and extra-vascular. Intravascular devices are placed in the circulatory system and enable blood flow to supply oxygen and nutrients through the immunoprotective membrane to the perfusion chamber (91). This system is not widely adopted as it is prone to promoting the formation of blood clots (92). Extravascular macroencapsulation devices are of three major configurations; rods (93), tubes (94, 95) and sheets (96), and are made from polymers such as polytetrafluoroethylene or silicon. These systems provide the advantage of being able to carry greater numbers of cells and implantation and extraction carry a reduced risk of infection (92). Insulin independence has been seen using a range of these devices (97, 98) and has become the focus of commercial investment.

Viacyte has been the most prominent commercial operation investigating the use of macroencapsulation of stem cell-derived insulin-producing cells. In 2011, the Juvenile Diabetes Research Fund (JDRF) announced it would be partnering with Viacyte to bring its macroencapsulation and differentiation technology to the clinic. In August 2014, Viacyte obtained approval from the FDA to enter a phase I/II trial of their macroencapsulated cell sheet replacement therapy, with mixed but overall positive published data (61, 67, 99). As previously stated, the first human recipient of the encapsulated cells was announced in October 2014. Viacyte's progress is followed in section 1.6.

1.5.2 Microencapsulation

Cells encapsulated and transplanted in mass rather than as a single device are classed as microencapsulation. An example of this is alginate encapsulation that involves hundreds of individual cells encapsulated in alginate spheres ranging from 400µm to 2,000µm in size. Purified alginate is a powder which when reconstituted in the laboratory with purified water forms a hydrogel. This hydrogel, which is negatively charged, is then mixed with cells and after generation of microcapsules, solidified by chelation with a cation, usually Ca^{++}, Ba^{++}, or a combination. It is estimated that over 93% of the alginate by volume is water, this greatly reduces the presentation of foreign antigens which can activate the immune system (100). There are several impurities in alginate that activate the immune system when implanted in immunocompetent recipients. These immunogenic impurities are proteins (101), polyphenols and endotoxins. Purifying the alginate will minimize these contaminants (102), but not completely remove them, even when the alginate is highly purified. Currently, free-flowing electrophoresis is the most effective method of removing protein contamination in alginate (103).

Alginate is an anionic polysaccharide extracted from the cell walls of brown algae. The unbranched polymers have two distinct linking patterns between homopolymeric blocks, 1,4-linked *β*-d-mannuronic (M) and *α*-l-guluronic (G) acid residues. These residues covalently link together in different sequences or blocks (104). The respective ratios of these linking acids affect the physical properties of the alginate capsules. High G alginate capsules are found to be more rigid, porous gels, which maintain their integrity for longer periods of time (105-109). Whilst high G alginate has more ideal physical properties, it has been shown to reduce metabolic and secretory activity in some situations, for example, growth inhibition of encapsulated mouse βTC3 cells (104).

Alginate capsules are porous enabling the passage of nutrients and signals to the cells while enabling metabolites to be excreted. The pore size can be quite variable, with some calcium alginate microbeads' pores being 5-200 nm in diameter (110). Small molecules, such as cytokines and chemokines, which are usually of molecular weight ≤ 20,000Da, can readily enter through the pores, whilst large molecules

(>70,000Da), for example, IgM, and cells cannot. The smaller immunoglobulin molecule IgG, which is of molecular weight 150,000, is also unable to enter pores of diameter 5 nm (111). In addition to the presence of low levels of immunogenic chemicals, the geometry of the alginate can influence the host's foreign body reaction. Spherical microbeads that are of 1.5 mm in diameter or greater have been shown to elicit a significantly slower foreign body response compared to both their smaller-sized and none spherical counterparts (112). Most recently stem cell-derived β cells achieved glucose-responsive, long-term glycaemic correction (>174 days) in an immune-competent diabetic mouse with no immunosuppressive therapy. This was achieved by the combined use of imidazole-modified alginate capable of mitigating the forging body response and larger capsule size (65). Encapsulation of drugs is very different from encapsulation of living cells, which need to remain alive after encapsulation. An example of this is insulin, which has been placed in capsules for oral delivery, in order to avoid degradation by the acidity of gastric juices once ingested. The blood glucose levels of diabetic rats administered this treatment are lowered (113). Oral administration of insulin has moved to encapsulation with nanoparticles of biodegradable polyester as the excipients used for nanoparticles manufacturing are well accepted worldwide in the pharmaceutical field (114). Clinical trials are underway with this product.

1.5.2.1 Differentiation while microencapsulated

As covered in section 1.4.7 differentiation of hESCs is carried out either as aggregates known as embryoid bodies or as two-dimensional monolayer cultures on an extracellular matrix. However, these differentiation formats do not provide the same structure and signalling that the cells would experience during development. One way to replicate the structure (and therefore the mechanical signalling) the cells would experience during development is through the use of biomaterials. These biomaterials can play an important role in promoting cell to cell interaction, proliferation, and differentiation (115). The goal of this combination of biomaterial and stem cell differentiation would be to combine a biomaterial that drives stem cell differentiation as well as has a clinically useful purpose *in vivo*. The differentiation of hESC while encapsulated in alginate has previously been taken to the definitive endoderm stage (116). This is a key

proof of concept that cells can be differentiated while encapsulated in biomaterials which will serve a purpose *in vivo*.

1.6 Bioengineered pancreatic organoids

Organoids are 3D *in vitro* culture systems derived from self-organizing stem cells. They can recapitulate the *in vivo* architecture, functionality, and genetic signature of original tissues. Thus, pancreatic organoids have been rapidly applied to understanding organogenesis and the stem cell differentiation process (117). The simplest derived organoids can be sourced from human pancreatic tumour cells and have proven to be a valuable tool to predict patient-specific sensitivities and clinical outcomes for pancreatic carcinomas (118). Mouse embryonic pancreatic progenitors have been cultured on Matrigel™ to produce complex organoids that spontaneously undergo pancreatic morphogenesis and differentiation (119). These experiments informed pancreatic development and differentiation. It was shown small groups of cells better maintain progenitor properties and expand more efficiently than isolated cells, as well as the biochemical properties of the niche and requirement for three-dimensionality.

Human pancreatic organoids have been grown from HuES6 human pluripotent stem cells. These organoids had the ultrastructural, global gene expression and functional hallmarks of the human pancreas in the dish (120). As a model, the cells were then used to investigate the pancreatic facets of cystic fibrosis. Other hESC derived organoids have been used to investigate materials which could be used in differentiation and transplantation (121). A number of studies demonstrated that stem cells could generate functional pancreatic organoids (POs), able to restore normoglycemia when implanted in different preclinical diabetic models which face the same post-transplantation hurdles outlined previously (122).

1.7 Commercial stem cell companies and trials

The current field of human embryonic stem cell treatments for T1D is dominated by several key researchers and their collaborations. Due to the commercial nature of treatment development, results can be tightly

guarded and announcements framed in a positive light. With this in mind, one of the most advanced researchers currently working on the field is Dr Douglas Melton from Harvard who has successfully differentiated human embryonic stem cells into mature beta-cells (64). Coupled with this, he has recently announced at the American Diabetic Association conference that his group has been able to successfully differentiate alpha cells and delta cells from human embryonic stem cells. With this, they hope to recreate the composition of endocrine cells found in human islets for transplantation and treatment of T1D (Semma Therapeutics). This research has been achieved *in vitro* and *in vivo*. But now the main challenge for them and others is employing a delivery system to transplant these cells. From lessons learned from donor islet transplant, it is common knowledge in the field that the hepatic site is not hospitable for transplanted cells (123).

1.7.1 Current trials and companies working on devices to house insulin-producing cells

Various companies, such as Semma Therapeutics are currently working on encapsulation devices to protect the embryonic stem cells while implanted. In combination with his group's endocrine differentiation work, Dr Melton has been working with bioengineer Dr Daniel Anderson at the Massachusetts Institute of Technology to develop a capsule for the successful transplantation of cells. A patent filing from Dr Anderson's lab describes a container made of layers of hydrogels, some containing cells and others anti-inflammatory drugs to prevent the capsule from being covered with fibrotic tissue when transplanted into the abdominal cavity. Dr Anderson has published previously on the effect of size and shape of alginate hydrogels has on the host's fibrotic response (65, 124). This work has been developed by Sigilon Therapeutics which licenced the product to Eli Lily in April 2018.

Alginate delivery systems have recently taken several different designs. The Thread Reinforced Alginate Fibre for Islet enCapsulation (TRAFFIC) devices uses a nylon string to provide increased integrity and retrievability of the device. While the device is durable, transplantation with rat islets into mice had a ~28% failure to maintain normoglycemia (125). Coupled with noted inflammation when transplanted into dogs the device is still in the development phase. Novo Nordisk has set up a stem cell production facility with

the University of California San Francisco and a collaboration with Cornell University, which developed the TRAFFIC device.

BetaO_2 Technologies acknowledged that one of the limitations of beta-cell transplantation is the lack of sufficient oxygen to maintain cell function. As a result, the company has developed a device which is a combination of live cells in an alginate and Teflon membrane, this device is then transplanted subcutaneously. To overcome poor oxygenation at the transplant location the device also includes an oxygen reservoir which must be replenished daily through a port also located subcutaneously. While some human trials have been conducted the most recent publication has only shown limited success in a non-human primate (126).

Another strategy that can potentially enhance cell survival in a subcutaneous transplant location is increasing microvasculature. The Australian Foundation for Diabetes Research (AFDR) has taken a novel approach by use of alginate microcapsules to immuno-isolate the cells inside a sophisticated 3D printed scaffold that allows neo-vascularisation to occur after transplantation subcutaneously. The scaffold is made by melt electrospin writing that forms micro-meter thin strands of polymers on which blood vessels can grow in close proximity to encapsulated beta-cells. The device can be pre-vascularised or treated with pro-angiogenic molecules to improve oxygen and nutrient supply. The research is in the pre-clinical phase, testing ß cells derived from human embryonic stem cells, supplied by Kadimastem Ltd.

Similar to the AFDR's approach is the Sernova Cell Pouch™, which is about the size of a business card. The pouch is made of a scaffold of non-degradable polymers that are formed into small cylindrical chambers. This pouch is then placed subcutaneously and becomes incorporated with the tissue and micro vessels. After tissue incorporation, plugs on the cylindrical chambers are removed, leaving fully formed tissue chambers with central void spaces for the transplantation of therapeutic cells. The product is currently undertaking phase I/II clinical trial using immune suppression.

There are several other devices in the early stages of development. The intravascular bioartificial pancreas device (iBAP) is an intravascular device that isolates the desired cell therapy from the circulatory system by

a silicon nanopore membrane. Trialled in the carotid artery and vein of a pig, islets inside the device were able to maintain viability and respond to glycaemic challenges (127). NanoGland is a silicon device aimed at subcutaneous transplantation, the device has only undergone limited trials in immune-deficient mice (128).

Viacyte Inc. is a major commercial player in the field, with hundreds of patents for both the differentiation of human embryonic stem cells and devices for the transplantation/protection of these cells. The device currently in phase I/II clinical trials, which is the most advanced in clinical trials is the VC-01™. It is a plastic mesh capsule that is semi-permeable to nutrients and hormones while impervious to antibodies and immune cells. This device contains pancreatic precursor cells that are designed to differentiate upon implantation. In January 2018 ViaCyte announced a second cohort to be treated with their PEC-Direct device, this cohort will be most likely treated with immunosuppression drugs as the device had failed to provide the necessary protection (129).Another leader focusing on the development of the cells for transplantation is Dr Timothy Kieffer who works through the University of British Colombia and the company Betalogics which was a subsidiary of Johnson & Johnson, but in 2016 was taken over by ViaCyte Inc. The company works with protocols that differentiate human pluripotent stem cells into pancreatic progenitor cells *in vitro* and relying on the cells to mature into the desired insulin-producing cells *in vivo*. His work has achieved promising results in animal models with a yarn-based scaffold in a polyester shell (130). While not in clinical trials yet, any products brought to market will benefit from the substantial experience and support of their parent company.

Viacyte Inc. is keen on performing trials on transdifferentiation of cells. The company adopts the approach based on the notion that enabling beta-cells to mature in vivo allows them to differentiate better and attain full functionality. Currently, regulatory agencies are exposed to strict controls being addressed regarding the support of their utilization in clinical trials (106). The approaches include the tumorigenic cells' antibody selective ablation and the detachment of pancreatic progenitors other cells. Viacyte, Inc. is supporting hESC

based clinical trials for diabetes by adopting the above strategies. In addition, the company adapted the encapsulation of the cells inside an immunoisolation device in its clinical trials that functions as a physical inhibitor to potential tumour-forming escapees.

The company Seraxis Ltd corrected blood glucose levels of immune-competent mice for 24 days using islets which had been reprogrammed to pluripotent cells using reprogramming plasmids (a non-integrating vector) and differentiated into insulin-producing cells. These cells were encapsulated in alginate microcapsules and transplanted into the peritoneum (131). In mice, these microcapsules were able to normalise blood glucose levels within 8 days.

Table 1.2: Summary of cell therapies and stage of development.

Product Name	Cell type	Type of device	Type of biomaterial	Company	Application	Clinical trial phase	Outcome of the trial	Reference
PEC-Direct	HESc	Macroencapsulation	Plastic exterior Hydrogel interior	Viacyte	T1D	I/II	Required immunosuppression	(129)
PEC-Encap	HESc	Macroencapsulation	Plastic exterior Hydrogel interior	Viacyte	T1D	I/II	Ongoing	(129, 132)
Unnamed	HESc	Macro+micro encapsulation	PCL scaffold + alginate	AFDR	T1D	Pre-Clinical	Successful in mouse studies	Unpublished data
Cell Pouch	Cadaver Islets	Macroencapsulation	Plastic exterior Hydrogel interior	Sernova	T1D	I/II	C-peptide detected in circulation	(133)
Unnamed (SC-β)	HESc	Microencapsulation	Alginate with surface modification	Semma	T1D	Pre-Clinical	Successful in mouse studies	(124, 134)
BAP	Cadaver or Xeno Islets	Macroencapsulation	Plastic exterior Hydrogel interior	BetaO2	T1D	Pre-clinical and I/II	Xenotransplantation without suppression in primate	(126, 135)
Unnamed (SR1423)	iPSC	Microencapsulation	Alginate	Seraxis	T1D	Pre-clinical	Successful mouse studies	(131)

1.8 Challenges and future perspectives of cell therapy for Type 1 Diabetes

For the immediate future, the used of transplanted donor islets and immunosuppression is likely to continue. Therefore, research is still conducted into enhancing islet transplant outcomes, these include optimising islet isolation methodology and pre-transplant islet care (136, 137). These coupled with novel non-pharmacological interventions to enhance islet graft survival (138) will ensure that cadaver donor transplantations will continue. Nevertheless, the increasing number of newly diagnosed T1D cases and the scarcity of pancreatic donors highlights the need for alternative approaches such as cell replacement therapies.

As more companies enter clinical trials, they discover that the time taken to mature cells *in vivo* is a major limitation to the efficiency of the treatment. ViaCyte's pancreatic progenitors require 2 to 3 month to mature *in vivo*, Novo Nordisk presented data at the June 2018 NSW Stem Cell Workshop, that their glucose-responsive insulin-secreting cells required up to 2 weeks before blood glucose levels were normalized. This is much longer than the time adult islet transplants take when done in diabetic animals which is only 1 to 2 days to reach normoglycemia (139).

As mentioned in section 1.1.2.1 iPSCs can be generated from patient's somatic cells. These cells represent a potent pluripotent cell source for patient-specific cell-based organ repair strategies. However, their generation and subsequent differentiation into specific cells or tissues entail a number of challenges, including but not limited to, method of pluripotent induction, differentiation requirements and cell type target. It has been proposed that a biobank of IPSc from each major histocompatibility combination could be developed (140). Recent work has shown that mouse and human iPSCs lose their immunogenicity when major histocompatibility complex (MHC) class I and II genes are inactivated and CD47 is over-expressed (141). These hypoimmunogenic iPSCs retained their pluripotency and differentiation capacity. Other groups have specifically modified HLA-C with an HLA-class II knockout which could be immunologically compatible with >90% of the world's population (142, 143). It is important to note that Type 1 Diabetes is an autoimmune disorder and while the cells may have the same HLA class expression the hosts beta cells are immunogenic. Therefore any transplantation even with these iPSCs will still likely require immunosuppression. While this is a potential solution to the immunogenicity of non-autologous transplants there is still significant concern about transplanting a cell or tissue which is "invisible" to the host's immune system. Especially when the transplant was exposed to pluripotent factors or may still contain pluripotent cells.

Continued development is needed for successful cell therapeutic outcomes and persistent insulin independence. The emergence of β cell encapsulation strategies and implantation of islets in combination with MSCs could improve graft survival. This is expected to occur through aiding revascularisation but also by providing both pre-transplanted and post-transplanted islets with paracrine growth factors needed for proliferation and function. It is apparent in the short term that conventional T1D therapeutic approaches, including insulin replacement, SGLT2 inhibitors, immune therapies, and peptide agonists, will be combined with cell therapy approaches for optimum clinical therapeutic outcomes.

1.9 Summary and aims

With the advent of the Edmonton protocol, the potential for individuals with T1D to achieve insulin independence was realised. This was not the sought after cure, as the requirement for lifelong immunosuppression and diminished graft function over time-limited the appropriateness of this treatment to patients with hypoglycaemic unawareness or those who were already receiving kidney transplants. These limitations coupled with the shortage of organ donors are the reason so few islet transplants are carried out each year in Australia.

Stem cells provide a potentially limitless source of tissue for transplantation, yet, still elicit an immune response. By encapsulating the cells with an immunoisolative device the two largest limitations to islet transplant could be overcome. Currently, there is extensive work on differentiating stem cells into insulin-producing beta-cells and then encapsulating them in an immunoisolative device. While this work has yielded success *in vivo* immunocompetent studies, there is the potential for these protocols to face hurdles in scaling producing cells in the quantities and economy's suitable for a widely accepted treatment.

In this thesis, strategies have been implemented to overcome some of these factors.

The specific hypothesis of this study are:

1. hESC encapsulated in alginate will differentiate to PDX1 expressing pancreatic precursors.

2. hESC that undergo differentiation while encapsulated in alginate will mature in vivo after transplantation into diabetic mice.
3. iPSC from a person with T1D, encapsulated in alginate, differentiate to early pancreatic progenitors similarly to hESC.

The specific aims of this study are:

1. To determine if human embryonic stem cells can be differentiated to *PDX1* transcript expressing pancreatic precursors while encapsulated in alginate microcapsules.
2. To determine if partial differentiation, while encapsulated, *in vitro* followed by transplantation into a diabetic model will facilitate maturation *in vivo*.
3. To show that differentiation while encapsulated in alginate microcapsules is a viable option for induced pluripotent stem cells.

Chapter 2

Materials and Methods.

2.1 Cell lines

This section will briefly describe the cell lines used in this thesis. Further information about culture conditions and methodology can be found in section 2.3.

2.1.1 Endeavour 1 human embryonic stem cell (End1)

This line of cells was derived in Australia in 2008 and presents features of established embryonic stem cell lines. These include pluripotency both under *in vitro* and *in vivo* conditions as shown by the expression of embryonic stem–cell surface markers, positive staining for alkaline phosphatase, and the presence of the pluripotent gene marker (*NANOG*) with a normal karyotype (46XX)(144). When injected under the kidney capsule of immunodeficient mice they formed teratomas(144). These cells have been previously shown to differentiate towards endoderm while encapsulated after transplantation into NODSCID mice (145).

2.1.2 T1D#3 iPSC

Fibroblast cells from a person with T1D were donated to Monash University for reprogramming reprogramming to induced pluripotent stem cells (iPSC). This work was undertaken by Dr Jun Liu using Addgene pMX vector to deliver the 4 transgenes namely, *OCT4, SOX2, KLF4 and C–MYC*, (Shinya Yamanaka(146), Addgene plasmid #17217, 17218, 13370, 13375). Exogenous expression of these four genes reprogrammed the cell to a pluripotent state. The cell line was designated T1D#3 and cultured for over 20 passages at Monash University. It was routinely cultured on human foetal fibroblasts in knock–out serum replacement medium (section 2.3.1) to maintain self–renewal (Jun Liu, unpublished). Vials of T1D#3 were cryogenically stored in liquid nitrogen at both Monash University and The University of Sydney using 10% DMSO in KOSR.

2.1.3 Human foetal fibroblasts (HFF08)

HFF08 were derived from human foetal tissue at the Diabetes Transplant Unit, Prince of Wales Hospital (144) and grown in DMEM (11965092, Life Technologies, VIC, Australia) + 10% FBS in T150 flasks (CLS430825, Sigma-Aldrich, NSW, Australia). These cells were passaged and stored to form a cell bank

between passages 2 and 12. From the cell bank, the cells were grown to provide feeder layers for the hESC. Once the culture passed 20, a vial from the cell bank was thawed for use.

2.1.4 Cell line storage and thawing

Cells were cryogenically stored submerged in liquid nitrogen. The hESC were stored as either single cells post trypsinisation or colonies post passage (section 2.2.2). These cells were then suspended in 10% DMSO, 90% KOSR medium in a 2mL cryovial (CLS430659, Sigma-Aldrich, NSW, Australia). Fibroblasts were stored in 10% DMSO, 90% FBS. The cryovials were then placed in a room temperature Mr Frosty™ Freezing Container (5100-000, Life Technologies, VIC, Australia) filled with Isopropanol. Mr Frosty™ was then stored overnight in a –80˚C freezer. The next day the cells were transferred to a storage box and submerged in liquid nitrogen for storage.

To thaw the cells, first they were retrieved from the liquid nitrogen and onto dry ice for transportation. The cryovials were then rapidly thawed in a 37˚C water bath. Once thawed 500µL of culture media (KOSR for hESC, 10% FBS DMEM for HFF08) was slowly added to the cryovial and removed into a 15mL tube. Once this process had been repeated 6 times all of the liquid from the cryovial as well as the cells was now in the 15mL tube. The 15mL tube was then centrifuged at 500g for 5 mins and the supernatant removed. The cells were then resuspended in the appropriate cell culture media and plated (see section 2.2.2).

2.2 *In vitro* experiments

2.2.1 Cell culture conditions and PBS preparation

All cells were cultured in a humidified cell culture incubator at 37˚C with 5% CO_2. Cells were passaged weekly unless otherwise stated.

PBS solution was prepared by dissolving commercially available tablets (AMRESO, OH, USA, Cat#E404) in water (1 tablet per 100mL). The final concentration of this solution contained 137mM NaCl at a pH 7.3–7.4. PBS solutions were sterilised either by autoclaving or by passing through 0.2µM filter.

2.2.2 hESC medium and maintenance

Endeavour 1 cells were maintained and grown on a fibroblast feeder monolayer of HFF08 cell line. The preparation of this monolayer is outlined in section 2.2.3. The medium used for the maintenance of the End1 cells line was KOSR medium (Knock Out DMEM [10829–018] supplemented with 20% knockout serum replacement [10829–018], 1% (v/v) ITS [41400–045], 1% (v/v) NEAA [111040–50] from Life Technologies, VIC, Australia and 4ng/mL bFGF [233–FB] R&D Systems, MN, USA). The cells were passaged weekly either manually or enzymatically. To manually passage the cells, a 16G needle (BD, NSW, Australia, Cat#305197) was used to cut the week-old colonies into squares with ~100µm sides. These squares were then pipetted onto a freshly made HFF08 monolayer. Enzymatic passaging was carried out by first washing the week-old hESC colonies and monolayer with PBS and then applying 0.25% trypsin (Life Technologies, VIC, Australia, Cat#25200072) for 1min at room temperature. The cells were then dislodged from the culture ware with a cell scraper (Sigma-Aldrich, NSW, Australia, Cat#SIAL0010) and resuspended in KOSR medium. The cell suspension was spun down at 500*g* for 3min and the supernatant removed. The cells were resuspended in KOSR medium as a mixture of small clumps and single cells ready for plating onto a fresh monolayer.

2.2.3 HFF08 culture and monolayer preparation

The HFF08 fibroblasts were propagated to serve as feeder monolayer for the End1 hESC. These HFF08 cells were grown in high glucose (25mM) DMEM (Life Technologies, VIC, Australia, Cat#11960–069,) with 10% FBS (AusGeneX, QLD, Australia, Cat#FBS500–S,). These cells were passaged once a week at a ratio of 1:5; i.e., 1 confluent T150 culture flask was split into 5 T150 culture flasks. This passaging was carried out by first washing the fibroblasts with PBS then applying 0.25% trypsin and returning the cells to the incubator for 5min. Centrifugation to remove the supernatant was not required, since fresh medium (DMEM and 10% FBS) subsequently added to the cell suspension inactivated the enzyme. The diluted cells in suspension were plated onto new culture ware.

Feeder layer preparation was initiated when the fibroblasts reached 80% confluence by adding mitomycin C (Sigma-Aldrich, NSW, Australia, Cat#M2487) 10µM into the culture medium and incubating for 2.5h under

normal cell culture conditions. Mitomycin C was received as a powder and dissolved in sterile water at 1mg/mL; aliquots were then stored at –20˚C. Cells were washed once with PBS and trypsinized with 0.25% trypsin for 5min at 37˚C. These cells were then centrifuged at 400*g* for 5min, the supernatant discarded and the cells resuspended in DMEM supplemented with 10% FBS. This resuspension was seeded at 20,000 cells/cm^2 on gelatin-coated plates. These plates were prepared by adding 2mL/10cm plate 0.1% porcine gelatin (Sigma-Aldrich, NSW, Australia, Cat#G9391) and placed in an incubator for 30min. The cell count methodology is covered in section 2.2.5. The following day the medium was changed to KOSR medium so that the hESC or iPSC could be plated onto them. Cells were grown in a volume of medium appropriate to the culture dish being used (Table 2.1). This process was carried out one to two days before the hESC required passaging.

Table 2.1: Cell culture plasticware and growth medium volumes.

Cell culture plasticware	Volume of medium (mL)
6cm culture dish	6
10cm culture dish	10
T75 culture flask	10
T150 culture flask	20

2.2.4 Pluripotent stem cell isolation from the feeder layer

Prior to encapsulation in alginate or plating onto Geltrex®, the pluripotent stem cells were first separated from their fibroblast feeder layer. To purify the stem cells, the culture medium was removed and the cells were washed once with PBS. The cells were then covered in 4mL 5mg/mL dispase (Stemcell Technologies, VIC, Australia, #07923,) per 10cm plate for 20min in the cell-culture incubator. The dispase was aspirated and the same volume of TrypLE Express (Life Technologies, VIC, Australia, Cat#12604013) was added and

incubated as before. Following incubation, the colonies were gently scraped with a cell scraper (Sigma-Aldrich, NSW, Australia, Cat#SIAL0010) and resuspended in 10mL KOSR medium. The suspension was then gently pipetted into a 40µm cell strainer (Sigma-Aldrich, NSW, Australia, Cat#CLS431750) on top of a 50mL centrifuge tube. This removed any large clumps of cells. The strained suspension was then pelleted at 1,000*g* for 5min and resuspended in DMEM supplemented with 10% FBS. This suspension was then plated onto T150 flasks (~36,000 cells/cm^2). The flasks were incubated at 37˚C for 30min to allow the fibroblasts to attach to the culture plate, while the stem cells remained in suspension. The medium with stem cells was then removed and spun down as described previously in this section.

2.2.5 Cell counts via haemocytometer

To count the number of live cells being plated, a cell count using 0.4% trypan blue solution (GE Healthcare, NSW, Australia, Cat#SV30084.01) and a haemocytometer were used. First, 10µl trypan blue solution was added to a microfuge tube. Then, cells were suspended in the tube via gentle pipetting and inversion/tapping of the tube. The cells were thoroughly mixed with the trypan blue by repeated pipetting. 10µl of this suspension was then pipetted onto the haemocytometer, and their number counted. Live cells prevent the entry of trypan blue allowing total live cell counts to be made.

2.3 Encapsulation

2.3.1 Alginate preparation

Encapsulation of the pluripotent stem cells in alginate requires the alginate to be a rehydrated, viscous liquid. To do this, ultra-pure alginate powder (Pronova Biomedical, Oslo, Norway Cat#UP MVG BP1105 06,) was added to MilliQ water and dissolved overnight on a roller at room temperature to prepare a 2.2% (w/v) solution. The following day 0.2mL 0.9% sterile NaCl solution was added per 1.8mL alginate solution. The mixture was briefly vortexed then centrifuged at 500*g* for 5min to sediment undissolved alginate. The solution was sterilised by passing through a 0.22µm filter (Sigma-Aldrich, NSW, Australia, Cat#Z359904) and stored at 4˚C.

2.3.2 Encapsulation of cells

The cells were mixed in the reconstituted alginate in a ratio of 1:8 to form a suspension which can then be transformed into spheres by passage through an air droplet generator. End1 stem cells were resuspended in 2.2% alginate solution at a concentration of 2 x 10^6 cells/mL alginate. The suspension was gently mixed using a stirrer (commonly a 14G plastic catheter attached to a syringe). The mixture was then drawn into a 3mL syringe and the nozzle of the syringe placed into the encapsulation device as shown in Fig. 2.1. A constant–pressure automated plunger was attached to the syringe to force the alginate solution out of the syringe through the device at a flow rate of 1mL/min. Simultaneously, sterile air was passed through the encapsulation device at a rate of 6L/min and 80kPa pressure. This pressure and flow rate were optimised from previous work in the laboratory(147) to produce droplet spheres of 400 ± 150µm in diameter as measured on Cell^M (Olympus, NSW, Australia) software post solidification. The alginate droplets were collected into a 30mL bath of sterile barium chloride (20mM $BaCl_2$, 10mM MOPS, 119mM NaCl, pH 7.2), placed 15cm below the device. In the presence of $BaCl_2$ the alginate droplets solidified the microspheres/microcapsules. The microspheres were then washed in sterile PBS 3 times to remove excess barium chloride, settling under gravity and cultured at 37˚C, 5% CO_2 in 10cm dishes containing KOSR medium.

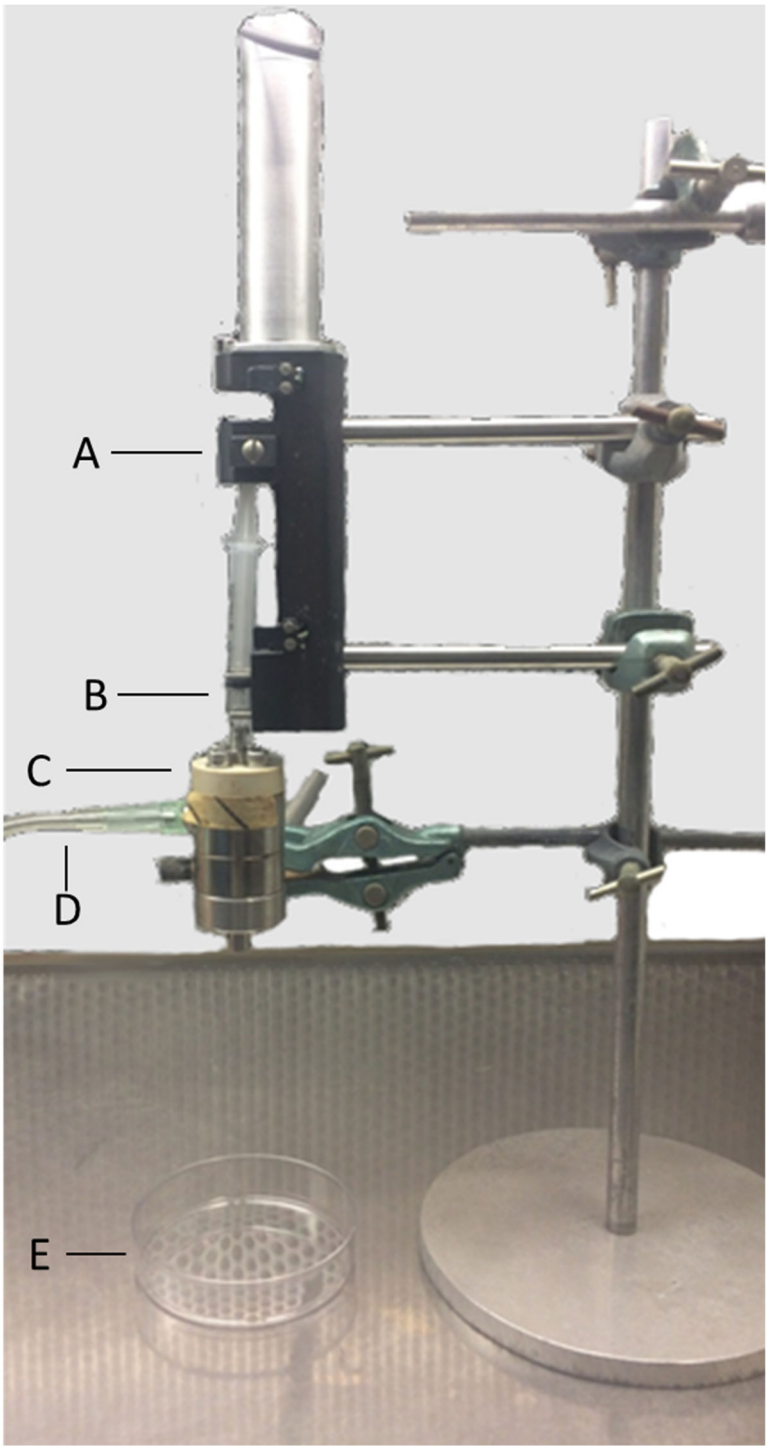

Figure 2.1: Encapsulation device shown with an empty syringe loaded into the constant speed machine. A) Syringe driver. B) A syringe filled with alginate/cell suspension. C) Encapsulation device. D) Sterile medical air. E) Petri dish which will contain $BaCl_2$ solution.

2.3.3 Differentiation of pluripotent stem cells to pancreatic progenitors

A previously published differentiation protocol was employed to take the hESC from pluripotent to the pancreatic precursor cell stage (61). To do this, End 1 pluripotent stem cells were plated onto Geltrex® (Life Technologies, VIC, Australia, Cat#A1569601) coated plates or encapsulated as per Section 2.3.2. Geltrex® is an hESC-qualified ready-to-use, reduced growth factor basement membrane matrix which stem cells require for proper adhesion and expansion in culture. To prepare the Geltrex® plates or flasks; a sufficient volume of Geltrex® was added to cover the entire surface area of the plate. The plate was then incubated at 37°C for 60min to enable the matrix to form. Any remaining liquid Geltrex® was aspirated before pluripotent stem cells were plated at $1x10^5$ cells/cm^2. These cells were grown for three days in KOSR medium supplemented with 10 µM Y27632 (Sigma-Aldrich, NSW, Australia, Cat#Y0503), a selective inhibitor of Rho-associated, coiled-coil containing protein kinase (ROCK inhibitor) (ROCK inhibitor was dissolved in DMSO at a stock concentration of 5 mM and stored at –20˚C.) Following this incubation, culture medium was changed to a differentiation medium and the medium replenished daily as summarised in Table 2.2. At the beginning of day 1, RPMI medium (Life Technologies, VIC, Australia, Cat#22400–105) was used supplemented with 100 ng/mL Activin A (R&D Systems, MN, USA, Cat#338–AC–050,) and 25 ng/mL Wnt3A (R&D Systems, MN, USA, Cat#5036–WN–010). For days 2 and 3, 0.2% FBS was also added. For the following 3 days (days 4-6) the RPMI medium was switched to contain 50ng/mL KGF (R&D Systems, MN, USA Cat#251–KG–050,) and 2% FBS. For the final 3 days (days 7–9) DMEM (Life Technologies, VIC, Australia, Cat#11960–069) was used containing 2nM retinoic acid (Sigma-Aldrich, NSW, Australia, Cat#R2625), 0.25nM Cyclopamine-KAAD (Merck Millipore, VIC, Australia, Cat#239804), 50ng/mL Noggin (R&D Systems, MN, USA, Cat#6057–NG–025) and 1% B27 (Life Technologies, VIC, Australia, Cat#17504–044).

Table 2.2: Pancreatic Progenitor differentiation protocol. Medium was changed daily. The concentrations of added growth factors were as follows: Activin A 100 ng/mL, Wnt3A 25 ng/mL, KGF 50ng/mL, Retinoic acid 2nM, Cyclopamine-KAAD 0.25nM, and Noggin 50ng/mL.

	Step 1		Step 2	Step 3
Differentiation Stage	Definitive Endoderm		Primitive Gut Tube	Posterior Foregut
Reagents	Activin A Wnt3A RPMI	Activin A Wnt3A 0.2% FBS RPMI	KGF RPMI 2% FBS	Retinoic acid Cyclopamine-KAAD Noggin DMEM 1% B27
Duration	1 day	2 days	3 days	3 days

2.3.4 Cell viability within capsules; cell live/dead assessment

Due to the stress placed on the cells during the encapsulation and/or differentiation process, we tested the viability of cells within the capsules. This assessment utilized 6-Carboxyfluorescein Diacetate (6-CFDA) (Sigma-Aldrich, NSW, Australia, Cat#C5041) as a live-cell marker and propidium iodide (PI) (Sigma-Aldrich, NSW, Australia, Cat#4170) as a counterstain for dead cells. To prepare the cells, they were washed twice with PBS. Non–encapsulated cells were centrifuged at 500*g* for 3min and encapsulated cells allowed to settle by gravity. The marker 6-CFDA, stored as a 10mM solution in DMSO at 4˚C, was diluted 1:9 in PBS and 2.5mL used to resuspend any number of pelleted cells or capsules in a 15mL tube. This was followed by a 30min incubation in the dark at 37˚C with the tube being gently tapped every 10min. The 6-CFDA was then removed with 2x PBS washes and resuspended in 200µl PBS. The cell marker PI stored as a 100µg/mL stock solution in sterile water 4˚C was diluted 1:19 into the cell suspension of 2.5mL and incubated at room temperature for 5min. The cells were then washed again in PBS and transferred to a glass slide and

visualised on a fluorescent microscope (section 2.3.12). Live cells were visible in the 520nm emission channel and dead cells at 620nm emission channel when excited by the USH-1030 ultrahigh-pressure mercury lamp (Olympus, NSW, Australia) at 490nm. The number of live and dead cells was counted per capsule and expressed as a percentage of the total number of cells in that capsule. Cells which stained both green and red from the live and dead markers respectively were counted as alive. 6-CFDA must be metabolised by intracellular esterase enzymes and bind to amine groups before fluorescence is visible therefore if green florescence is visible the cells is actively metabolising substrates. In addition to this, the fluorescence is contained within the cell indicating a non-permeable membrane.

2.3.5 Glucose stimulated insulin secretion (GSIS)

Beta-cells secrete insulin in response to blood glucose. It is important to investigate this characteristic when determining the effectiveness of cell therapy. GSIS was used to assess if insulin-producing cells were mature by exposing them to a high concentration of glucose. The capsules containing the cells were retrieved and initially cultured overnight at 37˚C in KOSR medium before performing GSIS. Two sterile 10cm culture dishes were filled with 10mL basal buffer (3.3mM glucose Krebs Buffer, [137mM NaCl, 4.7mM KCl, 1.2mM KH_2PO_4, 1.2mM $MgSO_4$, 2.5mM $CaCl_2$, 25mM $NaHCO_3$]). In addition, three vials were filled with basal buffer and another three filled with activation buffer (16.7mM Glucose in Krebs Buffer). Approximately 120 alginate capsules were placed into the first basal buffer culture dish for 30min at 37˚C. These were then placed into the second basal culture dish for an additional 30min at 37˚C. After incubation, the capsules were divided evenly between the 6 vials (0.3mL each) and incubated at 37˚C for 60min. The supernatant was removed and all samples were stored at –80˚C until analysed.

2.3.6 C-peptide measurement

To identify if human cells transplanted into mice had produced any (human) insulin, the concentration of human C-peptide in recipient mice plasma was measured. C–peptide is produced at a 1:1 ratio to insulin in beta-cells. An insulin assay is not used as it will measure any exogenous insulin given to help care for the animals. Insulin also has a much shorter half-life in the circulation compared to C-peptide. The assay was

conducted using a commercially available ultrasensitive human C-peptide ELISA kit (Mercodia, Uppsala, Sweden, Cat#10–1141–01,) according to the manufacturer's protocol. Briefly, the protocol is as follows: 50µl calibrators (solution of known C-peptide concentration), control samples and experimental samples (plasma) were pipetted into the antibody-coated wells. 50µl assay buffer was then added to each of the wells. The plate was then incubated on a plate shaker (700–900rpm) for 1h at room temperature. The wells were then washed five times with ~350µl of wash buffer. 200µl antibody-linked enzyme was then added to each well and incubated on a plate shaker for 1h as per previous steps. The wells were washed again as before. To each well 200µl substrate (3,3',5,5'-tetramethylbenzidine) solution was added and incubated for 30min on the bench at room temperature. The assay was completed by adding 50µl stop solution and the absorbance of each well was read on a plate reader at 450nm wavelength. A standard curve was generated using known concentrations of C-peptide (provided with the kit). Human C-peptide concentrations in test specimens were measured against the standard curve. A representative standard curve is shown in Fig. 2.2.

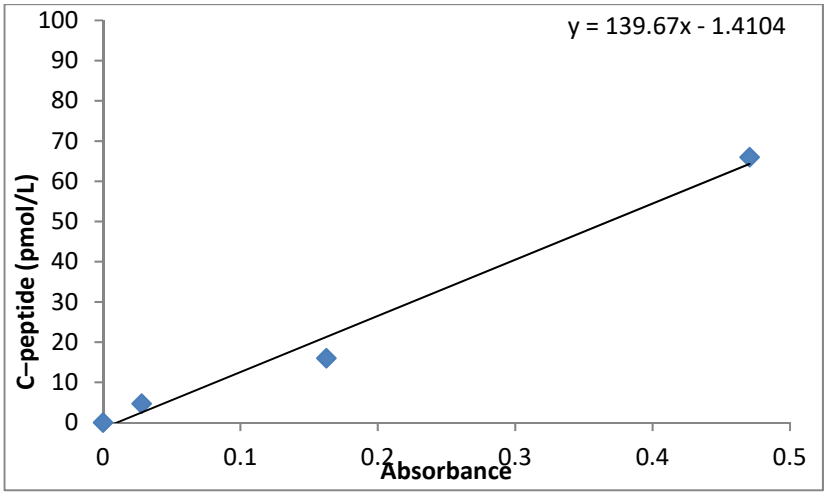

Figure 2.2: Absorbance curve of known standards in a C–peptide ELISA

2.3.7 Decapsulation

To retrieve the cells from the capsules decapsulation solution was used, consisting 50 ml 0.5M EDTA, 5 ml 1M HEPES in a total volume of 500 ml PBS. Sterilize using an autoclave at 121 °C for 20 min. First, the capsules were aspirated into a 15 ml centrifuge tube and allowed to settle at the bottom. The supernatant was then carefully aspirated and discarded. The capsules were washed PBS twice. Left to settle and the supernatant removed. 5 ml decapsulating solution was added to the capsules and the suspension was mixed thoroughly and incubated at 37^{o}C for 5 mins. The decapsulated cells were then centrifuged at 95 x g for 3 min and the supernatant discarded. The cell pellet was washed with PBS and centrifuged again 95 x g for 3 min. The decapsulated cells were then either immediately analysed or snap-frozen.

2.4 qPCR

2.4.1 RNA Isolation and cDNA generation

To assess gene expression, RNA was extracted from End1 cells being differentiated *in vitro* on days 0, 3, 6, 9 and *ex-vivo,* using 0.5mL TRIzol® reagent (Life Technologies, VIC, Australia, Cat#33251) per million cells and inverted 5 to 10 times. Samples were either snap-frozen in liquid nitrogen and stored at –80˚C or used immediately for RNA purification. During RNA purification, samples were kept on ice and chloroform (200µl/mL TRIzol®) was added to the samples, the mixture vortexed for 15s, and the phases allowed to separate first by incubating on ice for 5min followed by centrifugation at 12,000*g* for 15min at 4°C. The aqueous layer was removed and added to a microfuge tube followed by the addition of an equal volume of isopropanol. Samples were then vortexed and incubated at –20°C for 10min. The RNA was pelleted by centrifugation at 12,000*g* for 10min at 4°C and the supernatant discarded. The RNA pellet was washed in 1mL molecular grade 80% ethanol and centrifuged at 12,000*g* for 15min at 4°C. The ethanol was removed and the RNA pellet was air-dried for 15min to remove any residual ethanol. The RNA pellet was then dissolved in 50µl nuclease-free water and stored at –80°C.

To convert the extracted RNA to cDNA, the concentration of RNA must be known before the reverse transcription and assessment process can take place. The concentration of total RNA was measured on a Nanodrop 2000 (Life Technologies, VIC, Australia). The ratio of absorbance at 260nm to 280nm was used to determine protein contamination with a ratio of >1.8 considered to have very low protein contamination, whereas the 260 to 230 ratio was required to be > 1.7. The concentration of RNA present in each sample was determined from the absorbance at 260nm using an extinction coefficient of 0.025 $(\mu g/mL)^{-1}$ cm^{-1}. The RNA was then reverse transcribed using the High Capacity cDNA Kit (Applied Biosystems, CA, USA, Cat#4368814). A 0.5µg aliquot of RNA was reverse transcribed in a 15µl reaction as per the manufacturer's protocol.

2.4.2 cDNA generation and qPCR

The cDNA was analysed on the Viia7 thermal cycler using a TaqMan Assay system (Thermo Fisher Scientific, VIC, Australia). 1µl cDNA (equivalent to 33ng original RNA) was loaded into each well of a TaqMan Array 96–Well Fast Plate with 4µl TaqMan Fast Advanced Master Mix and the appropriate TaqMan primer. The final concentration of this primer was 250 nM. Samples were then run and C_t values returned using the Viia7 thermal cycler software. Factory set conditions were selected for the 96–well Fast Plate and C_t values were exported for analysis into Excel. C_t values were normalised to housekeeping gene 18s by adjusting the difference in value between the housekeeping gene in the control sample and the housekeeping gene in the experimental sample. These adjusted values were then expressed as a fold change over the detectable limit (39 cycles) of the machine. The detection limit is the number of cycles required to detect a single transcript of the gene of interest (148). Expressing the values in this format is a relative measure to the sensitivity of the machine to detect a single transcript. This expression is in the form of the final formula $2^{(39-CT)}$ where C_t is the adjusted C_t value. The efficiency of the primers was not tested as they were off the shelf TaqMan primers which are guaranteed to be 100 %. Further, off the shelf TaqMan primers cross exon-exon boundaries to ensure no genomic contamination .

Table 2.3: TaqMan probes used in qPCR. Probes were selected from a commercially available catalogue of sequences known to be specific for the reverse-transcribed mRNA sequence. The Life Technologies probe ID is listed for retrieval of the specific sequence. The gene which each probe is specific for as well as alternative names are provided. FAM and VIC are reporter dyes attached to the specific probe. It is important that the qPCR machine is set to read these fluorescent reporters. Finally, the role of each of the genes is listed.

Probe ID (Life Technologies)	**Gene name**	**Probe**	**Role**
Hs00999632_g1	*OCT3/4 (POU5F1)*	FAM	Pluripotency marker(149)
Hs02387400_g1	*NANOG*	FAM	Pluripotency marker(150)
Hs00751752_s1	*SOX17*	FAM	Definitive Endoderm Marker(151)
Hs00232764_m1	*FOXa2 (HNF3b)*	FAM	Definitive Endoderm Marker(152)
Hs01001602_m1	*HNF1β*	FAM	Primitive foregut(153)

Hs00230853_m1	*HNF4α*	FAM	Primitive Foregut(154)
Hs00236830_m1	*PDX1*	FAM	Primitive Pancreatic Marker(87) Mature β Cell Marker
Hs03003631_g1	*18S*	VIC	Housekeeping Gene(155)
Hs00165775_m1	*SLC2A2 (GLUT2)*	FAM	Late Pancreatic Marker(156)
Hs00360700_g1	*NGN3*	FAM	Endocrine Progenitor Marker(157)
Hs00232355_m1	*NKX6.1*	FAM	Late Pancreatic Marker(158)
Hs01651425_s1	*MAFA*	FAM	Mature β Cell Marker(159)
Hs02741908_m1	*INS*	FAM	Mature β Cell Marker(21)
Hs00173014_m1	*PAX4*	FAM	Endocrine Cell Marker(160)

2.5 Microscopy, sectioning and staining

2.5.1 Cryo-sectioning of capsules and grafts

Histological and immunohistochemical staining requires access of the stains to the tissue, grafts and antigen sites. To facilitate this, cryo-sectioning was employed to enable permeation and visualization of the stains. Pluripotent stem cells encapsulated prior to their implantation into mice and *ex vivo* grafts from these animals were immersed in Optimal Cutting Temperature (OCT) solution (Sakura, Osaka, Japan, #4583) at room temperature and solidified by placing in –80°C and stored for later use. Using a cryostat (Leica Microsystems, NSW, Australia Model#1510S), 10µm sections were cut and placed on charged microscope slides (Lomb Scientific, NSW, Australia, Superfrost Plus, #4951PLUS4). These slides were stored at –80˚C until analysed.

2.5.2 H&E staining

Haematoxylin and Eosin staining enable the identification of cells and structures within tissue. Cryo-sectioned slides (see Section 2.5.1) of grafts removed from recipient mice were taken out from –80°C storage and air-dried for 10min and fixed in 100% methanol for 5min. The slides were then rehydrated by placing them briefly (1 to 2s) in 100% ethanol followed by 70% ethanol and finally water. The staining was

initiated by immersion in Haematoxylin solution (POCD, Sydney, Australia) for 5min. The slides were then washed by three brief submersions in fresh deionised water. Following washing, the slides were submerged in acid alcohol solution (1% HCl acid v/v, 99% ethanol) for 1 to 2s. The cells were then washed in deionised water again and finally submerged in Eosin (1% w/v, 95% v/v ethanol, 4% water) (POCD, Sydney, Australia) for 2min. Finally, the slides were dehydrated by submersion first in 70% ethanol, then 100% ethanol for 5 min per solution. Mounting medium (Entellan™ New, Sigma-Aldrich, NSW, Australia) was placed over the sample and a coverslip was then fixed in place with clear nail polish on the corners of the coverslip.

2.5.3 Immunofluorescent staining

The following samples were immunostained:

a. hESC undergoing differentiation on geltrex at days 0, 3, 6 and 9.
b. hESC undergoing differentiation while encapsulated at days 0, 3, 6 and 9.
c. Cryosectioned kidneys of mice which had pancreatic progenitors matured under the kidney capsule *in vivo.*
d. Encapsulated pancreatic progenitors matured *in vivo* cryosectioned after retrieval.

Confirming that key protein expression was occurring is another key step in confirming developmental progression. Proteins such as FOXA2 are known to be turned on at set time points and enable development (161). The above-listed samples were stained with antibodies of known key proteins; see Table 2.4 for a list of these. Slides containing cryosectioned specimens were air-dried and fixed in 100% methanol for 5min. Samples on tissue culture plates were fixed with 4% PFA for 20min at room temperature. Following fixation samples were washed with TBST (0.1% Triton in TBS [50mM Tris, 150mM NaCl, pH 7.6 with HCl]) for 10min at room temperature. The samples were then blocked for 1h at room temp with 2% BSA in PBST (0.2% Tween–20 in PBS) on a rocker. After blocking, the samples were incubated overnight at 4˚C with 1˚ antibody diluted as per Table 2.4 in 2% BSA in PBST. The following day, the samples were washed three times for 5min with PBST at room temperature. The 2˚ antibody was then added as per Table 2.4 and incubated for 2h at room temperature on the rocker. The samples were then washed with 2% BSA in PBST and ProLong®

Gold Antifade (Life Technologies, VIC, Australia Cat#P10144) was added. Coverslips (Chase Scientific Glass, Rockwood, USA, 22x40mm No.1 thickness) was applied to the slides and fixed into place with the use of clear nail posh on the corners.

Table 2.4: List of immunohistochemistry antibodies used in this work. Antibodies were diluted in 2% BSA in PBST. Aliquots were stored in volumes of less than 20 µl at –20^{o}C. Once thawed, all antibodies were stored at 4^{o}C; secondary antibodies also were stored in the dark.

Antibody	Manufacture	Cat#	Dilution
Goat polyclonal primary Antibody to HNF1β	Abcam	Ab59118	1:200
Mouse monoclonal primary Antibody to HNF4α	Abcam	ab55223	1:200
Mouse monoclonal primary Antibody to FOXA2	Abcam	ab60721	1:200
Mouse monoclonal primary Antibody [BC24–3.5CH] to SOX17	Abcam	ab192453	1:200
Goat anti–Mouse IgG (H+L) Cross–Adsorbed Secondary Antibody, Alexa Fluor 488	ThermoFisher Scientific	A–11001	1:2000
Goat anti–Mouse IgG (H+L) Cross–Adsorbed Secondary Antibody, Alexa Fluor 594	ThermoFisher Scientific	A–11005	1:2000

Goat anti–Mouse IgG (H+L) Cross–Adsorbed Secondary Antibody, Alexa Fluor 647	ThermoFisher Scientific	A–21235	1:2000
Goat anti–Rabbit IgG (H+L) Highly Cross–Adsorbed Secondary Antibody, Alexa Fluor 488	ThermoFisher Scientific	A–11034	1:2000
Goat anti–Rabbit IgG (H+L) Secondary Antibody, Alexa Fluor 405	ThermoFisher Scientific	A–31556	1:2000
Goat anti–Rabbit IgG (H+L) Highly Cross–Adsorbed Secondary Antibody, Alexa Fluor 594	ThermoFisher Scientific	A–11037	1:2000

2.5.4 Microscopy

All slides were visualised on an Olympus BX51 with DP70 camera (Olympus, NSW, Australia). Live culture photos were taken on the Olympus IX81 and images analysed with Cell^M software.

2.6 *In vivo* experiments

2.6.1 Animal studies

The model chosen to assess the encapsulated differentiated pluripotent cells continued differentiation *in vivo* with the end goal of correcting induced diabetes were streptozotocin (STZ) treated female non-obese diabetic, severe combined immunodeficient (NOD/SCID) mice. These mice were maintained at the pathogen-free (SPF) Animal Facility of the Medical Foundation Building, University of Sydney, Australia. All

experimental protocols were approved by the Animal Ethics Committee of The University of Sydney, Australia (Protocol No. 2015/890).

7 to 8 week old NOD/SCID mice weighing >18g were obtained from the Animal Resource Centre (Perth, Western Australia). Five mice were housed per cage with a 12h dark/light cycle and were provided with normal rodent diet (Meat Free Mouse Feed, Specialty Foods, Perth, Australia) and water *ad libitum*. After 1-2 weeks of adaptation, mice were made diabetic while others served as non-diabetic controls.

2.6.2 Induction of diabetes

Diabetes was induced in mice by intraperitoneal injection of STZ (Sigma-Aldrich, NSW, Australia, Cat#S0130) dissolved in sterile-filtered acetate buffer (0.1M glacial acetic acid, 0.05M sodium acetate trihydrate, 0.05M anhydrous sodium acetate, 0.154M sodium chloride, adjusted to pH 4.5). This toxin is a glucose analogue and selectively destroys pancreatic β cells in mice (162).

2.6.2.1 STZ treatment

STZ is unstable in solution and quickly decomposes. To ensure a reliable dosage, the STZ solution was freshly prepared prior to injection at 5 mg/mL in acetate buffer. Mice weighing 20g or more were injected intraperitoneally at a dose of 50mg/kg for 4 consecutive days. Blood glucose levels (BGL) were measured using a portable glucometer (OneTouch Verio IQ, CA, USA) by pricking the tail vein with a 25G needle (BD, NSW, Australia, Cat#305125). BGL was checked 3 days post final STZ dose and every 2nd day following. If mice were not diabetic 7 days after the 4th injection an additional dose of 50 mg/kg was administered. Mice were considered diabetic when three separate BGL readings were > 15mmol/L on separate days. Once mice were diabetic, no more than 3 mice were housed per cage. This was done to reduce risk of dehydration from emptying of water bottles (as a result of polydipsia) and to ensure the cages remained clean for 2-3 days before the bedding was changed (due to polyuria).

2.6.3 Intraperitoneal transplantation

Once the mice were confirmed diabetic, encapsulated End1 cells, which had reached day 9 in their *in vitro* differentiation protocol, were infused into the intraperitoneal cavity of the mice. All surgical procedures

were performed within a class II biosafety cabinet that was UV sterilised prior to use. Sterile drapes, surgical gloves and instruments were used during all steps of the surgical procedure. Prior to surgery, the mice were given a subcutaneous saline solution injection containing Buprenorphine (0.1mg/kg) (Indivior, Berkshire, UK) and meloxicam (Troy Laboratories, NSW, Australia) 0.5mg/kg to reduce pain and inflammation post-operatively. This was done so the drugs would be in effect once the mouse regains consciousness as per animal ethics. The mice were anaesthetized with 5% isoflurane given via a nose cone (Abbott Laboratories, IL, USA) which was reduced to 2% once they had lost consciousness. They were placed with ventral side up on a warm surgical mat and the abdominal area was shaved and cleaned with chlorhexidine solution 0.5% (Baxter Healthcare, Sydney, Australia, AHF7963). A small incision was made in the skin and a 14G intravenous catheter (BD, NSW, Australia, Cat#381709) was inserted into the intraperitoneal cavity. Alginate microcapsules suspended in 0.9% sterile NaCl were then infused through this catheter into the peritoneal cavity. Each mouse was given 2 x 10^6 encapsulated cells in ~10,000 capsules. Once the microcapsules were infused, the catheter was gently removed and the incision site closed by suturing the peritoneum. The skin was then closed using 7mm staples (CellPoint Scientific, MD, USA Cat#203–1000). Antiseptic Betadine ointment was applied to the surgery site over the staples, isoflurane administration ceased, and the mouse placed into a clean recovery cage positioned over a warm heat mat. Mice were monitored until they were mobile and alert. Food was provided on the cage floor for easy access. Buprenorphine/meloxicam analgesic combination was given once each day for the following 2 days.

2.6.4 Transplantation under the kidney capsule

Unencapsulated pancreatic progenitors differentiated from hESC on Geltrex® were transplanted under the renal capsule of STZ-treated mice. The mice were given analgesia and anaesthetized as per the intraperitoneal surgery and then positioned in the right lateral recumbent position. The operation site was shaved and sterilised with chlorhexidine solution. An incision was made in the flank of the animal through the skin and then another smaller incision through the peritoneum. The kidney was then massaged out of the incision with the aid of a blunt set of forceps. The exposed kidney was kept moist with sterile 0.9% saline solution. An incision was carefully made across the top surface of the kidney capsule with a scalpel

blade. Using a straight and a curved forceps, a pocket was made by gently separating the renal capsule and loosening it from the body of the kidney. The $2x10^6$ cells in single-cell suspension were then made into a clot by mixing them with 10 to 20µl of blood taken from the tail at the beginning of the surgery. This enabled the cells to be easily handled and placed under the kidney capsule. The clot was then massaged further under the kidney capsule using a set of blunt forceps. The kidney was then returned into the abdominal cavity and the peritoneum stitched closed. Similar to intraperitoneal surgery, the skin was closed using staples and the mouse placed into a recovery cage. Postoperative care was the same as with intraperitoneal surgery.

2.6.5 Monitoring post-operatively

Regular measurements of the body weight and blood glucose concentration of diabetic mice were made post-operatively, weights second daily and glucose three times a week. If bodyweight dropped by more than 10% compared to the pre-STZ weight and the BGL was > 15mM, mice were injected with 0.5U Levemir Insulin (Novo Nordisk, NJ, America) administered subcutaneously, until further weight loss ceased. BGL was not measured within 24h of an insulin dose.

2.6.6 Blood collection for C–peptide measurement

2.6.6.1 Facial bleeding

To collect a sufficient volume of blood to be able to assay for human C-peptide, a facial bleed was conducted at monthly intervals post-transplantation. Mice were restrained by the scruff of their back and neck using the one-handed technique. Using a 5mm lancet (Braintree Scientific, Braintree, MA, Cat#GR 5MM) the superficial temporal vein was punctured. A blood collection tube with 10µl EDTA was then quickly placed under the site and up to 150µl blood was collected per mouse. Following the collection of the blood, cotton gauze was firmly applied to the cheek for 15s or until bleeding ceased. Animals were injected with 500µl warm saline solution into their intraperitoneal cavity to replace the fluid volume lost during the cheek bleed. The mice were then returned to the cage and monitored for the next 10min for

signs of weakness. Whole blood was centrifuged at 2000*g* for 5min at 4°C and plasma collected and stored at –80˚C until assayed.

2.6.6.2 Terminal cardiac puncture

At the completion of experiments in the mice, a maximal amount of blood was collected via cardiac puncture for measurement of C-peptide. Mice were anaesthetised with isoflurane as previously described (sections 2.7.3). Mice were then placed on their back in a supine position and a 23G needle attached to a 1mL syringe was inserted into the chest cavity to puncture the heart while drawing the syringe to collect blood. The specimen was added to a 1.5mL tube containing 10µl 0.5M EDTA, and plasma collected and stored at –80C until analysed. The mice were then euthanized by cervical dislocation before collecting grafts and tissues.

2.6.7 Collection of grafts and tissues

At the completion of the animal experiments, grafts implanted beneath the renal capsule were collected for analysis. When the graft could not be readily identified macroscopically, the entire kidney was removed. In mice infused with microcapsules containing cells, the microcapsules were retrieved from the intraperitoneal cavity immediately post euthanasia. PBS was squirted into the peritoneal cavity to help dislodge them. They were then placed into a 15mL centrifuge tube, and allowed to settle. Capsules containing cells were set aside for immunohistochemistry, gene expression analysis, cell viability and stimulated insulin release. Samples for immunohistochemistry were immersed in OCT and snap-frozen in liquid nitrogen before storing at –80°C. Samples for RNA analysis were immersed in TRIzol® and snap-frozen. Samples for cell viability and stimulated insulin release were cultured overnight in High Glucose DMEM + 10% FBS.

2.7 Statistical analyses

All values are expressed as mean ± SEM, and statistical analyses were performed using GraphPad Prism Software Inc., CA, Version 7.02. A two-sample *t*-test was used to compare data between two groups. A one-way analysis of variance (ANOVA) with Tukey's *post–hoc* analysis was used to compare data from more

than two groups. The number of animals or measurements in each group is indicated in the figure legends. The significance level was set *at P* <0.05 for all comparisons.

Table 2.5: Complete list of reagents

Reagent	Company	Catalogue number
0.22µm filter	Sigma-Aldrich	Z359904
14G intravenous catheter	BD	381709
14G intravenous catheter	BD	381709
16G needle	BD	305197
25G needle	BD	305125
2mL cryovial	Sigma-Aldrich	CLS430659
40µm cell strainer	Sigma-Aldrich	CLS431750
5mm lancet	Braintree Scientific	GR 5MM
5mm lancet	Braintree Scientific	GR 5MM
6-Carboxyfluorescein Diacetate (6-CFDA)	Sigma-Aldrich	C5041
Activin A	R&D Systems	338–AC–050
B27	Life Technologies	17504–044
bFGF	R&D Systems	233–FB
chlorhexidine solution 0.5%	Baxter Healthcare	AHF7963
chlorhexidine solution 0.5%	Baxter Healthcare	AHF7963

Coverslips	Chase Scientific Glass	22x40mm No.1 thickness
C-peptide ELISA kit	Mercodia	10–1141–01
cryostat	Leica Microsystems	1510S
Cyclopamine-KAAD	Merck Millipore	239804
dispase	Stemcell Technologies	7923
DMEM	Life Technologies	11965092
FBS	AusGeneX	FBS500–S
Geltrex®	Life Technologies	A1569601
High Capacity cDNA Kit	Applied Biosystems	4368814
ITS	Life Technologies	41400–045
KGF	R&D Systems	251–KG–050
Knock Out DMEM	Life Technologies	[10829–018]
knockout serum replacement	Life Technologies	10829–018
microscope slides	Lomb Scientific	4951PLUS4
mitomycin C	Sigma-Aldrich	M2487
Mr. Frosty™ Freezing Container	Life Technologies	5100-000
NEAA	Life Technologies	111040–50
Noggin	R&D Systems	6057–NG–025

Optimal Cutting Temperature (OCT) solution	Sakura	4583
PBS tablets	AMRESO	E404
pMXs-c-Myc plasmid	Addgene	13375
pMXs-hOCT3/4 plasmid	Addgene	17217
pMXs-hSOX2 plasmid	Addgene	17218
pMXs-Klf4 plasmid	Addgene	13370
porcine gelatin	Sigma-Aldrich	G9391
ProLong® Gold Antifade	Life Technologies	P10144
propidium iodide (PI)	Sigma-Aldrich	4170
retinoic acid	Sigma-Aldrich	R2625
RPMI medium	Life Technologies	22400–105
STZ	Sigma-Aldrich	S0130
T150 flasks	Sigma-Aldrich	CLS430825
TRIzol® reagent	Life Technologies	33251
trypan blue solution	GE Healthcare	SV30084.01
TrypLE Express	(Life Technologies	12604013
trypsin	Life Technologies	25200072
ultra–pure alginate powder	Pronova Biomedical	UP MVG BP1105 06

Wnt3A	R&D Systems	5036–WN–010
Y27632	Sigma-Aldrich	Y0503

Chapter 3

Differentiation of human embryonic stem cells to primitive foregut while encapsulated in alginate microcapsules

3.1 Introduction

The usefulness of human islet transplantation is limited by two major factors: Availability of donor tissue and the need for immunosuppression post-transplantation. The shortage of donor tissue might be addressed with the differentiation of human embryonic stem cells (hESC) into glucose-sensitive insulin-secreting cells. Alginate encapsulation can provide immune isolation of transplanted cells from the host, and therefore may relieve the need for immunosuppression. Current protocols (21, 64, 163) focus on differentiating hESC on a 2D matrix in culture dishes and then encapsulating post differentiation. While these cells secrete insulin in response to glucose and correct hyperglycaemia in diabetic mice, improving differentiation and production techniques are needed. Currently, the cells are exposed to mechanical stresses when scaling production using bioreactors in addition to the differentiation process is long and costly.

Undertaking the differentiation process while encapsulated in alginate provides a solution for the mechanical stress issue. Through the use of alginate, it is possible to differentiate in a 3-dimensional differentiation matrix which provides protection both from the immune system once transplanted as well as physical protection to shear forces in a bioreactor during the differentiation process. It is these advantages that may improve the differentiation process if it was undertaken while the cells are encapsulated in alginate.

hESC transition through a number of progenitor states during differentiation to beta-cells. These stages can be identified by the gene transcript expression profile. Each stage is initiated by changing signalling molecules in the culture media. Our differentiation process moves the cells through four distinct stages (Chapter 1, Table 1.1). The cells start as undifferentiated pluripotent stem cells. This can be verified by the expression of *OCT4* and *NANOG.* These genes are members of the core pluripotency network and the most widely used markers for pluripotency. The cells are then differentiated into the definitive endoderm primary germ layer and so express *FOXA2* and *SOX17*. The next stage is defined as a primitive gut tube in

which the cells express *HNF1β* and *HNF4α*. The final stage examined in this protocol is *PDX1* positive pancreatic endoderm.

3.1.1 Hypothesis

hESC encapsulated in alginate will differentiate to PDX1 expressing pancreatic precursors.

3.1.2 Aim

Investigate the stages of differentiation of hESC from pluripotent stem cells to pancreatic progenitors when grown in 2D-Geltrex® or encapsulated in alginate. The transitions through the developmental stages will be assessed using qPCR and immunohistochemistry.

3.2 Materials and methods

3.2.1 Cell culture

The hESC were cultured and purified as per Sections 2.2.2 and 2.2.4. They were then encapsulated in alginate at $1x10^6$ cells per mL of alginate as per Section 2.3.2. Cells that were plated onto Geltrex®-coated plates were seeded at a density of 30,000 cells/cm^2 in 6 well plates.

3.2.2 Microencapsulation

The hESC were passaged as per Section 2.2.4 and suspended in highly purified 2.2% alginate solution at $1x10^6$ cells/mL. The microcapsule formation was carried out using an air-driven droplet generator (Torsten Steinau Verfahrenstechnik, Berlin, Germany) as described previously (Section 2.3.2). The microencapsulated hESC were then cultured for a further 3 days in ROCK inhibitor supplemented KOSR (Section 2.3.3).

3.2.3 Cell viability

Viability and death of encapsulated cells were assessed using 6-CFDA and propidium iodide, respectively, as described previously (Section 2.3.4). The percentage of green cells (live) to red cells (dead) was measured to evaluate the viability (live/total x 100 = % viability). Co-stained cells were counted as live as 6-CFDA requires active esterase enzyme activity to be cleaved to its amine-reactive form. Samples were analysed under Olympus IX81 (Olympus, NSW, Australia) microscope using Cell^M software.

3.2.4 RNA Isolation, cDNA Generation and qPCR

Total RNA from cells was isolated using the organic extraction method of phenol-based TRIzol® reagent described in Section 2.3.7. The RNA was then reverse transcribed and transcripts measured using fluorescent probes on ViiA7 (Life Technologies) as described in Section 2.3.8. TaqMan® probes are listed in Table 3.1 of Section 2.3.8. Data were plotted normalised to the expression of the reference gene 18S and expressed as “Fold over detectable”. This represents a relative measure of the number of copies present in the sample. This methodology has previously been published by collaborating laboratories(148).

3.2.5 Immunohistochemistry

The hESC grown on Geltrex® were fixed with 4% paraformaldehyde (PFA) solution for 20 min at room temperature. Following fixation, samples were washed with TBST for 10 min at room temperature. The samples were then blocked for 1 h at room temperature with 2% BSA in PBST on a rocker. After blocking, the samples were incubated overnight at 4˚C with 1˚ antibody diluted as per Table 3.1 in 2% BSA in PBST. The following day, the samples were washed three times for 5 min with PBST at room temperature. Secondary antibodies diluted in 2% BSA in PBST were then added as per Table 3.1 and incubated for 2 h at room temperature on the rocker. The sample was then washed with 2% BSA in PBST and ProLong® Gold Antifade was added before visualisation using an EVOS Microscope (Life Technologies).

Table 3.1: Table depicts the catalogue numbers and dilution factor of the antibodies used in immune-staining of cells at each differentiation stage.

Antigen	**Primary Antibody (source/catalogue no.)**	**Dilution**	**Secondary Antibodies (Source/catalogue no.) All diluted 1:2000**
Human FOXA2	Mouse monoclonal (Abcam/ab60721)	1:200	anti-Mouse Goat IgG AlexaFluor488, (ThermoFisher A11001)
Human SOX17	Mouse monoclonal (Abcam/ab192453)	1:200	anti-Mouse IgG AlexaFluor488, (ThermoFisher A11001)
Human HNF1β	Goat polyclonal (Abcam/ab59118)	1:200	Anti-Goat IgG AlexaFluor488 (ThermoFisher A11055)
Human HNF4α	Mouse monoclonal (Abcam/ab55223)	1:200	anti-Mouse IgG AlexaFluor488, (ThermoFisher A11001)

3.2.6 Microscopy

Images of viable and non-viable cells were taken on the Olympus IX81 with UPLSAPO 10x and 20x objective (Olympus, NSW, Australia). Immunohistochemistry images were taken on the Evos® plate microscope using a 40x objective. Images were then stitched together using Evos® on-board software to give a complete picture of the stained well.

3.2.7 Statistical Analysis

Statistical analyses were performed using GraphPad Prism, Version 7.02. Student's *t*-test was used to analyse differences between conditions in the viability assessment. Two-way ANOVA with Tukey's *post-hoc* analysis was used to compare groups between all conditions in the qPCR analysis with data being considered parametric.

3.3 Results

3.3.1 Viability of Encapsulated Cells

The hESC were cultured for three days in KOSR + ROCK inhibitor post-encapsulation. As encapsulation exposes the cells to $BaCl_2$, which is toxic to cells, cell viability was measured prior to, as well as at the completion of, differentiation. Fig. 3.1A shows a bright-field image of hESC within microcapsules that are regular round spheres with a diameter of 440 ± 140 µm. Viable cells stain with the 6-CFDA (green). Fig. 3.1B. Counterstained with PI to determine the proportion of dead cells as shown in Fig. 3.1C. The merge of these two panels is shown in Fig. 3.11D. There is some co-staining of cells with both PI and 6-CFDA; these were considered to be alive due to the mechanism through which 6-CFDA produces fluorescence described in Section 2.3.4. The viability of the hESC after encapsulation in alginate on day 0 and day 9 of differentiation was quantified, there was no statistical difference between days (Student's t-test $P>0.05$).

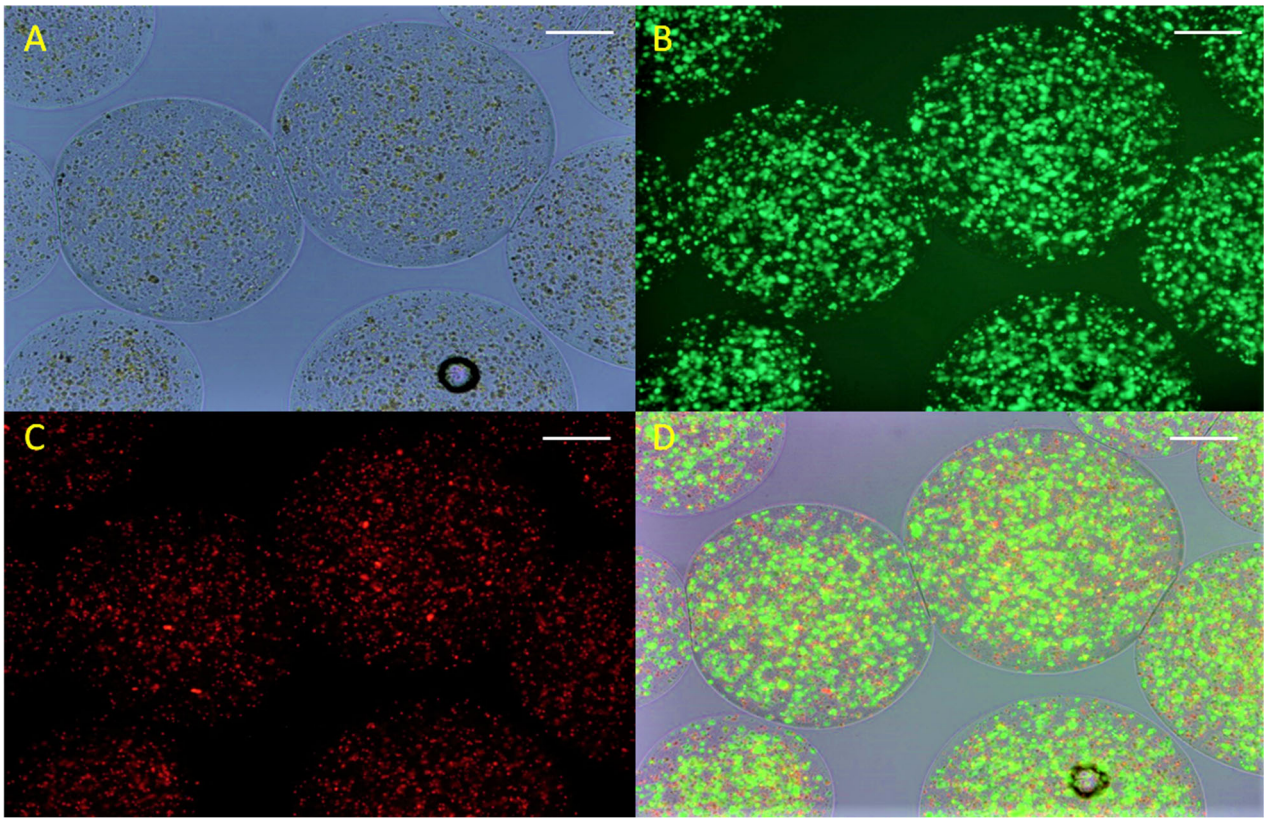

Figure 3.1: Effect of alginate encapsulation on the viability of hESC three days post-encapsulation (Day 0 of differentiation). hESC were encapsulated in 2.2% alginate and labelled with 6-CFDA and PI to determine the proportion of live and dead cells. A) Bright-field image of the alginate capsules showing the total number of hESC. B) Fluorescence observed under the green filter of encapsulated cells stained with 6-CFDA. C) Red fluorescence of PI staining indicating cells which have membrane permeability. D) Merged image of panels A to C showing the red/green staining exclusively within the capsule. Scale bar 100 µm. brighter/more aggregated 6-CFDA

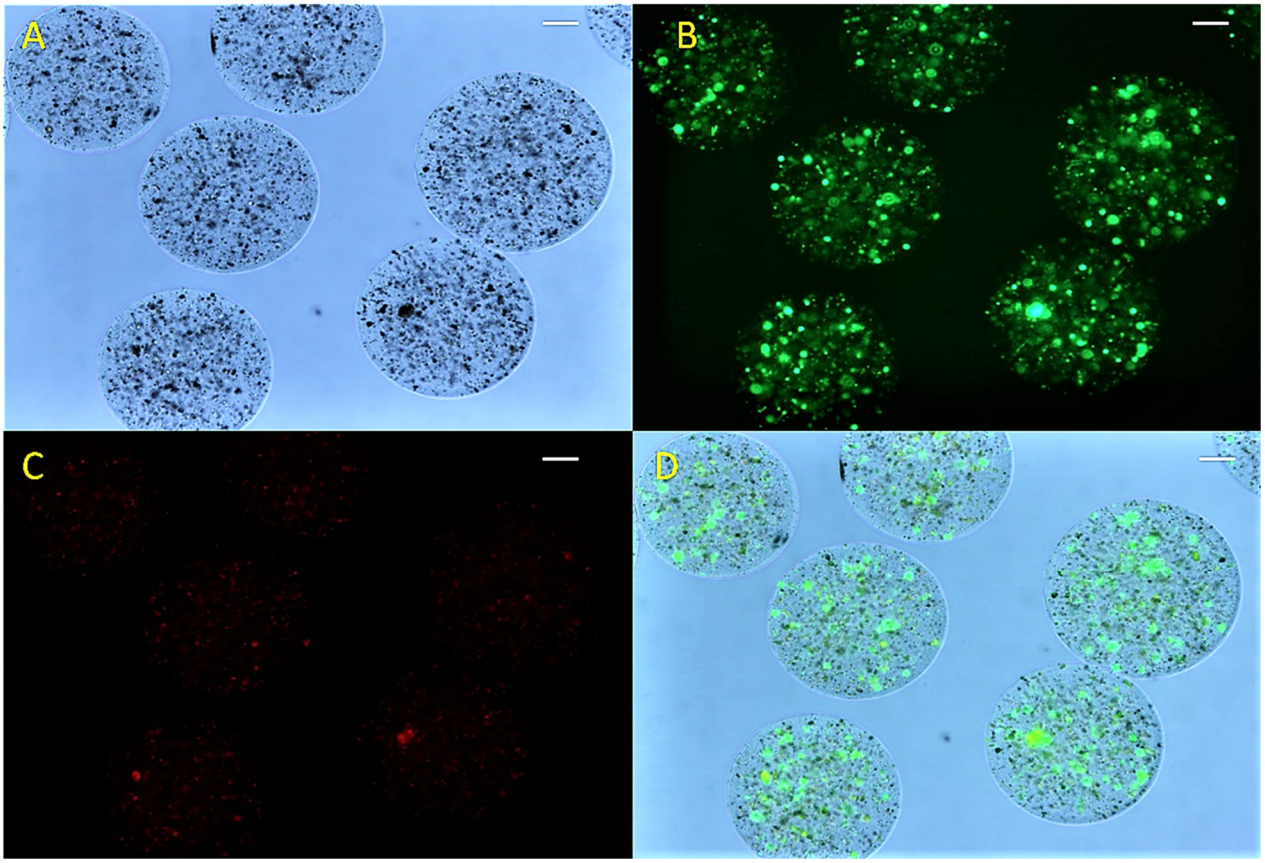

Figure 3.2: Viability of encapsulated hESC at day 9 of differentiation. hESC were encapsulated in 2.2% alginate and differentiated before being labelled with 6-CFDA and PI to assess viability. A) Bright-field image of the alginate capsules showing the total number of hESC. B) Fluorescence observed under the green filter of encapsulated cells stained with 6-CFDA. C) Red fluorescence of PI staining indicating cells which have membrane permeability. D) Merged image of panels A to C showing the red/green staining exclusively within the capsule. White scale bar 100 µm.

3.4.2 Transcript expression of key differentiation markers during differentiation while encapsulated in alginate.

3.4.2.1 Pluripotency markers *OCT4* and *NANOG* expression are downregulated during differentiation while encapsulated in alginate.

To investigate the difference in differentiation outcomes between hESC differentiated while encapsulated in alginate vs on Geltrex®, samples were taken and probed for known gene transcript markers. Before the differentiation protocol began (Day 0) expression of *OCT4* was high at $264x10^3$ and $131x10^3$ fold-over detectable for the Geltrex® and encapsulated groups respectively (Fig. 3.4) with no statistical difference between the groups. This expression then markedly decreased by $26x10^3$ to between 100 and 200 fold over detectable for the Geltrex® group on days 3 to 9 and a drop of $13x10^3$ to between 200 and 1000 fold over detectable for the encapsulated group. While *OCT4* continued to be expressed, expression levels between experimental runs were variable at day 6 and day 9 time-points ranging from 1 to 4444 fold over the detectable limit (Fig. 3.4).

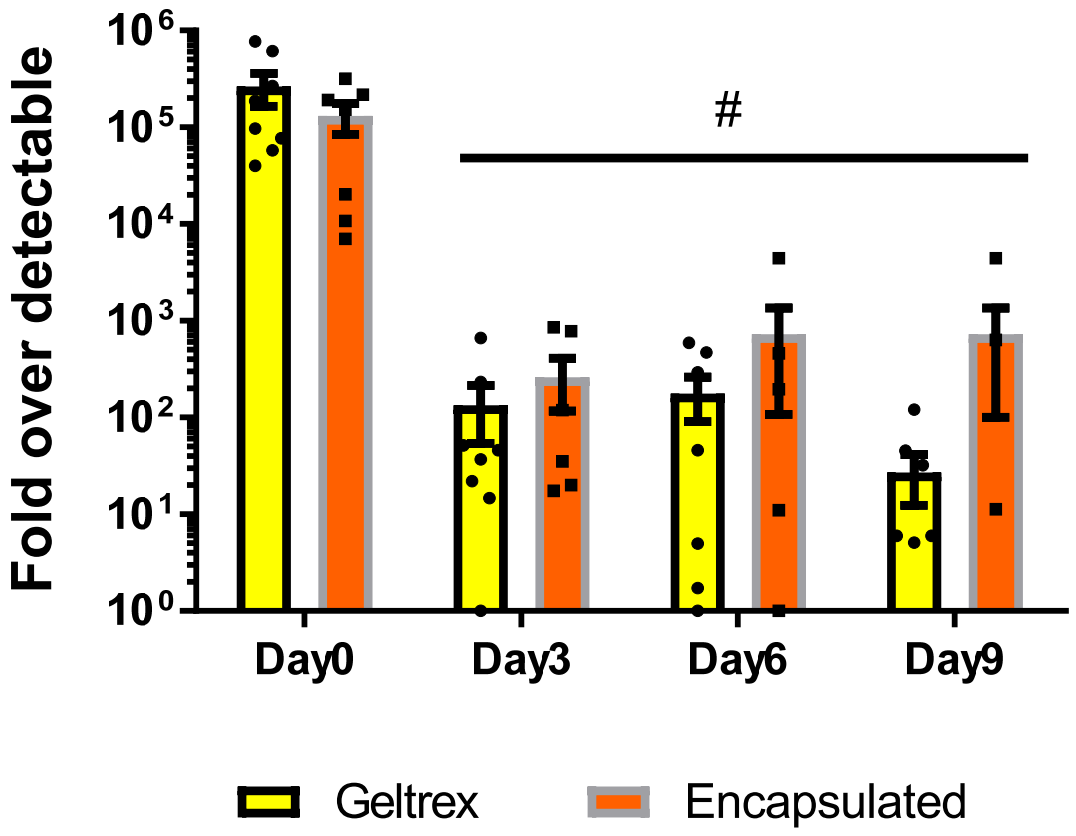

Figure 3.3: Relative expression of *OCT4* transcripts during the differentiation process from pluripotent hESC to pancreatic progenitors. Data are mean +/- SEM, n = 6-8/group, presented as fold over the detectable limit of the assay. Individual experiments are plotted as points with 0 values unable to be plotted on logarithmic graph. # Groups are all significantly different to Day 0 Geltrex® $P<0.001$, using a two-way ANOVA followed by Tukey's *post-hoc* test.

As expected the pluripotency marker *NANOG* followed a similar expression pattern to *OCT4.* The pre-differentiation samples returned values of $420x10^3$ and $93x10^3$ fold over detectable for Geltrex® and encapsulated samples respectively (Fig. 5). Once the differentiation was initiated the *NANOG* transcript levels dropped to near $1.5x10^3$ for both Geltrex® and encapsulated. This drop was significant and while Geltrex® samples continued to express transcript at around 400 fold over detectable. The encapsulated samples expression levels continued to drop to 17 and near undetectable on days 6 and 9 respectively. Similarly, to OCT4 expression the samples were variable for day 3, 6, and 9 samples, ranging from 2800 to undetectable in Geltrex® and 8500 to undetectable in encapsulated.

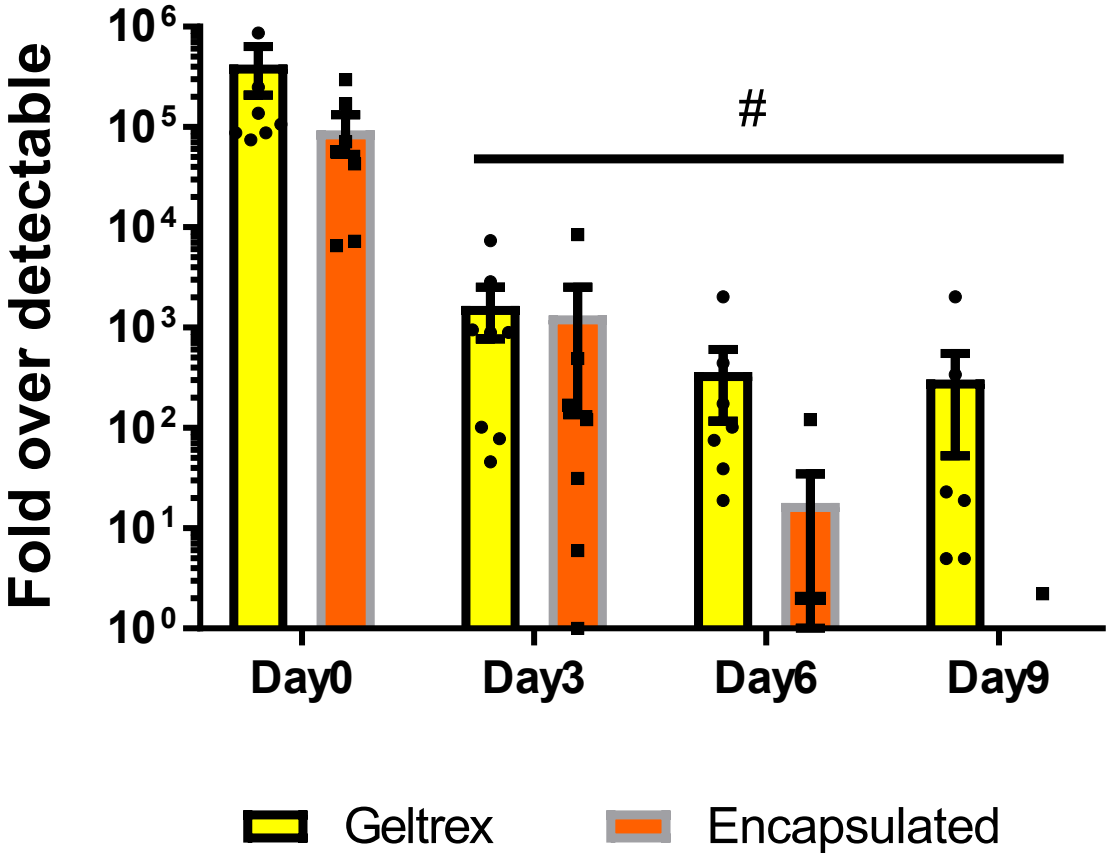

Figure 3.4: Relative expression of *NANOG* transcripts during the differentiation process from pluripotent hESC to pancreatic progenitors. Data are mean +/- SEM, n = 6-8/group, presented as fold over the detectable limit of the assay. Individual experiments are plotted as points with 0 values unable to be plotted on a logarithmic graph. *P*<0.001 Statistical difference tested with a two-way ANOVA followed by Tukey's *post-hoc* test.

3.4.2.2 Definitive Endoderm markers *FOXA2* and *SOX17* expression peaks at day 3 during differentiation.

The expression of definitive endoderm marker *SOX17* initially appears at day 0. However, this is only detectable in 3 of the 8 differentiation experiments (Fig. 6). At day 3 high levels of *SOX17* transcript are detectable with a mean expression of $235x10^3$ fold over detectable in the Geltrex® and $181x10^3$ in the encapsulated group. The expression pattern of SOX17 in the Geltrex® group then decreased over the next two time points at 1858 to 586 for day 6 and 9 respectively. The inverse occurred in the encapsulated samples moving from a mean of 3608 on day 6 to 5654 on day 9. However, due to the variability between experiments, none of these changes was significantly different.

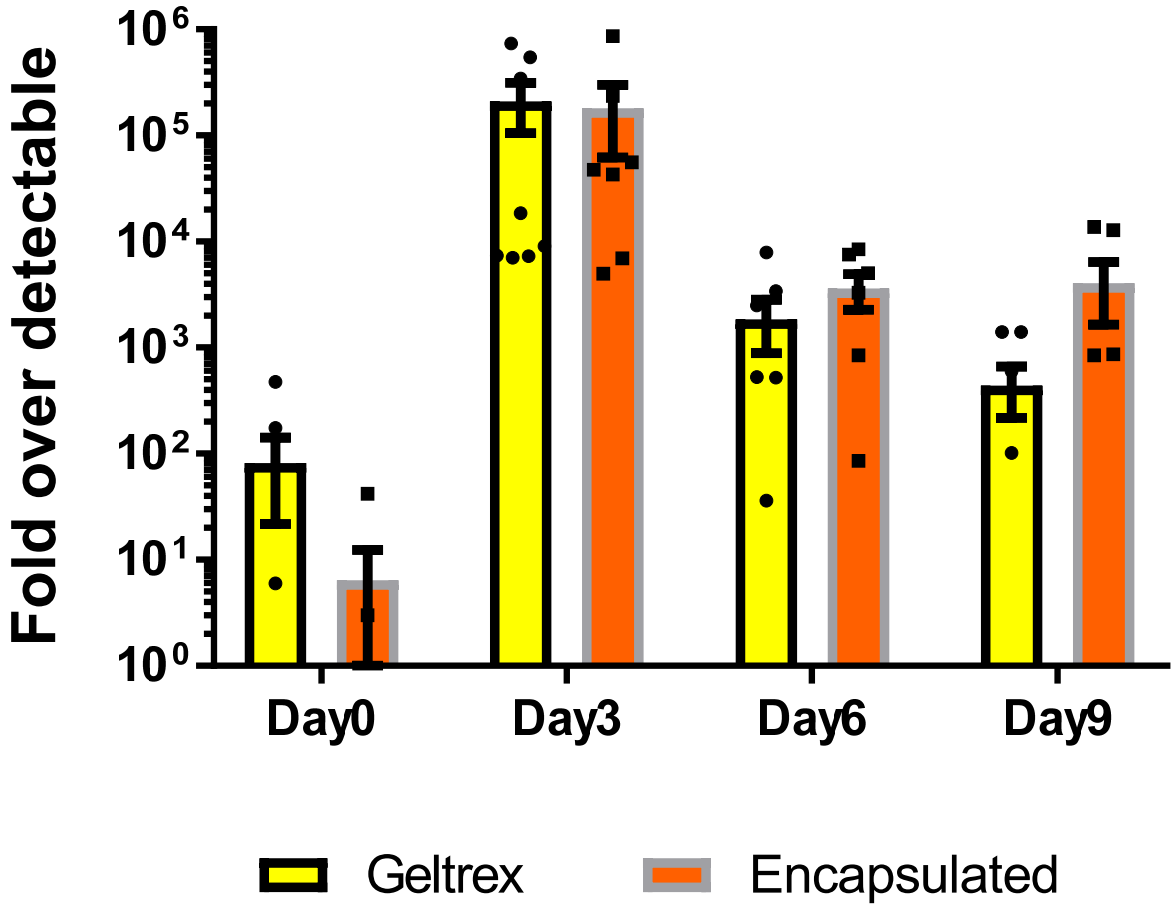

Figure 3.5: SOX17 transcript expression expressed as fold over detectable. Data are mean +/- SEM, n = 6-8/group, presented as fold over the detectable limit of the assay. Individual experiments are plotted as points with 0 values unable to be plotted on the logarithmic graph. Statistical difference tested with a two-way ANOVA followed by Tukey's *post-hoc* test.

Definitive endoderm marker *FOXA2* is first detected at day 3 contrary to the expression of *SOX17* at day0, but expressing a similar expression pattern to *SOX17* initial at $105x10^3$ and $92x10^3$ in Geltrex® and encapsulated groups respectively. The change over the following time points is not statistically significant but represents a ~-20 mean relative fold change in both groups of the *FOXA2* data. The lack of statistical significance is due to the large variation between differentiation experiments ranging from undetectable to 5000 fold over detectable (Fig. 3.7).

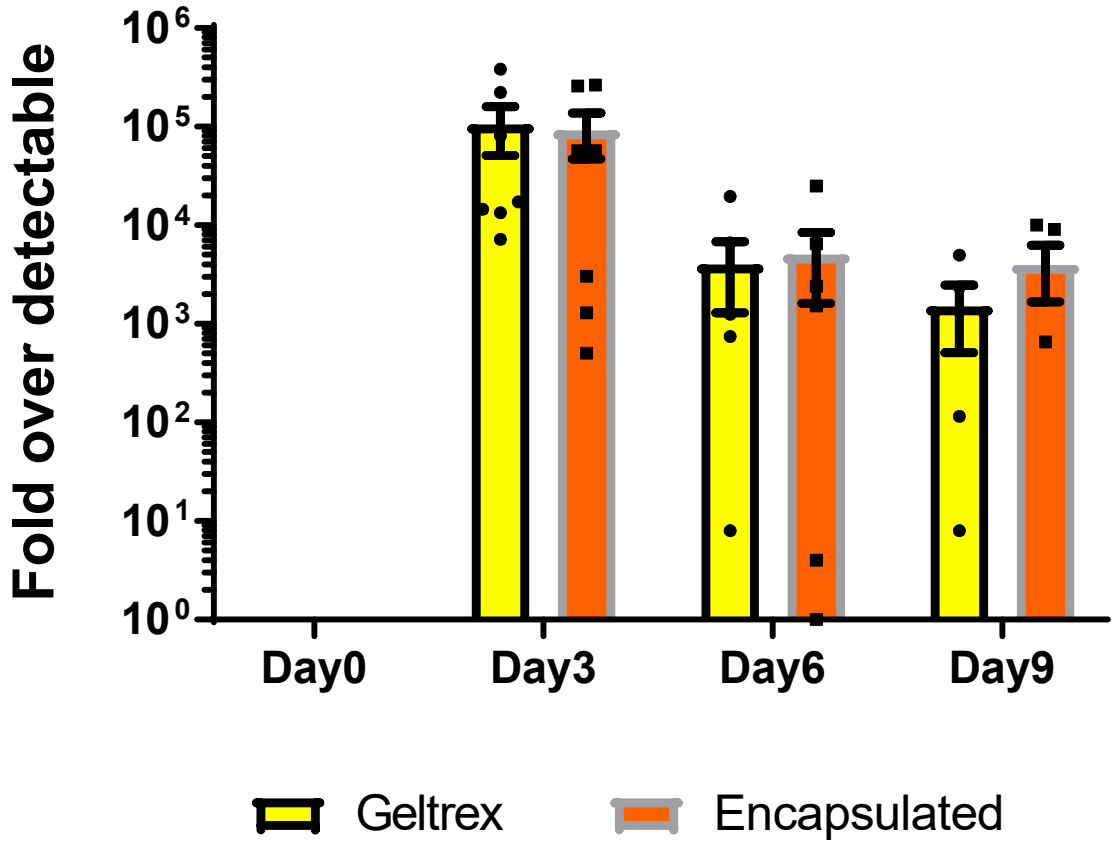

Figure 3.6: FXOA2 transcript expression expressed as fold over detectable. Data are mean +/- SEM, n = 6-8/group, presented as fold over the detectable limit of the assay. Individual experiments are plotted as points with 0 values unable to be plotted on the logarithmic graph. Statistical difference tested with a two-way ANOVA followed by Tukey's *post-hoc* test.

3.4.2.3 Primitive foregut/pancreatic endoderm markers *HNF4α*, *HNF1β* and *PDX1* expression peaks at day 9 of differentiation.

At day 3 the primitive gut tube markers *HNF4α* and *HNF1β* were first detectable in 4 of the 8 experimental runs. Expression of *HNF4α* increased on day 6 to $103x10^3$-fold over the detectable limit in the Geltrex® group and $152x10^3$ in the encapsulated group. This expression was maintained through to the 9th day with no statistical difference between the groups. There is a great deal of variation of transcript expression among differentiation experiments; this is evident especially in the day 6 and 9 samples (Fig. 3.8).

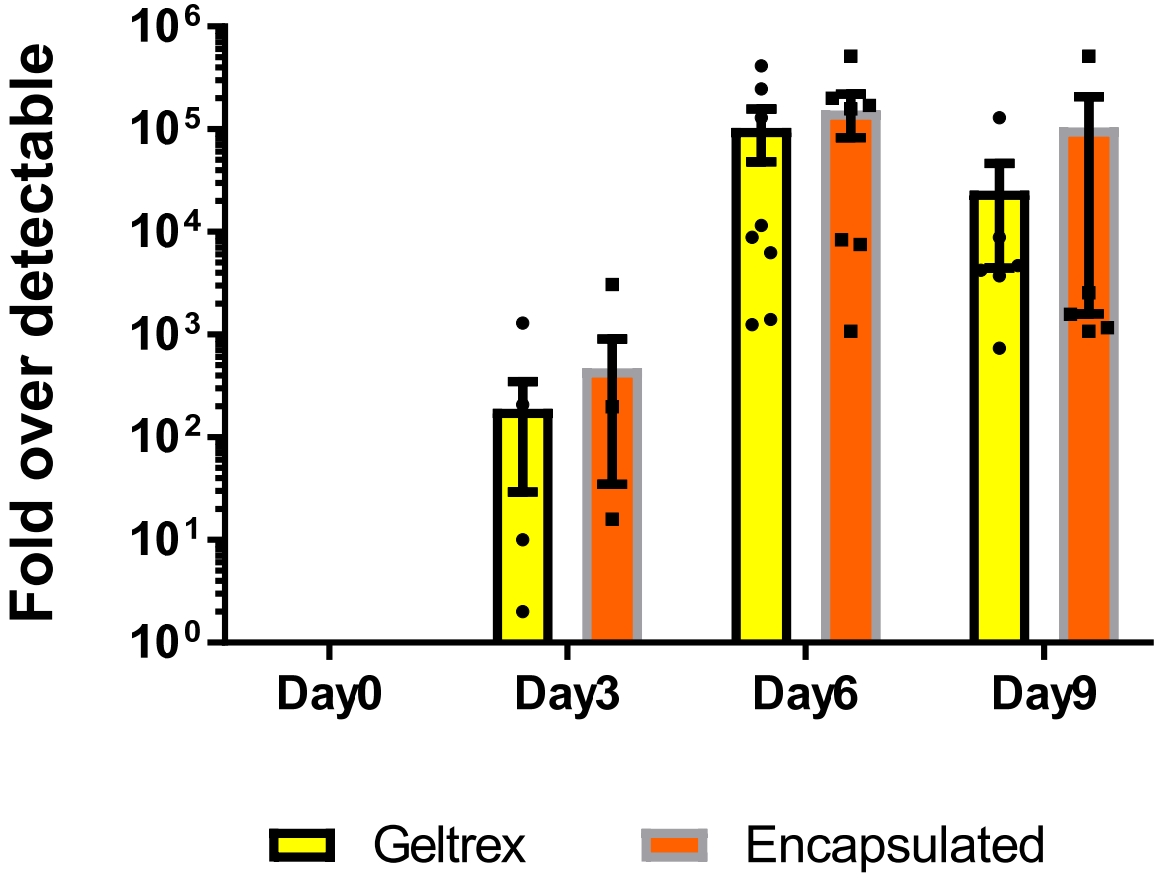

Figure 3.7: *HNF4α* transcript expression expressed as fold over detectable. Data are mean +/- SEM, n = 6-8/group, presented as fold over the detectable limit of the assay. Individual experiments are plotted as points with 0 values unable to be plotted on the logarithmic graph. Statistical difference tested with a two-way ANOVA followed by Tukey's *post-hoc* test.

The *HNF1β* transcript expression pattern was similar to *HNF4α*, first appearing at day 3 with low levels of expression with 55 and 75 fold over detectable for the Geltrex® and encapsulated groups respectively (Fig. 3.9). This mean expression then increased to $60x10^3$ and $103x10^3$ on day 6. Continued expression through the day 9 samples were also found with no statistical difference between groups.

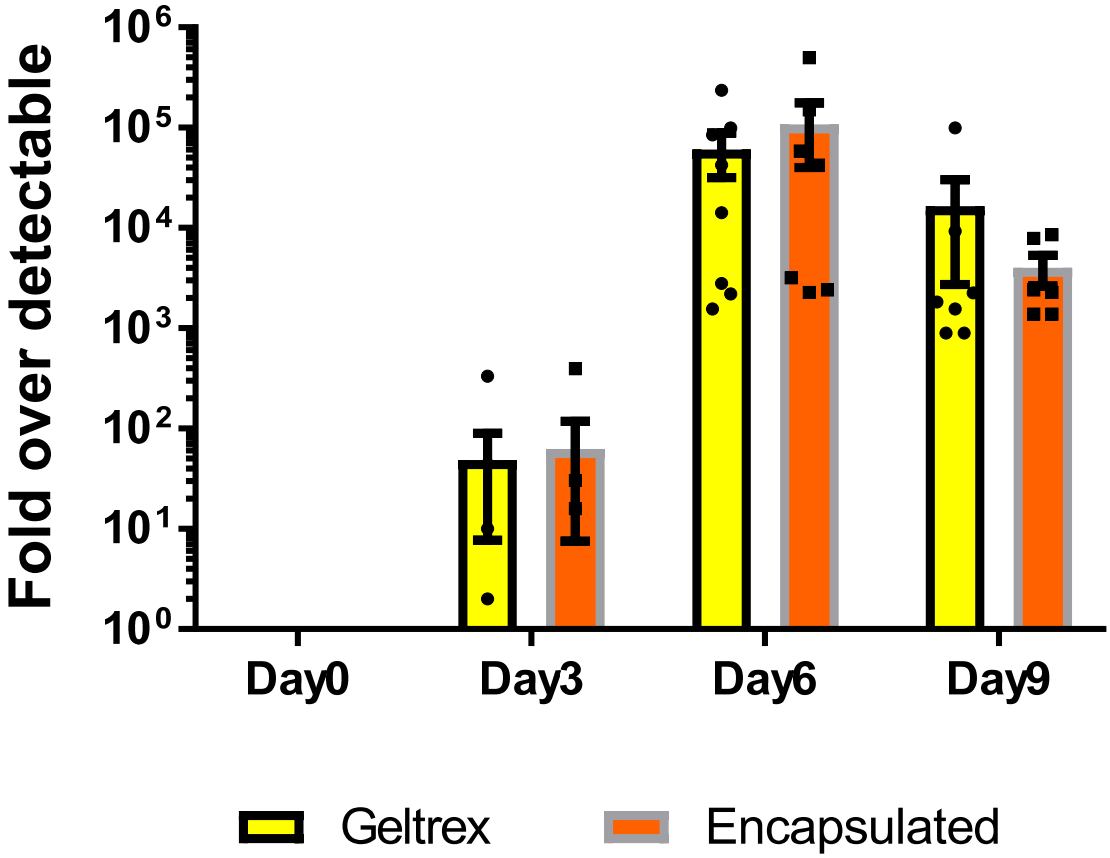

Figure 3.8: *HNF1β* transcript expression expressed as fold over detectable. Data are mean +/- SEM, n = 6-8/group, presented as fold over the detectable limit of the assay. Individual experiments are plotted as points with 0 values unable to be plotted on the logarithmic graph. Statistical difference tested with a two-way ANOVA followed by Tukey's *post-hoc* test.

The differentiation process culminates in *PDX1* expression on day 9 (Fig. 10). PDX1 expression was consistent, being detectable in all five differentiation experiments taken to day 9. There was no statistically significant difference in *PDX1* expression between the differentiation protocols undertaken on Geltrex® or

while encapsulated in alginate. The genes *NGN3* and *NKX6-1* were also probed however were undetectable at any time point in these experiments (data not shown).

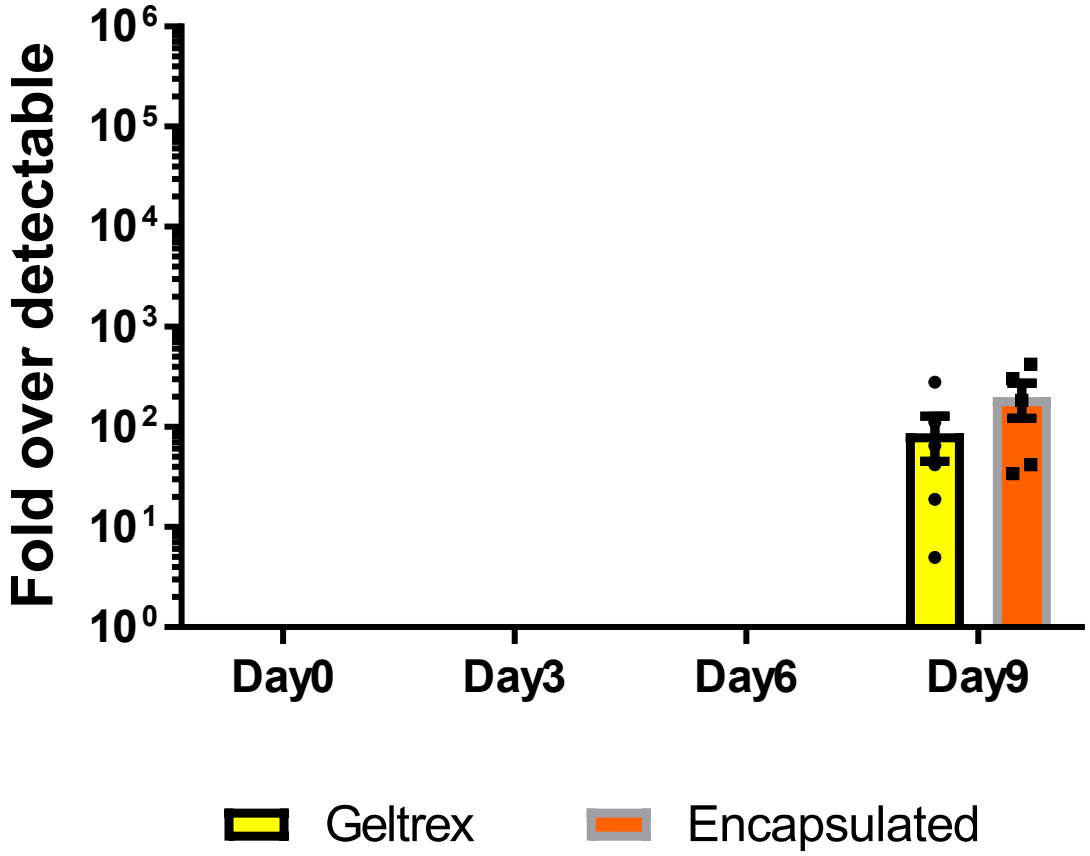

Figure 3.9: *PDX1* transcript expression expressed as fold over detectable. Data are mean +/- SEM, n = 6-8/group, presented as fold over the detectable limit of the assay. Individual experiments are plotted as points with 0 values unable to be plotted on the logarithmic graph. Statistical difference tested with a two-way ANOVA followed by Tukey's *post-hoc* test.

3.4.3 Confirmation of key protein expression at peak transcript expression

3.4.3.1 FOXA2 and SOX17 protein expression on day 3.

To determine if the transcript expression shown in Section 3.4.2 was reflective of the protein expression, Geltrex® samples were fixed and stained for genes at their peak expression time points. Attempts were made to stain the encapsulated differentiated cells but due to alginate preventing the antibodies reaching the cells and difficulty sectioning the cells and staining no useful images were generated (164). In the Geltrex® differentiation samples definitive endoderm markers SOX17 and FOXA2 were stained at day 3 and were positive for protein expression (Fig. 3.11 & 3.13, and 3.12 & 3.14 respectively). As shown in Fig. 3.11, SOX17 expression was not as ubiquitous as FOXA2 with subsets of cells clearly not expressing the protein (red circle). These cells tend to be close to the centre of the Geltrex® colonies as seen in Fig. 3.12.

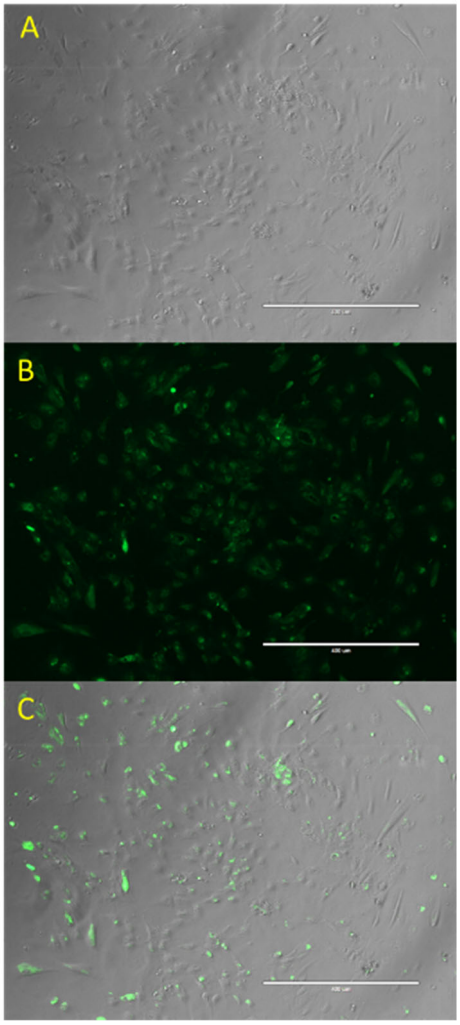

Figure 3.10: FOXA2 protein localisation of hESC grown on Geltrex® at day 3 of the differentiation process. A) Bright field showing typical morphology of hESC at day 3 B) Green fluorescence indicates cells stained for FOXA2 protein C) The bright florescent fields merged. White bar = 400 µm

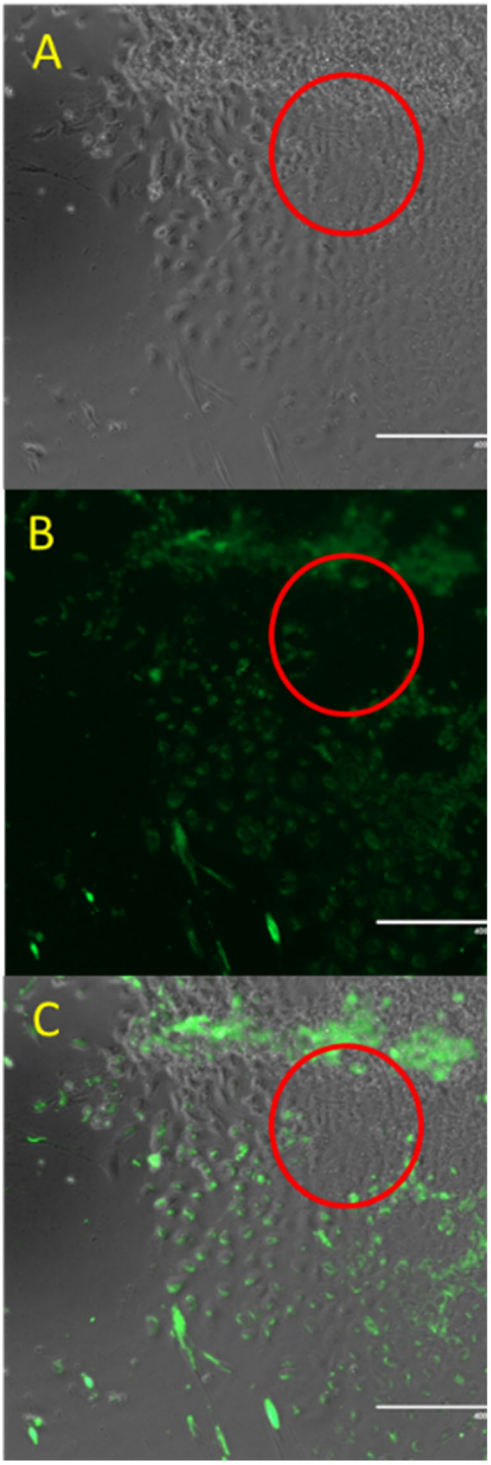

Figure 3.11: SOX17 protein localisation of hESC grown on Geltrex® at day 3 of the differentiation process, red circle highlights the region of live cells which are not positive for SOX17 staining A) Bright field showing typical morphology of hESC at day 3 B) Green fluorescence shown indicates cells stained for SOX17 protein C) The bright and florescent fields merged. White bar = 200 µm

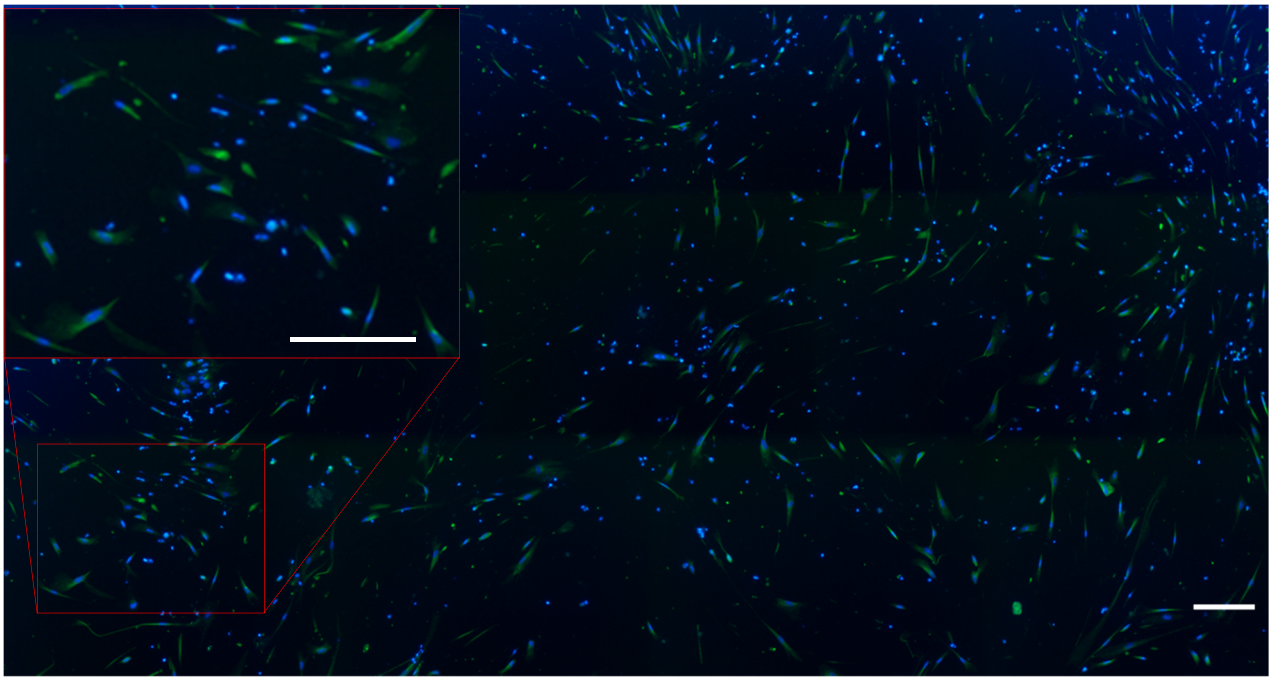

Figure 3.12: Day 3 FOXA2 protein staining. Cells fixed in 6 well culture dish and stained with DAPI (blue) nuclear stain and FOXA2 (green). Whole well Imaged on EVOS microscopy system and final image stitched together with on-board software. The inset is a zoomed view of stained cells. Cropped to reduce lens flare from the curved edges of the well. White bar = 100 µm

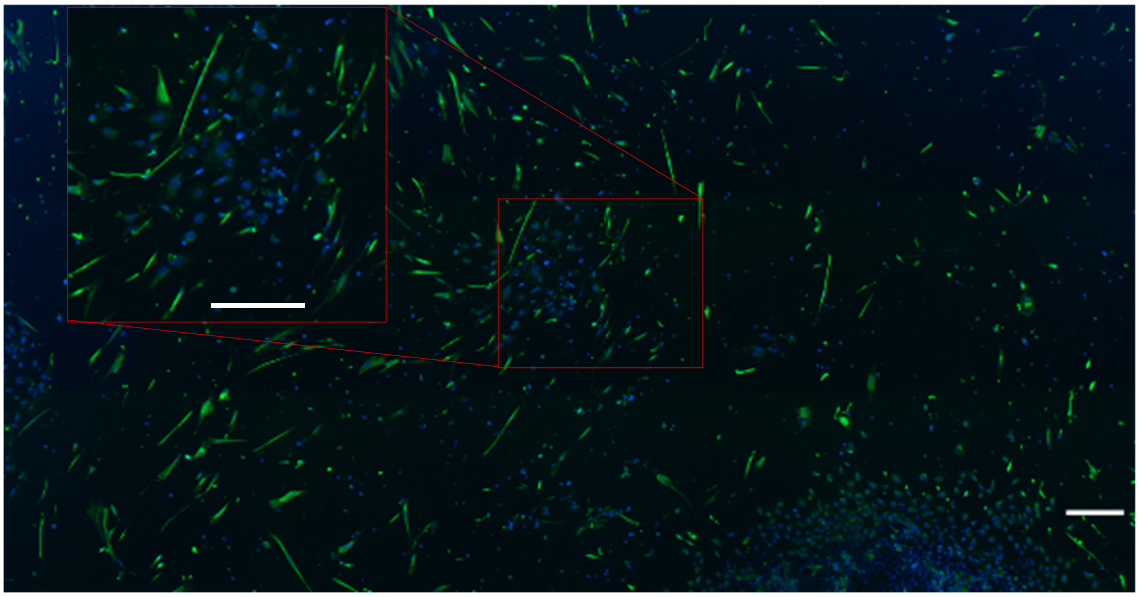

Figure 3.3: Day 3 SOX17 protein staining. Cells fixed in 6 well culture dish and stained with DAPI (blue) nuclear stain and SOX17 (green). Whole well Imaged on EVOS microscopy system and final image stitched together with on-board software. The inset is a zoomed view of stained cells. Cropped to reduce lens flare from the curved edges of the well. White bar = 100 µm

3.4.3.2 HNF1β and HNF4α protein expression on day 6.

Primitive foregut marker HNF1β is present in most cells (Fig. 3.15) similar to the staining for FOXA2. However, HNF4α is only expressed in a subset of cells (Fig. 3.16). In both cases, the positively stained cells were localised towards the edges of the culture dish suggesting the differentiating cells had an affinity for vertical structure. This can be seen in Fig. 3.15 which is a view centred on the middle of a dish with greater staining being seen to the edges. Fig. 3.16 is centred on the lower middle of a culture dish, showing greater staining at the very bottom of the photo relative the top. One PDX1 antibody was investigated, it was negative for positive control MIN6 cells as well as the differentiated cells. Antigen retrieval was also performed on the cells which did not improve the results (data not shown).

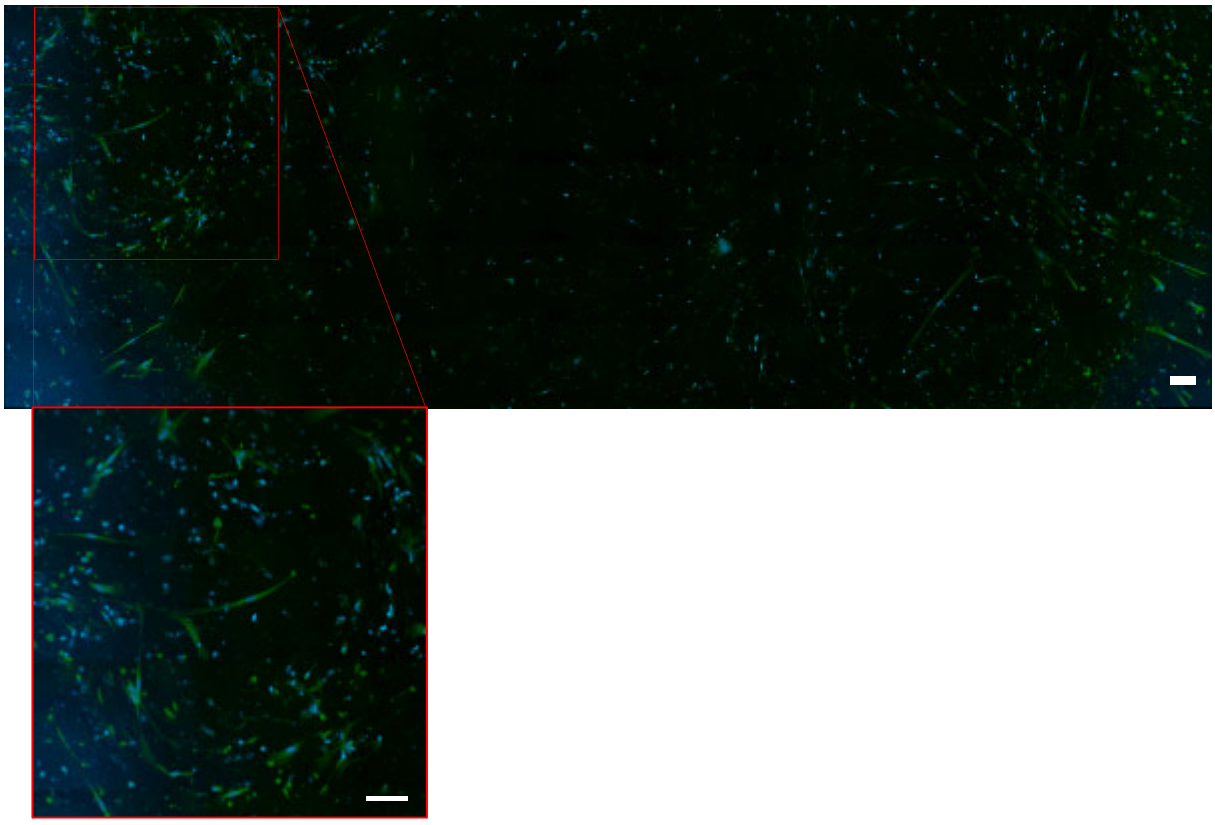

Figure 3.4: Day 6 HNF1β protein staining. Cells fixed in 6 well culture dish and stained with DAPI (blue) nuclear stain and HNF1β (green). Whole well Imaged on EVOS microscopy system and final image stitched together with on-board software. The inset is a zoomed view of stained cells. Cropped to reduce lens flare from the curved edges of the well. White bar = 100 µm

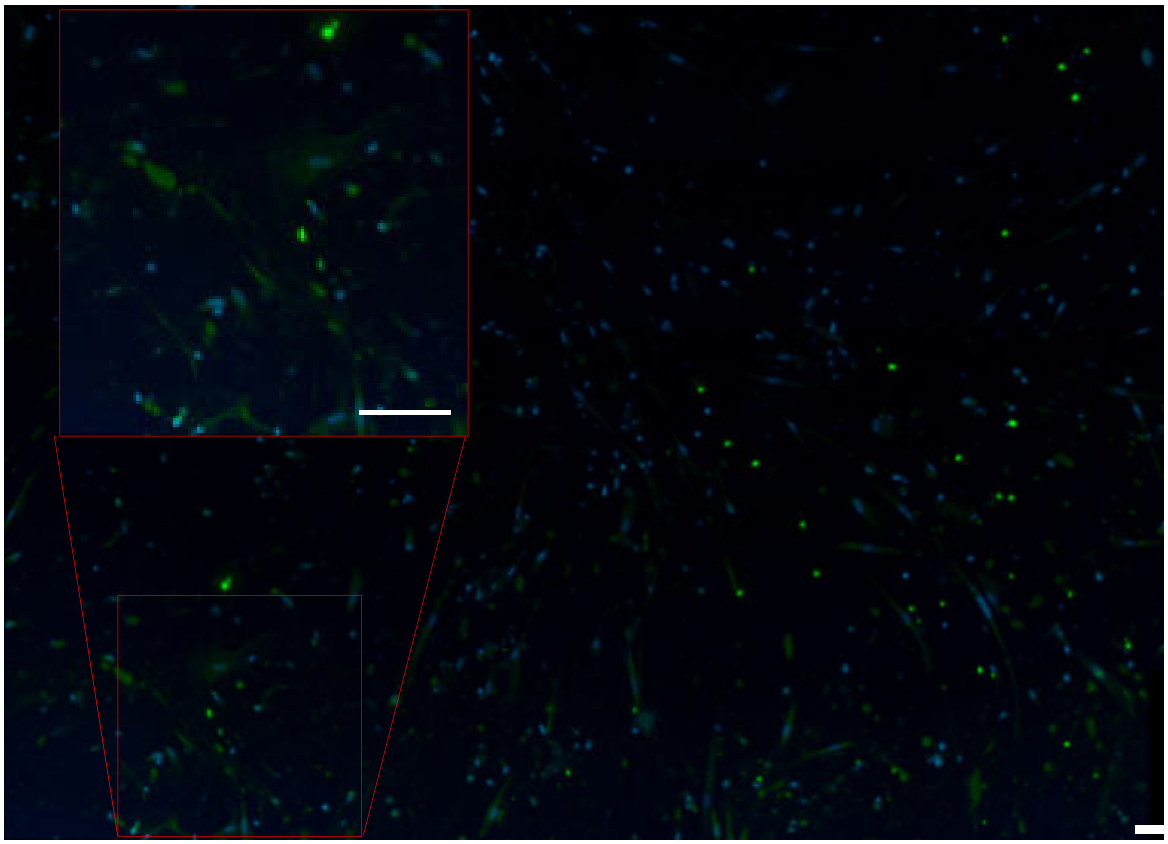

Figure 3.5: Day 6 HNF4α protein staining. Cells fixed in 6 well culture dish and stained with DAPI (blue) nuclear stain and HNF4α (green). Whole well Imaged on EVOS microscopy system and final image stitched together with on-board software. The inset is a zoomed view of stained cells. Cropped to reduce lens flare from the curved edges of the well. White bar = 100 µm

3.5. Discussion

Past studies have focused on the immuno-isolation of hESC post-differentiation (65). These studies have focused on viability and insulin secretion post-encapsulation. A leader in the area of encapsulation post differentiation is Don Anderson's group with mature stem cell-derived β cells encapsulated in modified triazole–thiomorpholine dioxide alginate (65). To the best of my knowledge, my study is the first to examine the effect of alginate encapsulation prior to the differentiation process reaching the *PDX1* expression stage. Whether encapsulation prior to differentiation had any effect on viability or differentiation outcome of the transplant was unknown prior to my study. I found that very few transcription factors were affected by encapsulation, with almost all showing no statistical difference to the current standard, which is using Geltrex® differentiation.

Previously the most extensive work on differentiation while encapsulated had been conducted by Methichit Chayosumrit (116). This paper greatly informed the research conducted in this chapter as it was the first paper to show the successfully differentiated alginate encapsulated hESC to definitive endoderm. A notable similarity between the results shown in this chapter was the expression of definitive endoderm markers *SOX17* and *FOXA2* at the same time point post Activin A exposure. This is encouraging as it reinforces the robustness of the differentiation to this time point.

As our method for mRNA quantification extrapolates absolute levels of mRNA. The previously published work in this field does not. The cited works in this thesis express mRNA relative to the pluripotent cells or the final stage of differentiation. For this reason it is only possible to say that this work is comparable to the cited previously published work.

As with the Chayosumrit paper, the effect of hESC differentiation within microcapsules on the viability of these cells was studied. To do this, hESC were either grown the traditional way on Geltrex® or encapsulated in alginate at 3 days prior to differentiation. The hESC were shown to maintain viability throughout the differentiation process. The hydrolysed 6-CFDA is seen to fluoresce green for quantification due to the activity of intracellular esterase's. Therefore, cells which express this fluorescence must have functioning

esterase's and were judged to be alive. The use of PI as a marker for dead cells is common in flow cytometry and microscopy (165). Under normal physiological conditions, cell membranes are impermeable to PI. However, physiologically stressed, apoptosis or necrotic cells have compromised cell membranes wherein PI is able to enter the cell. Upon entering the cell, PI will bind to cellular DNA and fluoresce, enabling the visual identification of dead/dying cells (with permeable membranes).

It can be seen from Fig.3.2 that as the differentiation progressed the 6-CFDA staining concentrated into foci. A possible explanation for this is the survival and proliferation of cells within their alginate niche. This concentration of staining made absolute quantification of numbers difficult as the 6-CFDA staining merged cells together. Further, as these 3D clusters of cells were not in a single plane, the fluorescence signals overlapped making quantification of individual cells numbers difficult. This likely lead to an underestimation of the "live" cell count and consequently the viability. Another factor which possibly affected viability assessment at the day 9 endpoint was the breakdown and removal of cell debris. The PI could stain only DNA still present in the capsules. As cells undergo apoptosis and necrosis, the resultant debris may have been small enough to leave the alginate capsule. This likely reduced the "dead" cell count of the viability assessment.

The cells stained positive for live cell marker CFDA at day 9 in as shown in figure 3.2 and 3.3. Encapsulation leads to some cell death but this is the case if the cells are encapsulated while pluripotent or terminally differentiated. DE marker transcript is detected from the encapsulated cells and this level of transcript expression is shown to match protein expression in the 2D differentiation cells. The CFDA stain is the equivalent of actin, mitochondria, or GAPDH live/dead assays.

During the differentiation process, the cells are exposed to a series of stressful environments including serum-free media and the differentiation process. Cell numbers were not quantified during the differentiation process; however, others have shown the proliferation of cells during the later stages of differentiation (72, 166). Indeed, the article my protocol is based on cites the need for an investigation into the mode of differentiation and suggests the mode is likely inductive rather than selective (72). Inductive

differentiation signals cells to develop towards the desired cell type. This is different from selective differentiation wherein cells, not of the desired lineage, become apoptotic (selected against). From our viability studies, it is not possible to distinguish between these processes as proliferating cells are unable to migrate away from one another, appearing as a homogenous 6-CFDA positive spot. None the less, my results show the cells survive the encapsulation and differentiation process.

The cell number appears to have dropped as dead cells degrade and live cells can only replicate within their niches in the alginate as they are unable to migrate. It is likely true that the capsule has fewer total cells, these cells are concentrated and still viable, therefore the % of cells in the capsule which are still viable remains around the same. This idea is supported by the data in supplementary figure 1.

Next, the transition of the hESCs through the different developmental stages was compared between Geltrex® and encapsulation strategies. To achieve this, semi-quantitative RT-qPCR analysis was used to determine the relative expression of various markers during the defined stages of development. Pluripotency makers, such as OCT4 and NANOG are widely used as markers of stem cell pluripotency. At day 0 expression of the *OCT4* transcript was very high in hESC grown in Geltrex® as well as when encapsulated. Similarly, day 0 expression of *NANOG* was very high; this is supportive of the pluripotent nature of these cells. These trends were as expected and were reported during the initial description of the line (144). However, the more important finding of this research was that there was no difference in the relative amounts of these markers between cells grown on Geltrex® and in microcapsules. This establishes that encapsulation with alginate and the associated stress does not prevent the cells from differentiating.

Once the differentiation protocol was initiated the transition through definitive endoderm is seen with the upregulation of *SOX17* and *FOXA2.* Expression of *SOX17* is known to direct mammalian development through primitive and definitive endoderm (151). Likewise, *FOXA2* is highly expressed during endoderm development and is believed to help regulate polarity and epithelialization (152). The high levels of definitive endoderm marker expression are supported by the immunohistochemistry results in figures 3.11 and 3.12. Both the gene transcript and protein were maximally expressed at the day 3-time point.

Additionally, *FOXA2* continues to be highly expressed for the remainder of the protocol. This prolonged-expression on *FOXA2* is characteristic of pancreatic differentiation and has been shown to promote *PDX1* expression (161). Expression of definitive endoderm markers, both gene transcript, and protein, were as expected for cells transitioning through definitive endoderm.

This comparability is continued into the development of the cells to the primitive foregut. Key markers examined at the primitive foregut (day 6) time point were *HNF1ϐ* and *HNF4α*. *HNF1ϐ* has been shown to be expressed in the entire primitive gut tube of mouse and zebrafish embryos(153). *HNF4α* shows a similar pattern of expression to *HNF1ß*(154). In Figures 3.8 and 3.9 can be seen the upregulation of both of these markers in Geltrex® and encapsulated protocols. Confirming this is the positive expression of *HNF1ϐ* and *HNF4α* protein in figure 3.15 and 3.16. The presence of both the gene transcript and the protein at 6 days strongly suggests the transition through the primitive foregut stage.

The final key marker examined was *PDX1.* While also a posterior foregut marker; *PDX1* positive cells give rise to the pancreatic buds and eventually the whole pancreas. Detectable levels of *PDX1* can be seen in Figure 3.10, in the cells at day 9 of both the Geltrex® and encapsulated cells. This expression of *PDX1* was key to this project as the transplantation of PDX1 positive tissue leads to maturation and insulin secretion *in vivo* (87).

The most statistically significant change during the protocol was the clear transition of the cells from expressing clear pluripotent cell markers to pancreatic lineage markers. While *OCT4* and *NANOG* are significantly decreased after the commencement of the differentiation protocol, they are never undetectable. While these genes are associated with pluripotency *OCT4* is known to have a role in lineage specification through expression levels (167). The RT-qPCR results in this chapter follow the progression of the cells and replicate the data from Kroon 2008, (with the exception of *FOXA2*)(61). Our data show a plateau or possibly decrease in *FOXA2* expression post definitive endoderm stage while Kroon 2008 found levels continued to rise and peaked at days 9 and 10. *FOXA2* is a known upstream regulator of *PDX1* expression (161) which appears to be unaffected by this plateau.

Transcript expression levels were similarly expressed between encapsulated and Geltrex® differentiation protocols (Fig. 3.4 -3.10), with expression being statistically similar. This is supported by the reproduction of previously published transcript expression data of these cells passing through the expected stages (61).

It is common practice to use mRNA concentrations as a proxy for the abundance of the corresponding protein. There is increasing evidence that there are many regulatory mechanisms occurring after mRNAs are transcribed which alter protein expression. Studies have suggested while mRNA concentration does correlate with protein expression, there is up to 40% variance between expected and quantified values (168). In my study, I showed mRNA and protein expression in all transcription factors examined except for PDX1 but did not compare relative levels. Visualisation with a PDX1 antibody was attempted, the antibody did not produce reliable or meaningful binding to the positive control after multiple attempts. Because of this, it was not possible to visualise protein levels in the differentiated cells or positive controls.

The data presented in this chapter clearly showed the encapsulated cells expressed the same key transcription factors at known time points as the Geltrex® cells. These expression patterns matched that of previously published data indicating the cells were differentiating towards insulin-producing cells. In addition, it has previously been shown that immature cells will continue to mature once transplanted *in vivo* (67). The next step was to replicate this with the partially differentiated encapsulated cells.

Chapter 4

In vivo maturation of hESC to insulin-producing cells within alginate microcapsules

4.1 Introduction

Human foetal pancreatic endocrine cells or their precursors are potential sources of cells for clinical transplantation (55). Immature human PDX1-positive islet-like clusters differentiated from human pluripotent cells have been shown to successfully continue development into mature endocrine cells secreting insulin and lowering BGL within 100 days when transplanted under the kidney capsule of immunodeficient mice (163, 169). Similarly, PDX1-positive hESC have been shown to continue to mature into insulin-secreting cells *in vivo* when transplanted under the kidney capsule (61, 67).

While 100 days is the maximum time cells have been shown to mature in vivo, the lowering of blood glucose occurred between 25 and 50 days post-transplantation. This is important as NOD-SCID mice are at high risk of developing thymomas after 85 days (170). This is an important consideration both in experimental design as well as to animal ethics committees.

Maturation of hESC to glucose-sensitive insulin-secreting cells can be achieved *in vitro* (64). However, this protocol requires up to 5 weeks of differentiation in culture. This lengthy production time is expensive, increases the risks of maintaining appropriate quality control, and makes scaling production risky. One proposed method to increase the efficiency of stem cell-derived treatment is the mass production of partially differentiated cells, which would be allowed to mature *in vivo*. Differentiation of hESC to insulin-producing cells using an experimental murine model is the first step in producing these cells for clinical application.

Human insulin corrects hyperglycaemia in diabetic mice but it is difficult to achieve sustainable normoglycemia (171). A dose of 10 U/kg/day of Humulin administered by pump over a day corrects hyperglycaemia in NOD mice. However, some research has reported a requirement of up to 80 U/kg/day to achieve long-term survivability when using subcutaneous Lantus injections (171). In contrast, humans require 1 U/kg/day (171) which varies with carbohydrate consumption. This discrepancy may be explained by a number of factors: Firstly, while the insulin gene is highly conserved in vertebrates there is around 15% amino acid mismatch between *H. sapiens* and *M. musculus*. Secondly, the difference in dose of insulin

required to achieve normoglycemia could be attributed to increased metabolic rate and the proposed insulin resistance of NOD mice that may lead to decreased efficacy (172). We can use the relative requirements from the results in this chapter to infer the required number of cells to be transplanted into humans if normoglycemia is to be achieved. Given the challenges of *in vitro* differentiation, and the possibility that they may be overcome if the cells can mature *in vivo*, we propose the following hypothesis and aims.

4.1.1 Hypothesis

We hypothesize that hESC that undergo differentiation while encapsulated in alginate will mature *in vivo* after transplantation into diabetic mice.

4.1.2 Aims

1. To investigate *in vivo* maturation of encapsulated hESC in a diabetic murine model.

2. To examine the developmental gene expression profile of the hESC at the end of *in vivo* maturation

3. To measure physiological outcomes of *in vivo* maturation of encapsulated hESC in a diabetic murine model, including evidence of insulin secretion in the circulation.

4.4 Materials and methods

4.4.1 Cell culture and microencapsulation

hESC were grown and microencapsulated as per Sections 2.2.2 and 2.3, respectively. Briefly, hESC were maintained on a feeder fibroblast layer before being either encapsulated or passaged onto Geltrex®. Once the cells were divided into respective treatment groups, they were differentiated as detailed in Section 2.3.1. Empty alginate capsules were generated by passing alginate without the addition of the cell suspension through the encapsulation device using the same instrument settings.

4.4.2 *Ex vivo* viability

After 83 days post-transplantation, animals were euthanized and encapsulated cells were retrieved from the intraperitoneal cavity as per Section 2.6.7. These cells were then placed into sterile PBS and the viability measured as described in Section 2.3.2 using 6-CFDA and PI as markers of viable and dead cells, respectively.

4.4.3 Animal experiments

4.4.3.1 Induction of diabetes in mice

Female NOD/SCID mice at the age of 7-8 weeks, weighing >18 g were obtained from the Animal Resource Centre (Perth, Western Australia). Once the mice were >20 g in body weight they were administered low dose STZ (i.p.) as per Section 2.6.2 and monitored for symptoms of diabetes. The mice were considered diabetic once their BGL reached >15 mmol/L on three independent random measures taken on different days. These mice were then randomly assigned to treatment or control groups. Mice were given insulin if their body weight dropped more than 10% below their pre STZ weight (see Section 2.7.2).

4.4.3.2 Intraperitoneal transplantation

The mice received either empty alginate capsules (control) or encapsulated hESC that had been put through the 9-day differentiation protocol (see Section 2.3.1). Either empty microcapsules or those containing cells were transplanted intraperitoneally as per Section 2.6.3 and the mice were administered analgesia (s.c.)

for the following 3 days. For each mouse, body weight and BGL were monitored every 2nd day for the next 83 days for all groups.

4.4.3.3 Kidney capsule transplantation

Cells differentiated on Geltrex® (Section 2.3.1) were transplanted under the kidney capsule according to the procedure detailed in Section 2.6.4.

4.4.3.4 Blood collection and graft recovery

Over the experimental period, blood was collected by two facial bleeds (at 1 and 2 months post-transplantation) and terminally by cardiac puncture (Section 2.6.6). Plasma was extracted from blood and used to measure circulating C-peptide by ELISA (Section 2.6.6). At termination on day 83 post-transplant, the grafts were recovered. Capsules in the intraperitoneal cavity were removed and suspended in PBS and used for RNA extraction, histology and viability studies. Kidneys that were transplanted with Geltrex® differentiated cells were embedded in OCT and stored at -80°C until used for histological analysis.

4.4.4 RNA extraction and qPCR

Using a transfer pipette, ~100 capsules were placed into a microfuge tube. ~500 µL TRIzol® reagent was added to the capsules and mixed vigorously for 3 min and snap-frozen in liquid nitrogen. Samples were thawed on ice and RNA extracted as described in Section 2.4.1.

4.4.5 Microscopy

Histological samples were prepared for H&E staining as outlined in Section 2.5. These slides were examined under bright-field on the Olympus IX81 microscope and microphotographic images acquired at 200x and 400x.

4.4.6 Statistical analysis

Graphical representation and statistical analyses of data were performed in GraphPad Prism Version 7.02. Student's *t*-tests were used to compare differences between the two groups. A Two-way ANOVA with a

Tukey *post-hoc* analysis was used to compare difference involving three or more groups. A *P* value of <0.05 was considered statistically significant.

4.5. Results

4.5.1 Viability

The number of capsules required for transplantation is heavily dependent on the survival of the cells within the capsules during the experimental period. To determine cell survival within the capsules during the experimental period, capsules containing partially differentiated hESC were retrieved and viability measured 83 days post-transplantation. During retrieval, the capsules showed no macroscopic signs of fibrosis and were freely moving in the intraperitoneal cavity (Fig. 4.1). In addition, there were no visible signs of increased angiogenesis around the capsules or peritoneum. These observations were exemplified by the ease with which the capsules could be suspended in PBS during retrieval. Fibrotic attachment to the peritoneum would prevent the suspension and retrieval of the cells. These macroscopic observations were then evaluated under the microscope using viability quantification.

Figure 4.1: Encapsulated pancreatic progenitors (red arrows) in the intraperitoneal cavity of a NOD/SCID mouse at day 83 post-transplantation. Approximately 2 million hESC were encapsulated in 2.2% alginate, differentiated *in vitro* and transplanted into the intraperitoneal cavity. Mice were monitored for 83 days, euthanised and the grafts removed for analysis.

Encapsulated cells recovered from mice were stained with 6-CFDA and PI to quantify viability. The viability of cells post-transplantation decreased by 17% compared to those tested before transplantation (Fig. 4.2).

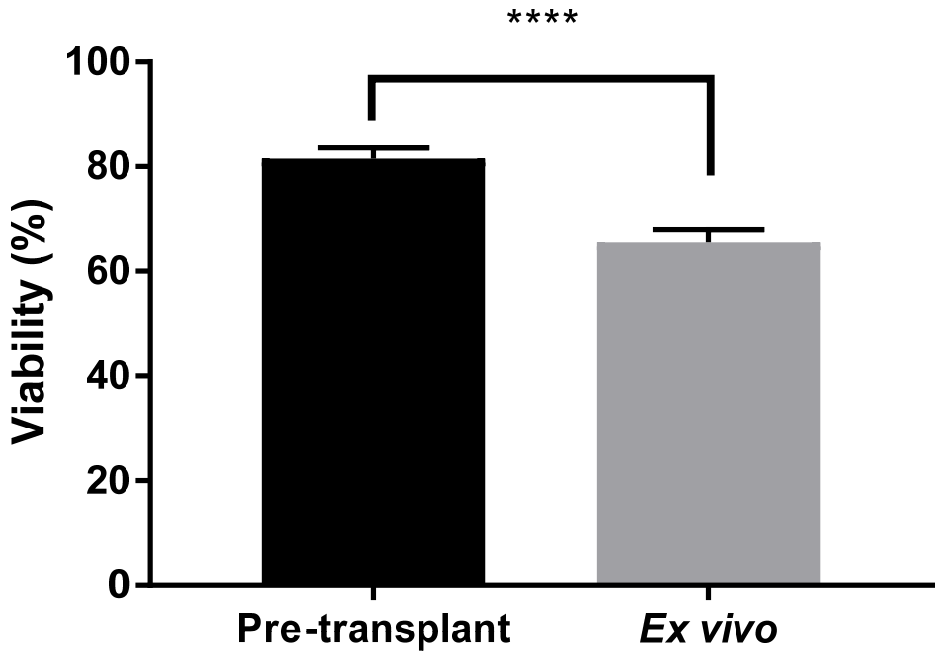

Figure 4.2: Pre-transplant vs *ex vivo* transplant viability of encapsulated pancreatic progenitor cells. *Ex vivo* capsules were stained with 6-CFDA and PI to asses for viability. Viability was scored as a percentage of live cells in each capsule. For each group at least 21 capsules were analysed. n = 3, $P < 0.001$, unpaired *t*-test.

Following isolation, the capsules showed no visible microscopic evidence of fibrosis and retained their smooth, regular exterior (Fig. 4.3). The cells remained viable seen by the continued 6-CFDA expression, an enlarged version on pannel D can be found in Supplementary figure 7.

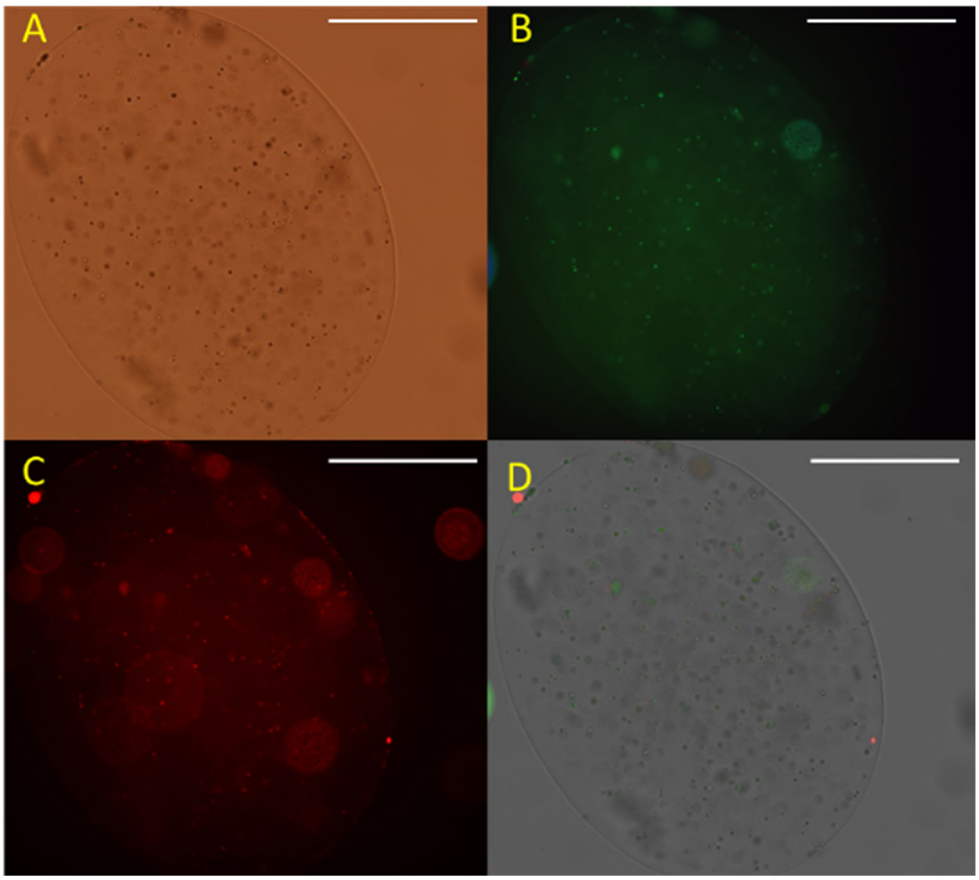

Figure 4.3: Encapsulated pancreatic progenitors *ex vivo* at day 83 post-transplantation. A) bright-field image of an alginate capsule showing the total number of hESC. B) 6-CFDA-positive viable cells (green), which have metabolised the stain. C) Dead cells with increased membrane permeability to PI stained red. D) Merge of images in panels A, B, and C. Scale bar 200 µm.

4.5.2 *In vivo* markers of cell maturation

4.5.2.1 Mice treated with encapsulated pancreatic progenitors had detectable levels of human C-peptide in their circulation.

Blood samples for C-peptide analysis were taken at three pre-defined time-points during the *in vivo* maturation experimental period. In the first two samples taken at days 30 and 60, the ultrasensitive ELISA returned values below its detection limit (2.5 pmol/L) indicating that there was no circulating C-peptide. However, the encapsulated pancreatic progenitor treatment mice were positive for circulating human C-peptide at the conclusion of the experiment (5.7 ± 2.7 pmol/L, n = 4) (Fig. 4.4). Along with these samples, pre-transplantation and ex vivo capsules were tested for glucose-stimulated insulin secretion (GSIS) but were undetectable (data not shown). The stress of retrieval, the low numbers of insulin producing cells or their maturity are the likely causes of this.

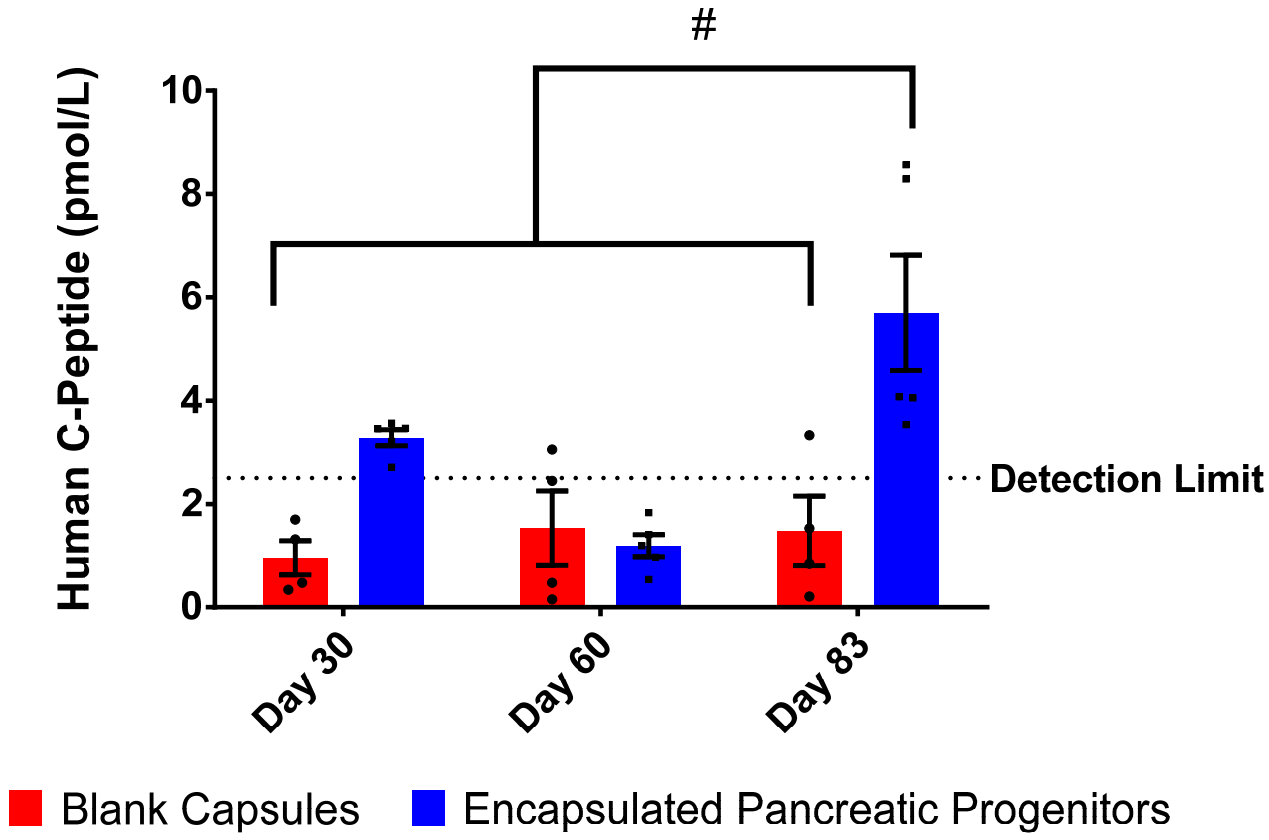

Figure 4.4: Circulating human C-peptide concentration in mouse plasma. At three time-points following transplantation of the capsules, blood samples were collected for detection of human C-peptide from

mouse plasma by an ultrasensitive ELISA. At termination (day 83), the encapsulated pancreatic progenitor treatment group had detectable levels of circulating human C-peptide. Pancreatic progenitor treatment, n = 5; Blank capsules, n = 4; # $P < 0.05$ when compared to Day 83 pancreatic progenitor capsules.

4.5.2.2 Effect of transplantation on body weight

Mouse body weight was measured at 2-day intervals from the time of transplantation to the end of the experiment (Fig. 4.4). At the time of transplantation (day 0), there was no difference in the mean weight of mice that received blank capsules (21.5 ± 0.7 g, n = 4) compared to those receiving the encapsulated pancreatic progenitor cells (21 ± 1.3 g, n = 7).There was no statistically significant difference in weight between the groups throughout the experiment.

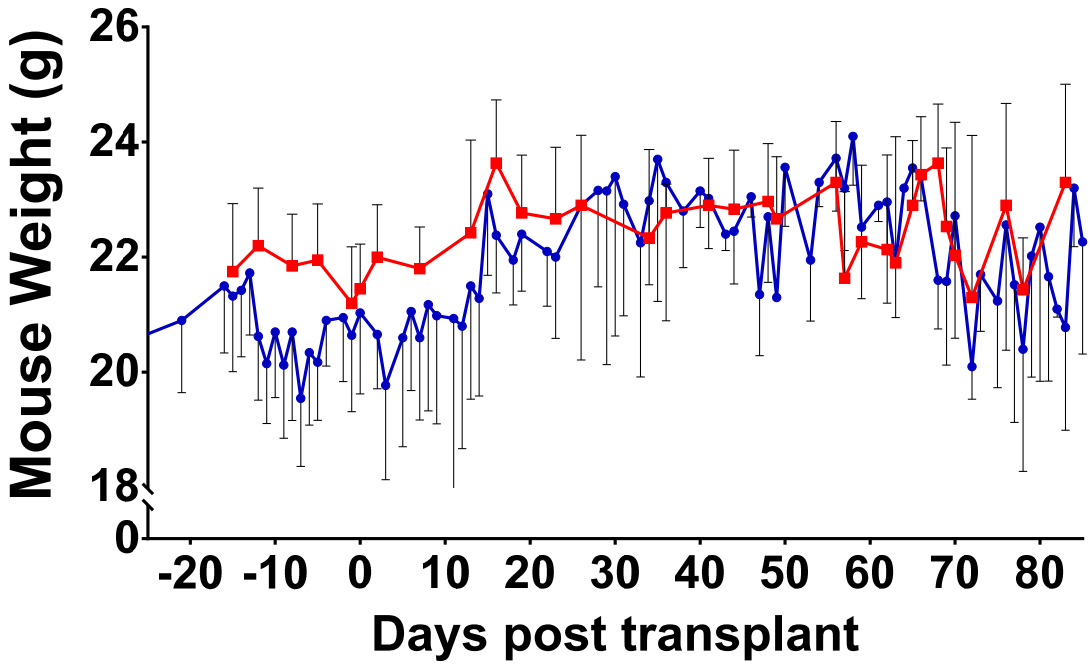

Figure 4.5: Bodyweight of mice post-transplantation of blank capsule controls or encapsulated pancreatic progenitor cells. At no time is there any significant difference between the weights of the two groups. Two-way ANOVA with a Tukey *post-hoc* analysis. Pancreatic Progenitor (Blue) n = 7, Blank capsules (Red) n = 4.

4.5.2.3 No difference in BGL over 12-week transplantation

Mouse BGL was measured three times a week from STZ treatment until the end of the experiment (Fig. 4.5). At the time of transplantation (day 0), there was no difference in the mean BGL of mice that received blank capsules (18.2 ± 3.1 mmol/L, n = 4) compared to those receiving the encapsulated pancreatic

progenitor cells (16 ± 4.5 mmol/L, n = 7). For the first two readings post-transplantation, the encapsulated pancreatic progenitor group had significantly lower BGL ($P < 0.05$). In addition to this, the blank capsule group quickly reached the detection limit of the blood glucose monitor (33.3 mmol/L) having statistically higher blood glucose at days 16 and 19. The only other statistically significant difference was found at day 33. For the remainder of the experiment, both groups regularly returned results above the detection limit of the blood glucose monitor. Diluting the blood in an EDTA solution to calculate a reading higher than the detection limit of the device was attempted but unsuccessful.

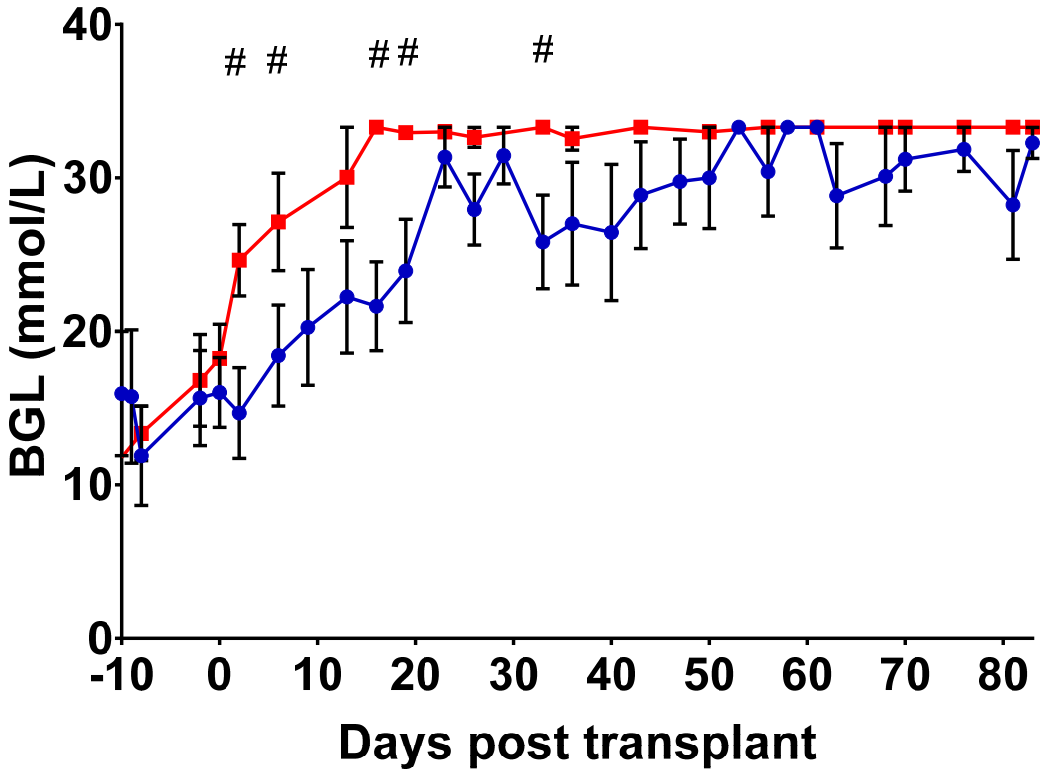

Figure 4.6: Blood glucose levels of mice post-transplantation of blank capsule controls or encapsulated pancreatic progenitor cells. Between days 0 and 83 post-transplantation mice with encapsulated pancreatic progenitor cells showed significantly lower blood glucose levels compared to controls at respective time points. # $P < 0.05$ by two-way ANOVA with Tukey post-hoc test. Encapsulated Pancreatic Progenitor (Blue) n = 7, Blank capsules (Red) n = 4.

4.5.2.4 Mice treated with pancreatic progenitor required less insulin.

Insulin was administered to any mouse whose weight dropped 10% below their pre-STZ weight, with each mouse receiving the same amount of insulin, 0.5 U Novorapid. The encapsulated pancreatic progenitor treatment group had a month without requiring exogenous insulin administration from weeks 4 to 8 (Fig. 4.7). This period correlates with a dip in average BGL of the mice and maintenance of weight (Figs 4.5 and 6). This, however, did not continue through to the end of the experiment.

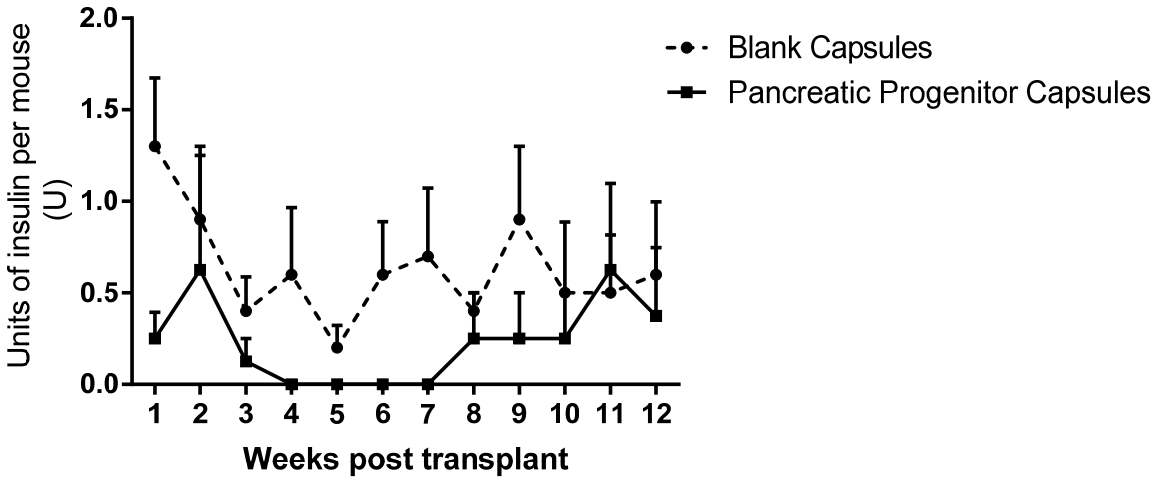

Figure 4.7: Average exogenous insulin administration per mouse per week. No statistical difference was found between the two groups at any time point (multiple t-tests); pancreatic progenitor treatment n = 7, blank capsules n = 4.

4.5.3 Gene transcript expression of *ex vivo* samples.

To better understand the maturation profile of the transplanted cells encapsulated cells were collected from the i.p cavity at day 83. In this section, these *ex vivo* results are presented with the pre-transplantation gene expression (the day-9 samples from Chapter 3). Geltrex® grafts placed under the kidney capsules were not included in the analysis as the cells could not be retrieved for mRNA extraction, see section 4.6.1.

4.5.3.1 Pluripotency markers *OCT4* and *NANOG* are expressed post maturation *in vivo.*

Expression of *OCT4* in the *ex vivo* samples maintained comparable levels with pre-transplantation on retrieval after 83 days *in vivo* (Fig. 4.8). Expression levels remain below $1x10^2$ fold over detectable, comparatively low to the pluripotent expression levels seen in Chapter 4.

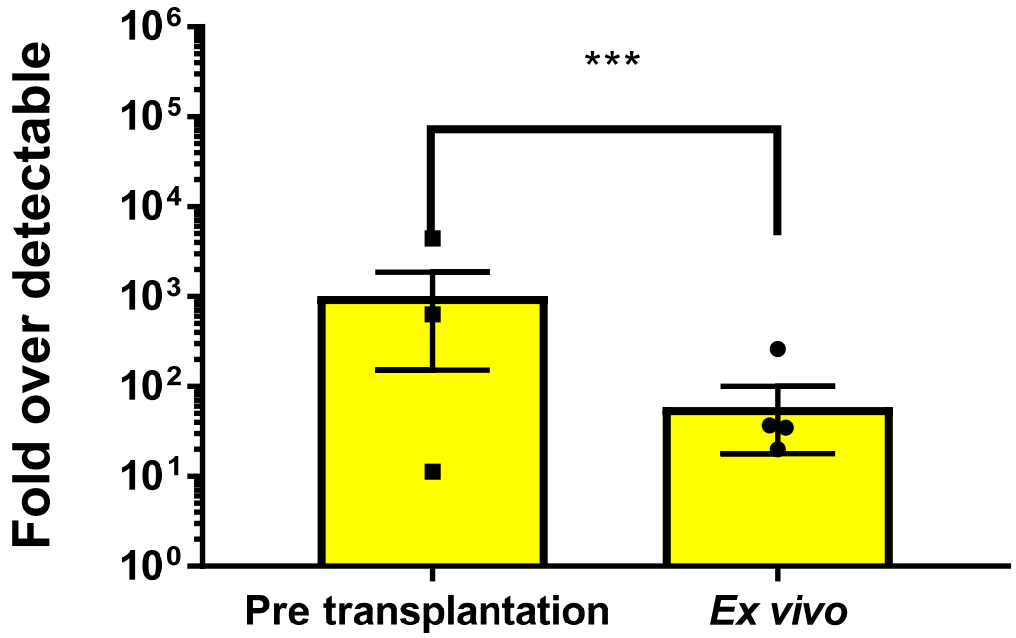

Figure 4.8: *OCT4* transcript expression of encapsulated hESC before transplantation and 83 days post-transplantation in the i.p cavity. Data are shown as mean ± SEM, y-axis $\log_{10}$ (fold over detectable), n = 6-8 per group presented as fold over the detectable limit. Samples which did not reach detection threshold samples can not be plotted on a logarithmic graph (n=2 for each group).

NANOG expression (Fig. 4.9) in the encapsulated cells prior to transplantation was undetectable. But, in samples retrieved 83 days post-transplantation there was found to be detectable levels of expression.

These levels were extremely low at 65 ± 36 fold over detectable and were significantly different from the pre-transplantation levels.

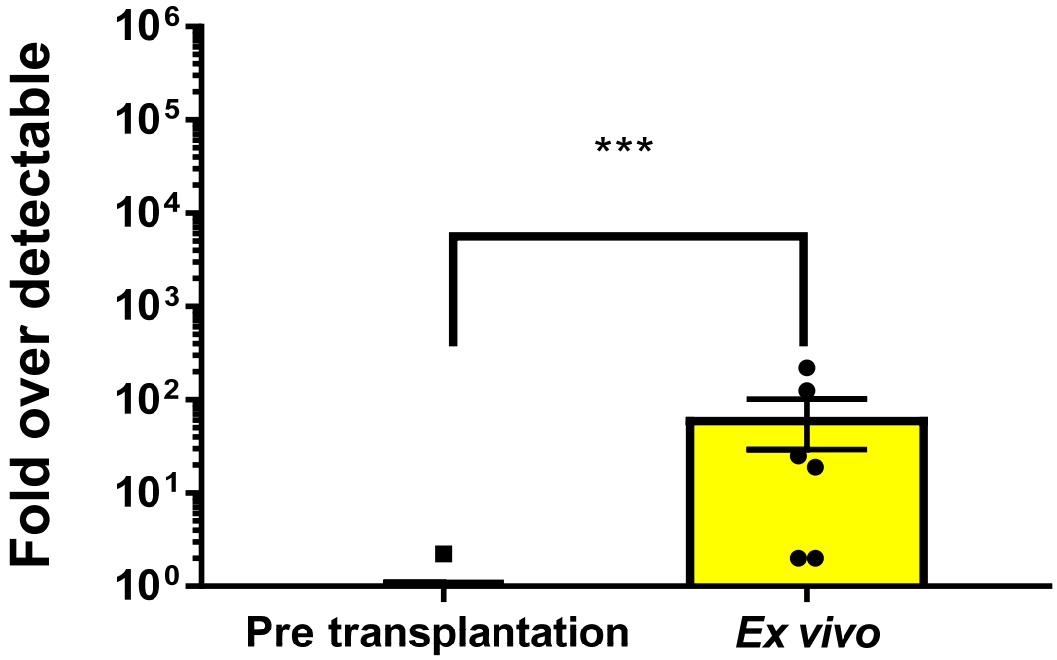

Figure 4.9: Encapsulated hESC *Ex vivo NANOG* gene expression. Data are shown as mean ± SEM, y-axis $\log_{10}$ (fold over detectable), n = 6-8 per group. $P < 0.0001$ by unpaired Student's t-test, samples which did not reach detection threshold samples cannot be plotted on a logarithmic graph (n = 4 for Pre transplantation).

4.5.3.2 Definitive endoderm markers *FOXA2* and *SOX17* expression remains unchanged during the *in vivo* maturation

The expression of definitive endoderm marker *SOX17* was unchanged when retrieved *ex vivo.* Of note is the variability near equal to their mean expression levels (*Ex vivo* 4329 ± 3270). This combined with comparable mean expression (5654 pre-transplantation vs 4329 *ex vivo*) meant there was no statistical significance between the two-time points (Student's *t*-test). On the other hand, the *ex vivo* profile for *FOXA2* was significantly different from the pre-implantation (label day-9) samples (Fig. 4.11). There is a drop from near 4000 fold over detectable to 600 *ex vivo.*

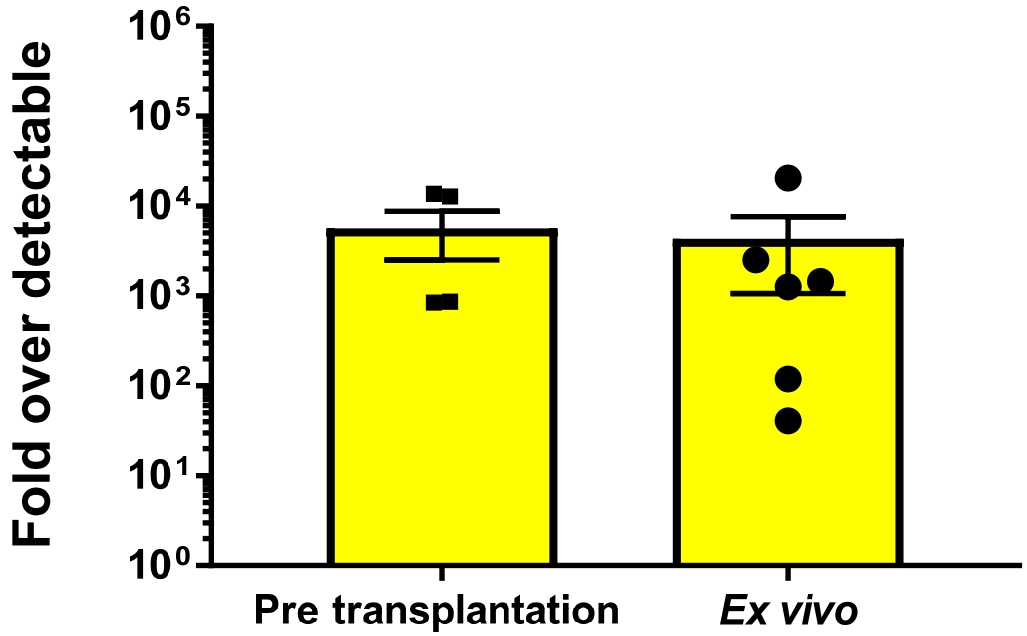

Figure 4.10: Encapsulated hESC *Ex vivo SOX17* gene expression. Data are shown as mean ± SEM, y-axis $\log_{10}$ (fold over detectable), n = 6-8 per group. Samples which did not reach detection threshold samples can not be plotted on a logarithmic graph (n = 1 for Pre transplantation).

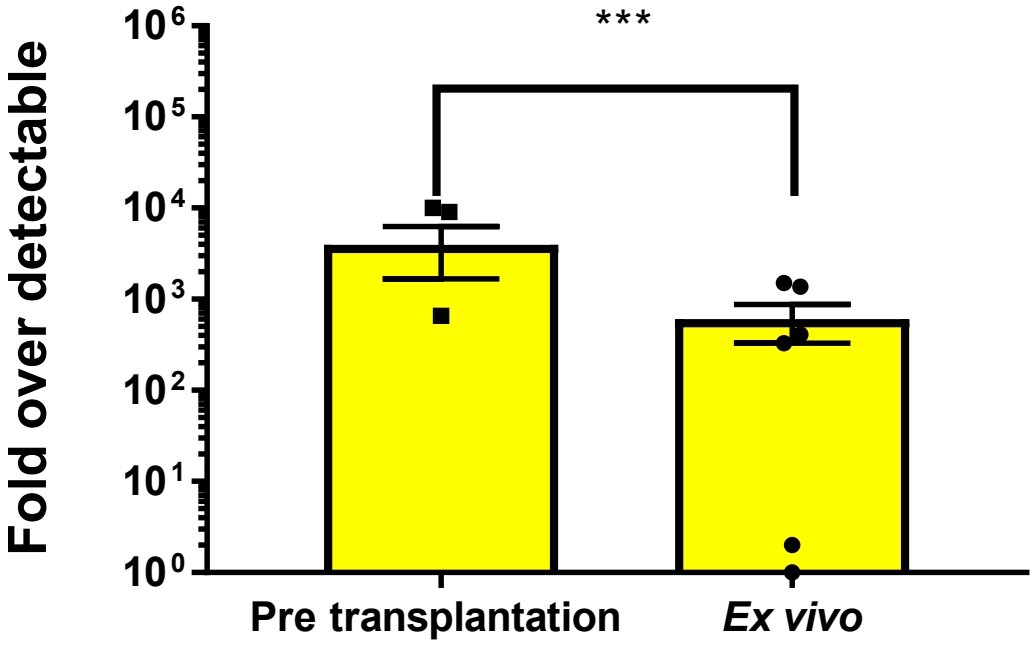

Figure 4.11: Encapsulated hESC *Ex vivo FOXA2* gene expression. Data are shown as mean ± SEM, y-axis $\log_{10}$ (fold over detectable), n = 6-8 per group. *P* = 0.0004 by unpaired Student's t-test, samples which did not reach detection threshold samples cannot be plotted on a logarithmic graph (n = 1 for Pre transplantation).

4.5.3.3 Primitive foregut/pancreatic endoderm markers *HNF1β* and *HNF4α* exhibited consistent expression post *in vivo* maturation.

Pre-transplantation through the primitive gut tube marker *HNF1β* had comparably low variation in expression levels (pre-transplantation 3994 ± 1362 vs ex vivo 3523 ± 1473) (Fig. 4.12). Yet there is a comparatively greater variation of transcript expression for *HNF4α* between *ex vivo* samples; this is consistent with the genes expression at earlier time points (Fig. 4.13). Both *HNF4α* and *HNF1β* are expressed pre-transplantation and at retrieval.

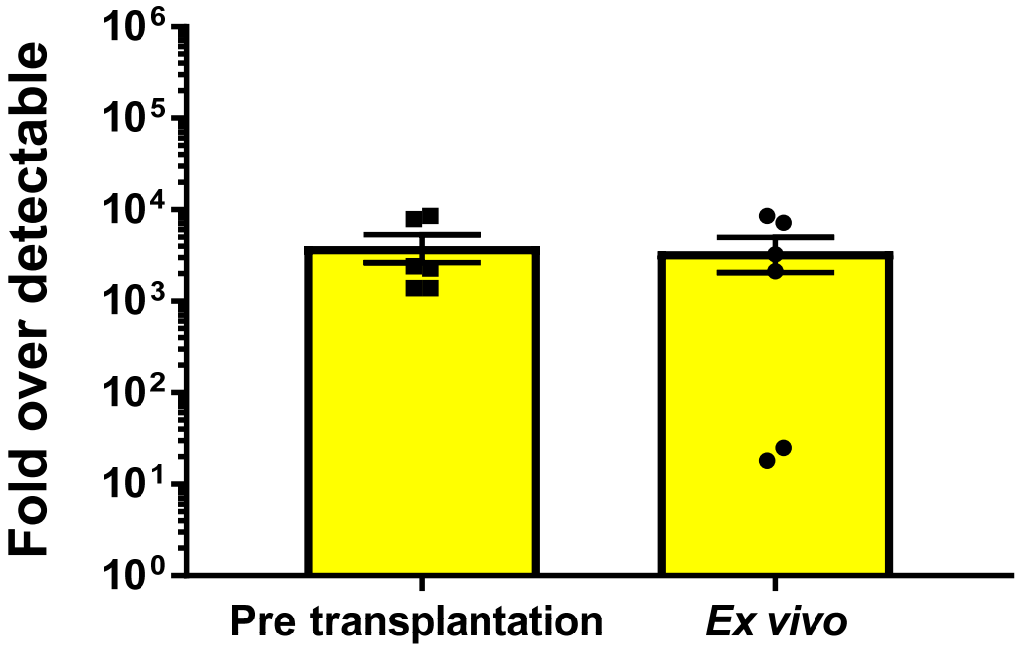

Figure 4.12: Encapsulated hESC *ex vivo HNF1β* gene expression. Data are shown as mean ± SEM, y-axis $\log_{10}$ (fold over detectable), n = 6-8 per group. All samples produced detectable signals.

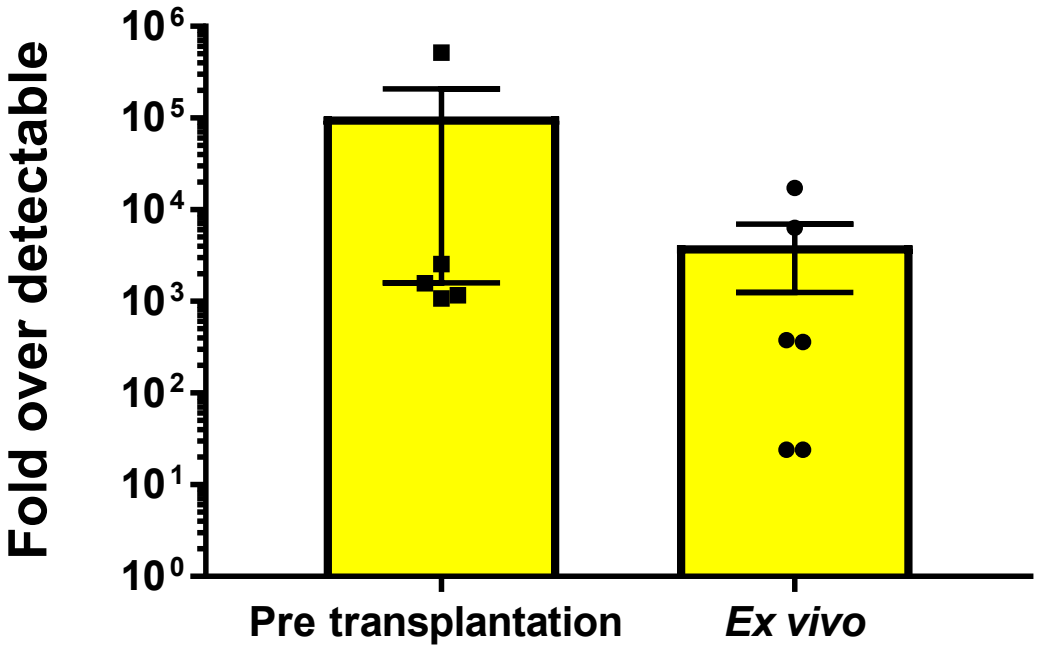

Figure 4.13: Encapsulated hESC e*x vivo HNF4α* gene expression. Data are shown as mean ± SEM, y-axis $\log_{10}$ (fold over detectable), n = 6-8 per group. All samples produced detectable signals.

4.5.3.4 Key pancreatic marker *PDX1* and beta-cell marker *INS* is detectable in *ex vivo* samples.

The expression of beta-cell marker *PDX1* on day 9 was the indicator which gave us the confidence to proceed to maturation *in vivo*. *Ex vivo* these cells continued to express *PDX1* transcript at comparable levels (Fig. 4.14). PDX1 expression was not statistically different between the Pre transplantation and retrieved samples and was detectable in all 5 *ex vivo* samples.

The mature beta-cell marker, insulin, had a significant detectable transcript in the *ex vivo* samples (Fig. 4.15). This marker was not detectable pre transplantation in either the encapsulated or Geltrex® differentiation protocol. *Ex vivo* this transcript was found to be detectable at 2272 ± 1593 fold over detectable. This result is further supportive of the circulating C-peptide findings in Fig. 4.4.

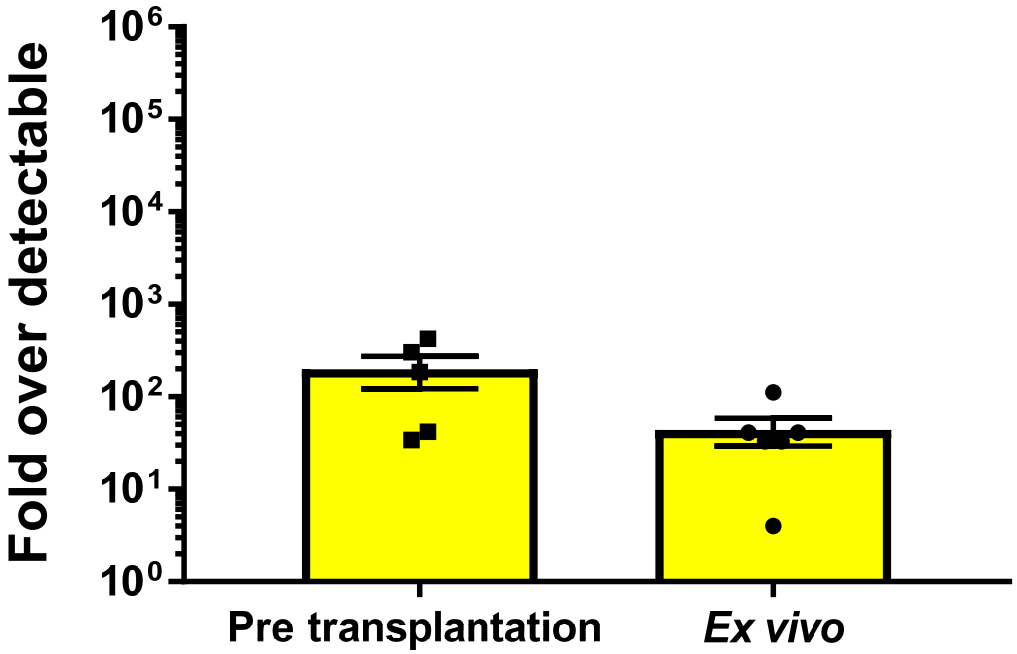

Figure 4.14: Encapsulated hESC *Ex vivo PDX1* gene expression. Data are shown as mean ± SEM, y-axis $\log_{10}$ (fold over detectable), n = 6-8 per group. All samples produced detectable signals.

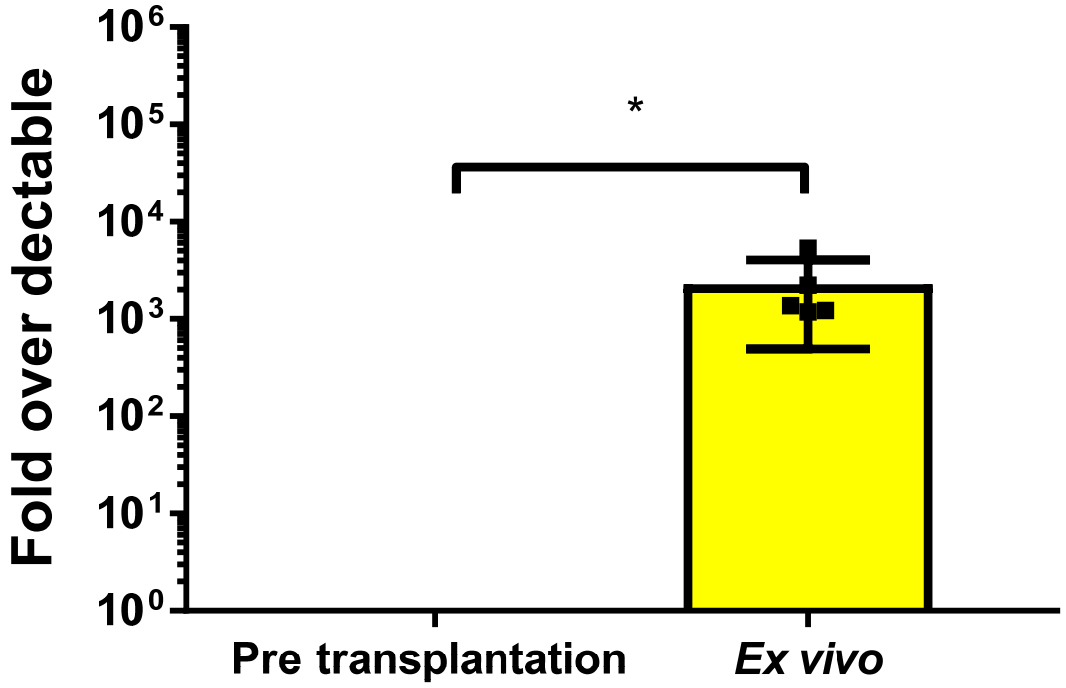

Figure 4.15: Encapsulated hESC *Ex vivo INS* gene expression. Data are shown as mean ± SEM, y-axis $\log_{10}$ (fold over detectable), n = 5-6 per group. An asterisk denotes P = 0.0116 by Student's t-test, all 6 Pre transplantation samples did not reach the detection threshold and are not plotted on the logarithmic graph.

4.6 Histology and Immunohistochemistry

Transplanted alginate capsules containing pancreatic progenitors and whole kidneys from the kidney capsule treatment group were retrieved from the mice at 83 days post-transplantation. These samples were set in OCT for histology and immunohistochemistry analysis. Slicing and mounting of alginate capsules was a significant challenge and produced poor results once mounted and stained (Fig. 4.16). The process of staining (histological and immunohistochemistry) resulted in the loss of many capsules and their contents.

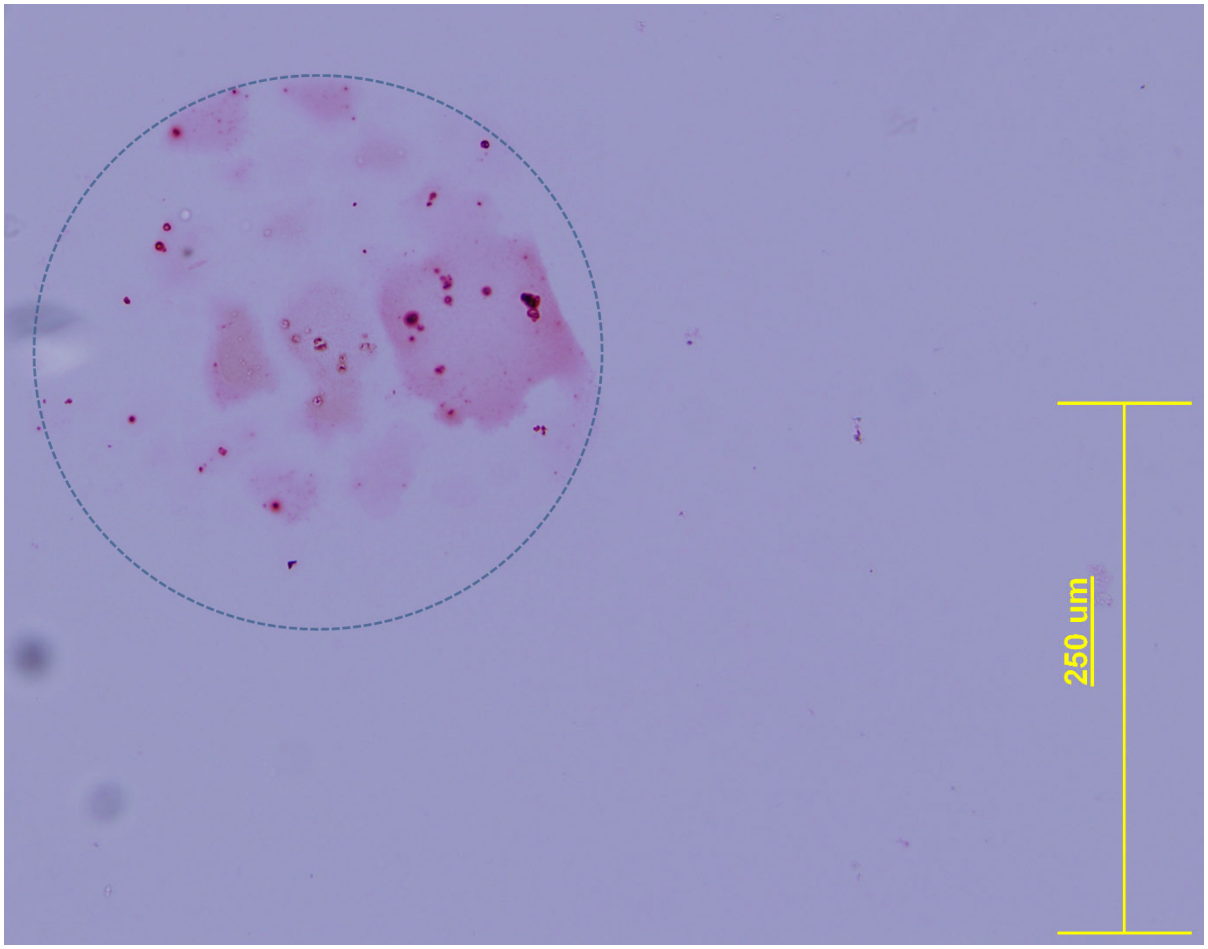

Figure 4.16: Remnants of a retrieved capsule H&E stained after 83 days post-transplantation in the i.p. cavity. Blue dashed line estimation of the former capsule boundary. Pale pink staining of the alginate (most of which has been dislodged from the slide). Dark pink staining of the cells within the capsule. Scale bar 250 micrometres.

4.6.1 Immunohistochemistry and H&E staining

Kidneys that had the Geltrex® differentiated pancreatic progenitors transplanted under the capsule showed macroscopic growths (Fig. 4.17). The kidneys were of normal shape, size and weight (data not shown) with no other apparent injuries. The kidneys were sectioned and H&E stained to examine histology and to identify the capsular growth tissue.

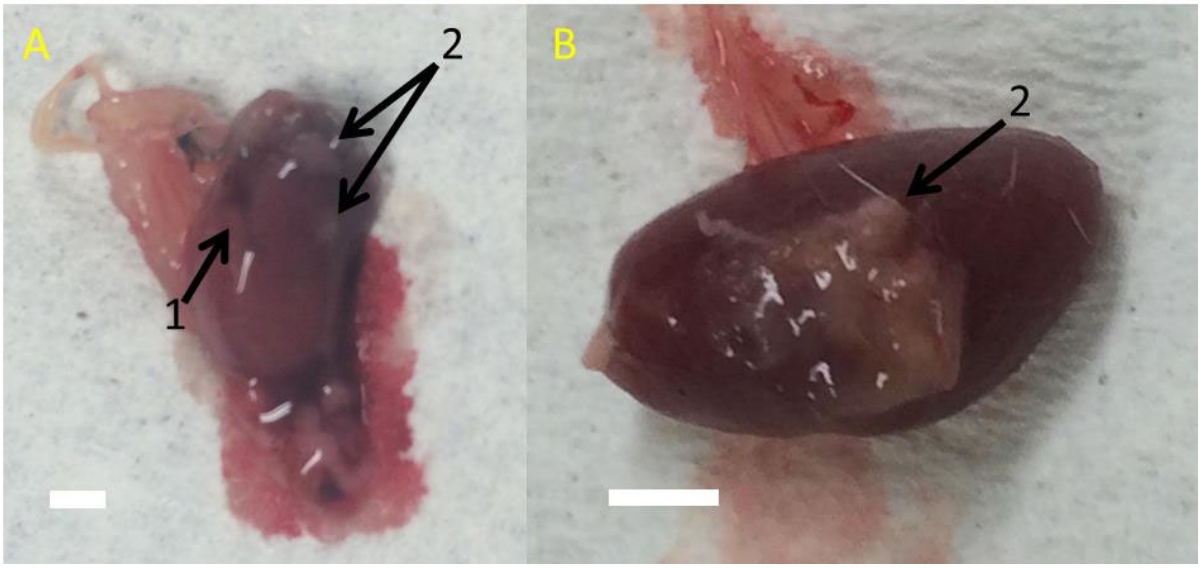

Figure 4.17: Mouse kidney retrieved 83 days post cellular transplantation under the kidney capsule. Representative images from two different mice (A and B) showing the site at which the kidney capsule was incised for implanting the cells (1) and the growths under the kidney capsules (2), white bar = 2mm.

These samples were then sectioned and mounted for H&E staining and showed a cellular infiltrate under the kidney capsule with no obvious signs of the graft (Fig. 4.18).

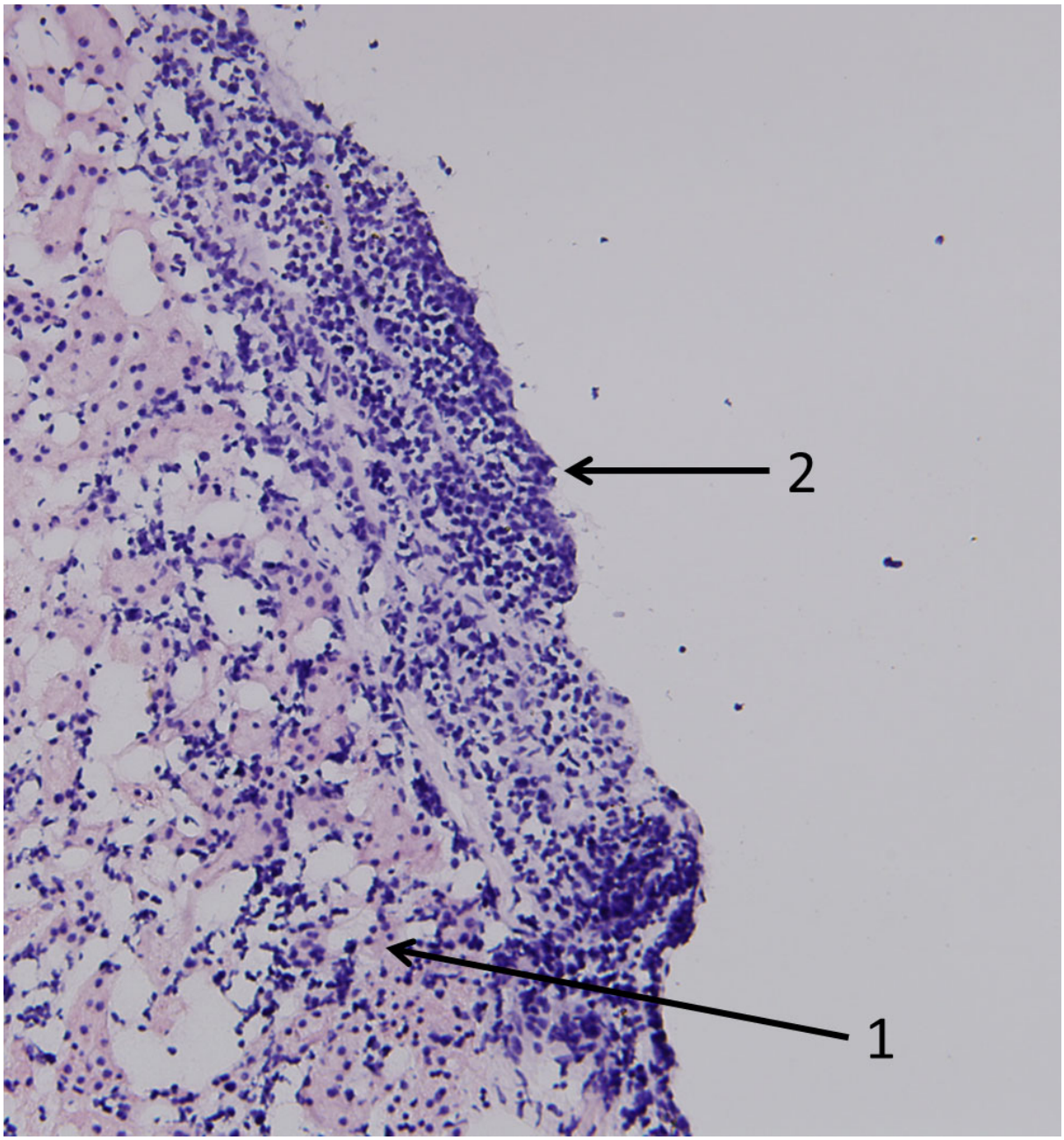

Figure 4.18: *Ex vivo* H&E staining of mouse kidney 83 days post-transplantation of partially differentiated stem cells under the kidney capsule. Normal kidney cortex containing cells with large cytoplasm's (1) adjacent to visually different, densely packed cells (2)).

4.6.2 Assessment of histology

The slides stained negative for PDX1 and human insulin (data not shown) and were referred to Dr Andrew Gal (senior pathologist, Laverty Pathology). His assessment of the grafts was that the cells were unlikely to be of human origin and were possibly an immune response from the host. Dr Gal's facility was not equipped to distinguish mouse cell types. However, it was confirmed that there were no human tissues present. The full report can be found in Appendix 1.

Figure 4.17 and 4.18 show masses on the kidney but these were not of human tissue. As discussed in section 4.7 the masses may have been the result of immune cell infiltration to destroy the transplant or technical error . While this does limit statements when comparing to the proposed positive control it does not prevent comparison to the negative control (blank capsules).

4.7 Discussion

PDX1-positive tissue transplanted into an induced diabetic mouse leads to the generation of insulin-secreting cells (87). To the best of my knowledge, this is the first time encapsulated human embryonic stem cells differentiated for 9 days *in vitro* have been transplanted with the goal of correcting BGL. It has been shown that cells continue to mature *in vivo,* and secrete insulin. This key finding is supported by the measurement of circulating human C-peptide found in the mice at day 83 (Fig. 4.4). The assay is extremely selective for human C-peptide and the blank capsule control mice had only 2 samples register above the detectable limit of the assay. One on day 60 and one on day 83, these samples were from different mice and can only be explained as false positives as they were just 0.5pmol/L over the detectable limit. At day 83 the mice treated with the encapsulated pancreatic progenitors had 5.7 ± 2.7 pmol/L of circulating human C-peptide. Although insulin is produced in a 1:1 ratio with C-peptide (173), it is metabolized at a much faster rate (through the liver as compared to the kidney for C-peptide), such that the level of C-peptide in the blood is ~5 times that of insulin (173). Thus, 5.7 pmol/L plasma C-peptide equates to 1.4 pmol/L plasma insulin, or 1.7×10^{-7} U/mL. Mice have around 58.5 mL/kg circulating blood (174), and therefore these mice, which weighed 22 g, had around 1.3 mL total blood volume. The insulin in the circulation from the capsules at this time point was around 1.07×10^{-6} U in total. As established in the introduction of this chapter (171) a 20 g mouse will require 0.25 U of human insulin to achieve normoglycemia. Assuming that the mouse has a steady-state of insulin in the blood of 1.7×10^{-7} U/mL and that C-peptide has a 30 min half-life we can calculate the excretion rate and therefore the total excretion of the cells over a day. Using the steady-state equation for pharmacokinetics ($k^0 = k_m K_p V_E C_{0,ss}$)(175) it is estimated that the cells are excreting 0.54×10^{-4} Units per day; ~3670 times less than required to achieve normoglycemia.

Consistent with the detection of circulating human C-peptide, the *ex vivo* cells also were positive for insulin transcript. It is likely that each cell within the capsules was at differing developmental stages, as the extracts from the capsules were positive for *OCT4* and *NANOG* pluripotent markers. While the mRNA transcript of NANOG went from undetectable to detectable it was still expressed at extremely low levels, additionally *NANOG* is expressed in low levels in a range of tissues (176). The later stage*SOX17,* and *FOXA2* definitive

endoderm markers, and *HNF1β* and *HNF4α* immature pancreatic markers were also found in the capsules. While some of these markers are expressed in mature beta-cells, it is likely that the variation in gene expression levels that we observe represents a heterogeneous population of cells within the capsule at different stages of differentiation. In a traditional transplant, this may place the recipient at risk of teratomas due to the presence of pluripotent cells. However, as the cells are unable to migrate through the alginate capsules the formation of teratomas caused by the transplantation of pluripotent cells may have been prevented, this is consistent with previous research (177). Due to the issues mounting the capsule sections, it is not possible to determine if there were any teratomas formed within the capsules. Encouragingly no abnormal growths were noted in the mice at the end of the 12-week period. It has been observed by others that transplantation of as few as 100,000 pluripotent cells has a 100% mortality rate at the 12-week time point in immunodeficient mice (178).

The inability of the encapsulated cells to correct hyperglycaemia may have been due to a number of factors. The point at which the random blood glucose level of the blank capsule mice was significantly different from the encapsulated pancreatic progenitor treatment mice was at the very beginning of the experiment. This coupled with the lack of detectable human C-peptide at this time makes it unlikely that the treatment was responsible. As previously discussed the dosage of human insulin was 3670 times lower than the optimal treatment dose. Additionally, both the blank capsule and pancreatic progenitor treatment mice had a BGL above the measurable limit of the device (33.3 mmol/L) for multiple readings past day 25. If there was any mild correction in the stem-cell-treated mice due to the presence of low levels of human insulin this would have occurred above the measurable limit. Several steps were taken to attempt to improve the sensitivity of the mice BGL measurements. Firstly, the blood samples from the mice were diluted in an EDTA solution. However, this was not compatible with the BGL testing machine. Secondly, the mice were also tested after overnight fasting, although this was also unsuccessful (measurements were still above 33.3 mmol/L; data not shown).

The loss of the Geltrex® differentiated cells transplanted under the kidney capsule may have been the result of several factors. The blood clot holding the cells may have moved free of the capsule once the kidney was re-inserted in the mouse. The pathology report did not find any human tissue in the samples, the two most likely causes of this are the cells dying during or after transplantation and being cleared over the 3-month experimental period. Alternatively, the transplant may not have been securely placed under the kidney capsule. Again no abnormal growths were noted in the peritoneum of the kidney capsule treatment group. The graft may have been destroyed by immune cells as some NOD/SCID mice will spontaneously develop partial immune reactivity (179). Additionally while NOD/SCID mice have non-functioning B and T cells, there is still NK cell activity. However placing cells under the kidney capsule is a very demanding technique and technical error cannot be ruled out. Concluding that the cells were not present in the kidney at retrieval, they may not have stayed in the kidney capsule or may have failed to vascularise and develop.

The detection of circulating human C-peptide is a significant achievement as it represents the continued maturation of progenitor cells in an alginate capsule when transplanted into a diabetic mouse. While dosage requirements need to be addressed there is an opportunity to increase cell numbers within capsules and with larger hosts (rats, primates and eventually humans) the number of capsules. With this progress in mind, the reduction in regulatory burdens facing this new paradigm is beneficial, specifically the implantation of non-autologous cells. One method, which will be examined in the next chapter, is the use of additional pluripotent stem cell sources.

Chapter 5

Differentiation of induced pluripotent stem cells derived from a person with Type 1 Diabetes to primitive foregut while encapsulated in alginate microcapsules

5.1 Introduction

In the previous chapter, the *in vivo* maturation of hESC differentiated while encapsulated was investigated. There are both advantages and disadvantages to using ESC as the source of stem cells for use as a therapy. The disadvantages of hESC are primarily governmental regulation around creation, prolonged storage and culture, and the risk factors associated with non-autologous transplantation in the clinic. While there are numerous existing hESC lines available, this only alleviates the creation restrictions. One option to ease some of these issues is the use of induced pluripotent stem cells (iPSC). As reprogramming technology improves, the evidence to use differentiated iPSC as autologous transplants strengthens. This would greatly reduce the risk to the patient from transplant rejection although not protect against autoimmune conditions.

iPSC is reprogrammed somatic cells that can be differentiated into the 3 germ layers. Most commonly fibroblasts taken from an individual are grown and reprogrammed under cell culture conditions. These cells can then be differentiated with differentiation protocols used for hESC to obtain similar outcomes (64, 180).

The ideal outcome in our case would be to take cells from a patient, reprogram them into iPSC and then differentiate them into insulin-producing cells. These cells could then be transplanted into a patient as an autologous cell therapy for the treatment of T1D. These cells would still require immunoisolation as T1D is an autoimmune condition.

It is important to consider if the genetic factors which predispose an individual to T1D would also prevent the generation of iPSC. There has been extensive work on the identification of genetic factors, which lead to the development of T1D. An example of this is the major histocompatibility complex RT1 (u) haplotype and Cblb (Casitas B-lineage lymphoma b) which contribute to the development of T1D in rat models (181) as well as many factors in the non-obese diabetic (NOD) mouse strain (182). This is a concern as previously the continual culturing of ESC from NOD mice has been unsuccessful (183). These results suggest a possible interplay between the T1D predisposing genetic background and the ability of the cells to maintain stable

pluripotency and differentiate. However recently there has been success with both ES and iPSC from NOD mice (184, 185).

The iPSC line derived from a person with T1D investigated in this chapter was reprogrammed by Dr Jun Liu at Monash University using the four Yamanaka factors. Using a lentiviral vector, the cells were transfected and expressed the reprogramming genes (unpublished data). Their pluripotent state was confirmed by transplantation by Dr Liu into a nude mouse where they contributed to the formation of the three germ layers (Supplementary figure 5.1). While cells from a person with T1D have been differentiated down the pancreatic lineage before (186), this chapter will explore this process while the cells are encapsulated.

5.1.1 Hypothesis

Induced pluripotent stem cells from a person with T1D, encapsulated in alginate, differentiate to early pancreatic progenitors similarly to hESC.

5.1.2 Aims

Investigate the stages of differentiation from induced pluripotent stem cells to early pancreatic progenitors of iPSC from a person with T1D, while the cells are encapsulated in alginate.

5.3. Materials and methods

5.3.1 Cell culture

The iPSCs were cultured and purified as per Sections 2.2.2 and 2.2.4. They were then mixed with alginate solution at a concentration $2x10^6$ cells/mL and encapsulated as described in Section 2.3. The iPSCs were also plated onto Geltrex®-coated plates seeded at a density of 30,000 cells/cm^2 in 6-well plates.

5.3.2 Viability

Viability of encapsulated cells was assessed using 6-CFDA and Propidium Iodide (PI), as described previously (Section 2.3.4). After staining, samples were analysed under an Olympus IX81 (Olympus, NSW, Australia) microscope using Cell^M software. The percentage of 6-CFDA positive (green) cells (live) to PI positive (red) cells (dead) was measured to evaluate the viability (live/total x 100 = % viability). Co-stained cells were counted as live because 6-CFDA requires active esterase enzyme activity to be cleaved to its amine-reactive form.

5.3.3 RNA isolation, cDNA generation and RT-qPCR

Total RNA from cells was isolated using the organic extraction method of phenol-based TRIzol® reagent described in Section 2.4.1. The RNA was then reverse transcribed and abundance of mRNA transcripts measured using specific fluorescent probes on ViiA7 (Life Technologies) as described in Section 2.4. TaqMan® probes are listed in Table 2.1. The relative abundance of each transcript of interest was normalised to the expression of a reference gene, 18S, and expressed as "fold over detectable". This represents an approximation of the number of copies present in a sample (148).

5.3.4 Statistical Analysis

Statistical analyses were performed using GraphPad Prism, Version 7.02. Student's *t*-test was used to analyse differences between conditions in the viability assessment. Two-way ANOVA with Tukey's *post-hoc* analysis was used to compare groups between all conditions in the RT-qPCR analysis with data being treated as non-parametric due to the small sample size.

5.4 Results

5.4.1 Viability

As with previous experiments, it was important to establish that the iPSC could survive within the alginate microcapsules. The cell survival was assessed in the same manner as the hESC in Chapter 3 with CFDA/PI staining of the cells before the commencement of the differentiation protocol and at its completion. The capsules can be seen with the CFDA-positive (i.e., live) iPSC inside (Fig. 5.1B). In addition to this, PI-positive cells were visible (Fig. 5.1C).

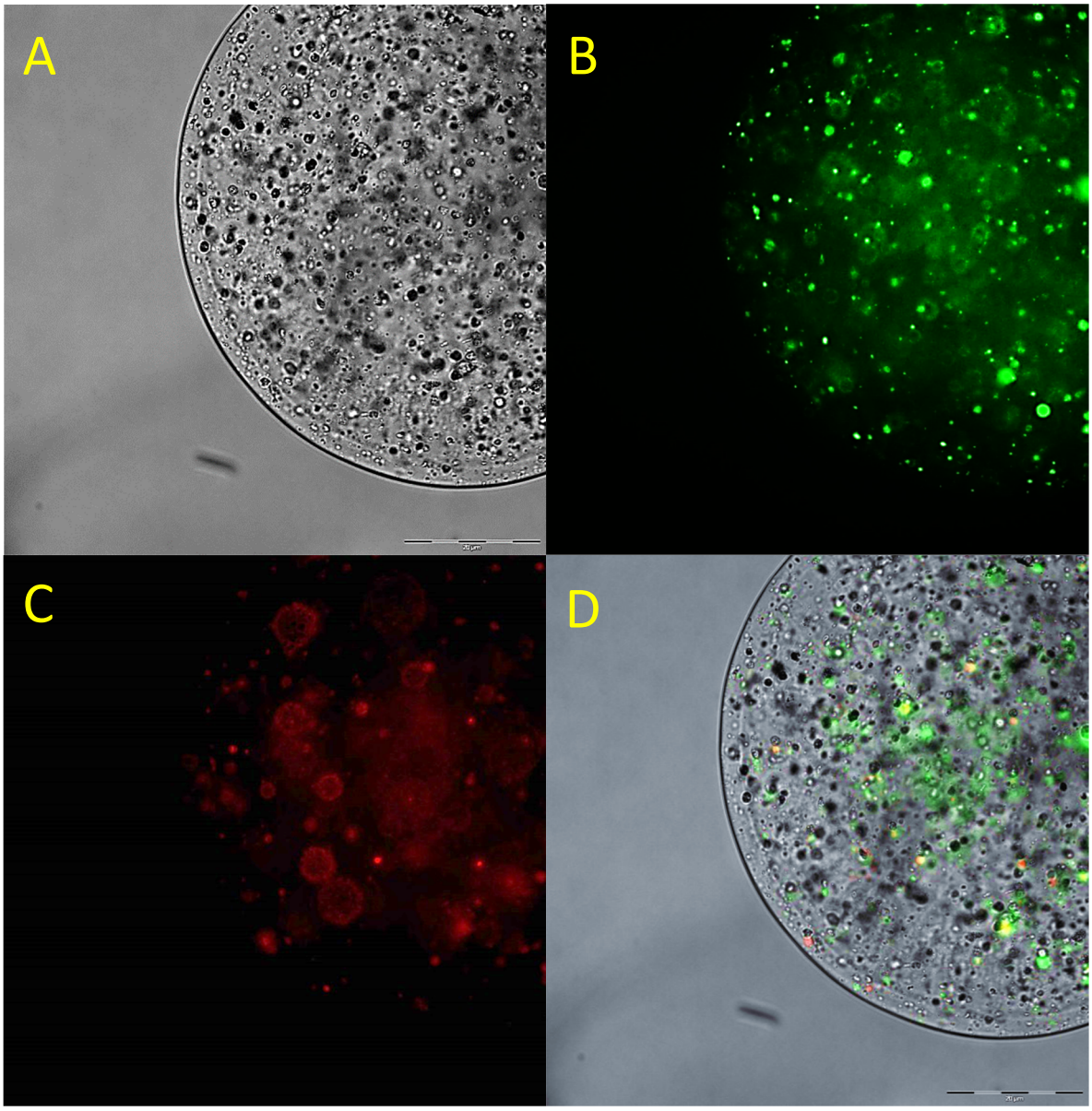

Figure 5.1: Effect of alginate encapsulation on the viability of iPSC prior to differentiation. iPSC were encapsulated in 2.2% alginate and stained with 6-CFDA and PI to determine the proportion of live and dead cells. A) Bright-field image of encapsulated iPSC. B) 6-CFDA-positive viable (green) cells. C) PI-positive dead (red) cells. D) Merged image of the capsule showing staining of live and dead cells. Black section of scale bar 20 µm

At day 9 of the differentiation the capsules were still intact and contained live cells (Fig. 5.2). The viability of cells was found to not change during the differentiation process (Fig. 5.3). The capsules contained 80% ± 13% live cells before differentiation. At the completion of the differentiation protocol, the percentage of viable cells in the capsules remained at 79 ± 10%.

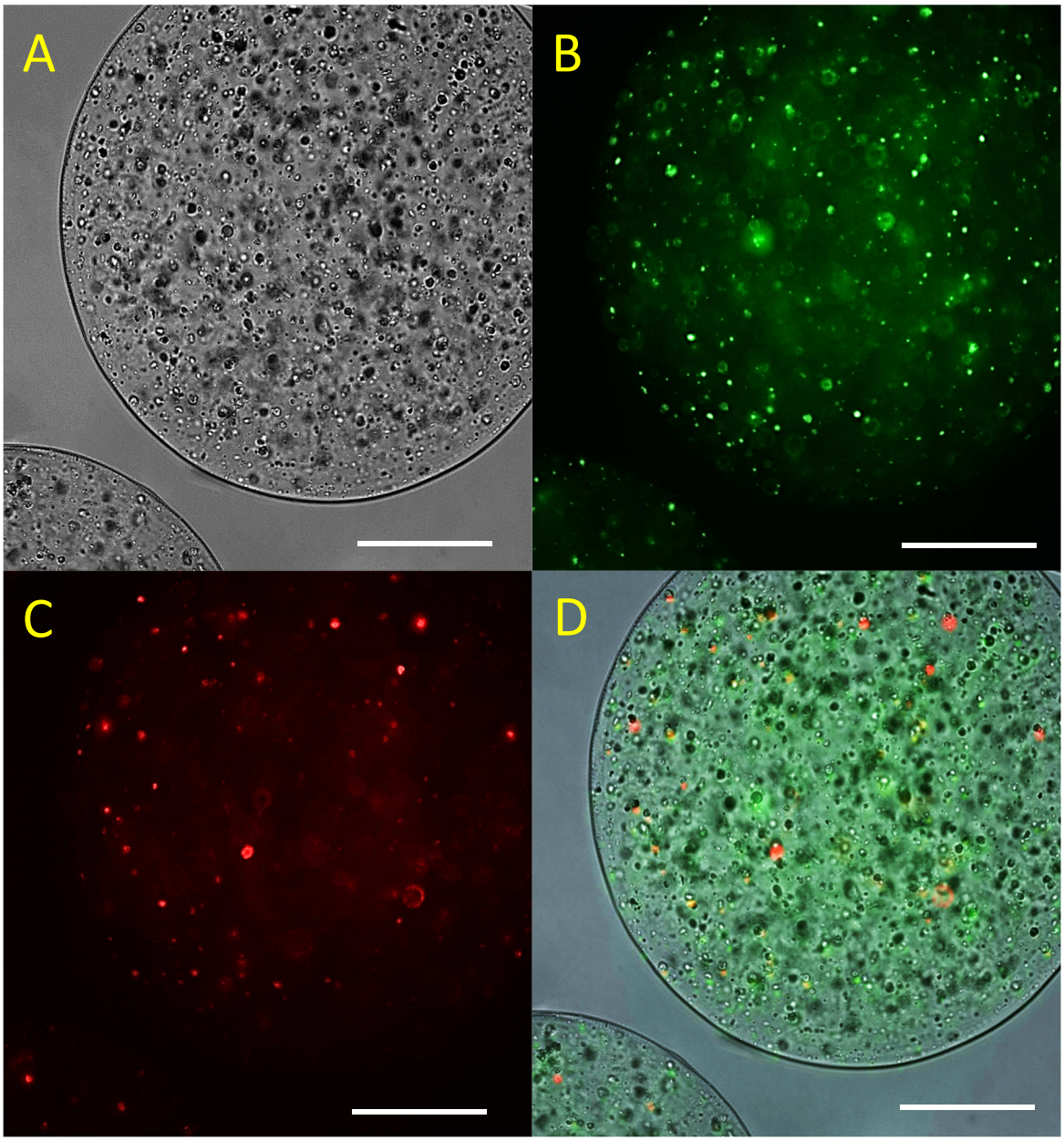

Figure 5.2: Viability of encapsulated hESC at day 9 of differentiation. hESC were encapsulated in 2.2% alginate and differentiated before being strained with 6-CFDA and PI to asses viability. Encapsulated Day 9 IPSC. A) Bright-field image of an alginate capsule showing the iPSC encapsulated in the spherical micro alginate capsule. B) 6-CFDA-positive viable (green) cells which have metabolised the stain. C) Dead cells with increased membrane permeability to PI stained red. D) Merged image of the capsule showing staining of live and dead cells. Scale bar 100 µm.

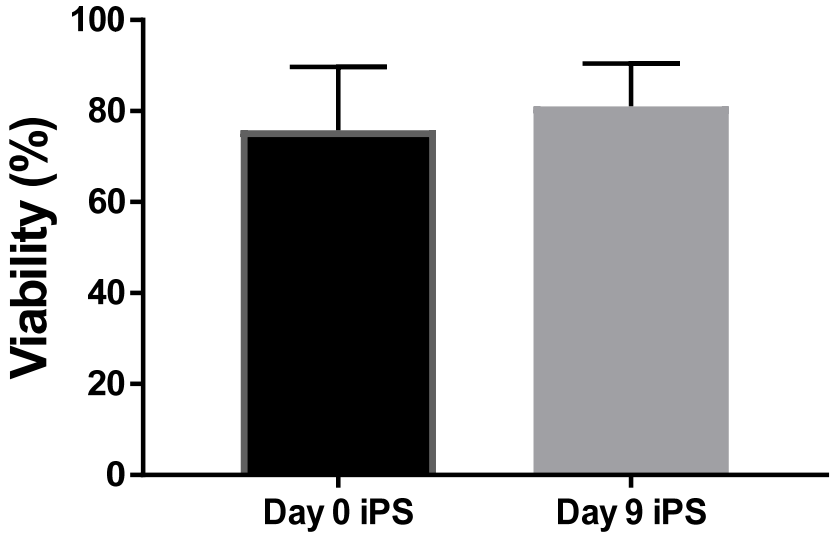

Figure 5.3: Quantification of the viability of the iPSC after encapsulation in alginate at day 0 and day 9 of differentiation. Cells were stained with 6-CFDA and PI to asses for viability. Viability was measured by counting the number of live and dead cells and expressed as a percentage of live cells to total cells. For each group at least 21 capsules from 4 experiments were analysed.

5.4.2 Gene transcript expression of iPSC samples during differentiation

To better understand the differentiation profile of the iPSC, gene transcript (mRNA) expression of key differentiation markers was analysed and compared to the encapsulated hESC differentiation data shown previously (Section 3.4.2). Encapsulated iPSC were differentiated following the same protocol as HESC and compared at the same key stages. Data are presented in the context of the gene expression profiles during differentiation (Fig. 5.4). Cells differentiated in Geltrex® were also analysed for expression of differentiation markers as shown in Fig. 5.11.

5.4.2.1 Pluripotency markers *OCT4* and *NANOG* are expressed similarly between cell types during differentiation in both hESC and iPSC.

Encapsulated iPSC data is compared to the encapsulated hESC data presented in Chapter 3. At the beginning of the differentiation protocol (Day 0) expression of *OCT4* was high at 350 x 10^3 and 131 x 10^3 fold over detectable for the encapsulated iPSC and hESC groups, respectively (Fig. 5.4) with no statistical difference between the groups. This expression then markedly decreased on day 3 to ~600 fold over

detectable for the iPSC group which continued to nearly undetectable levels for days 6 and 9. This change in expression was not statistically significant between the iPSC and the hESC.

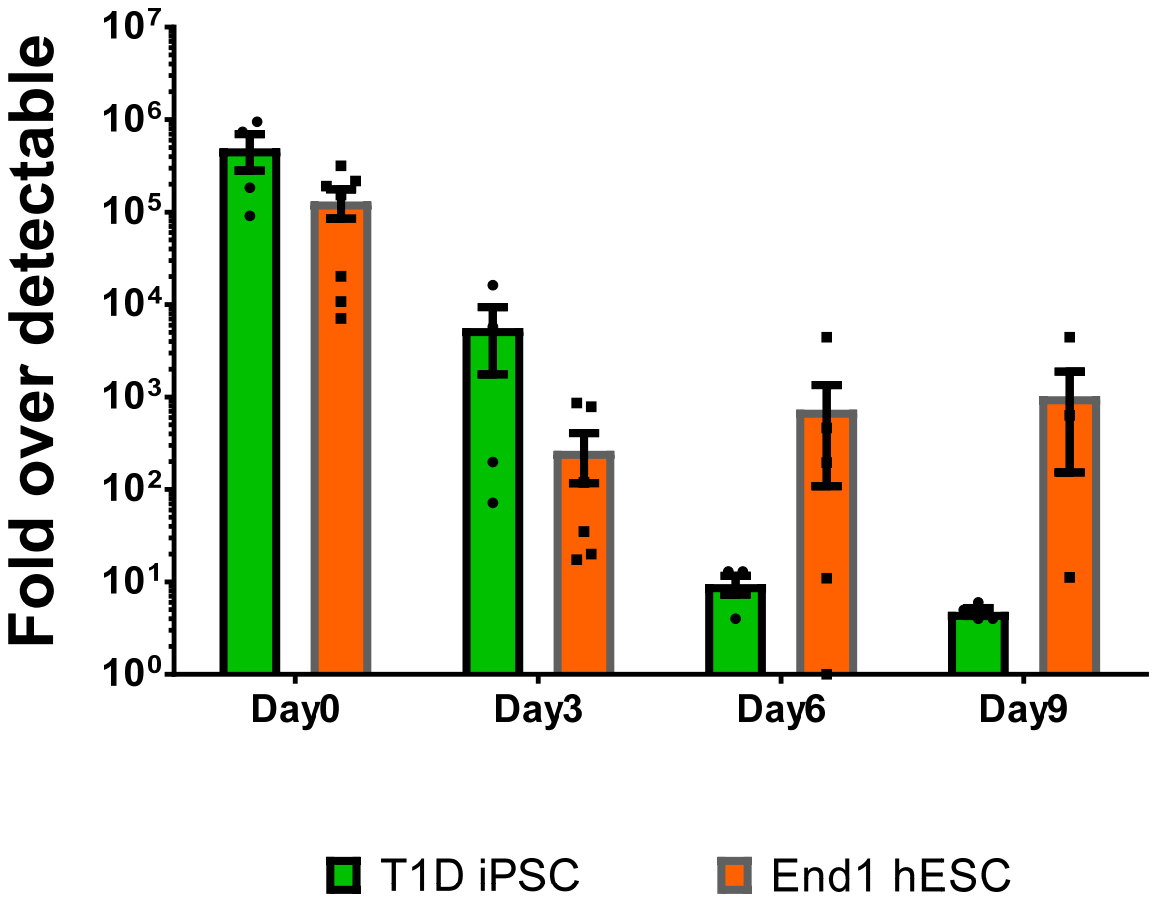

Figure 5.4: *OCT4* transcript expression of encapsulated iPSC compared to encapsulated hESC. Data shown as mean ± SEM, y-axis log10 (fold over detectable), n=4-8/group. Samples which did not reach the detection threshold could not be plotted on a logarithmic graph (n=2 for End1 hESC).

The pluripotency marker *NANOG* followed a similar expression pattern to *OCT4.* The pre-differentiation samples returned values of $4.2x10^5$ fold over detectable for iPSC (Fig. 5.5). Once the differentiation was initiated, the *NANOG* transcript levels dropped to near $1.5x10^3$ and very closely followed hESC differentiation expression for the following time points. The encapsulated samples expression levels continued to drop to 17 and near undetectable in days 6 and 9, respectively. Similarly, to *OCT4* expression, the expression of NANOG in the samples was variable for day 3, 6, and 9 samples, ranging from $8.5x10^3$ to undetectable.

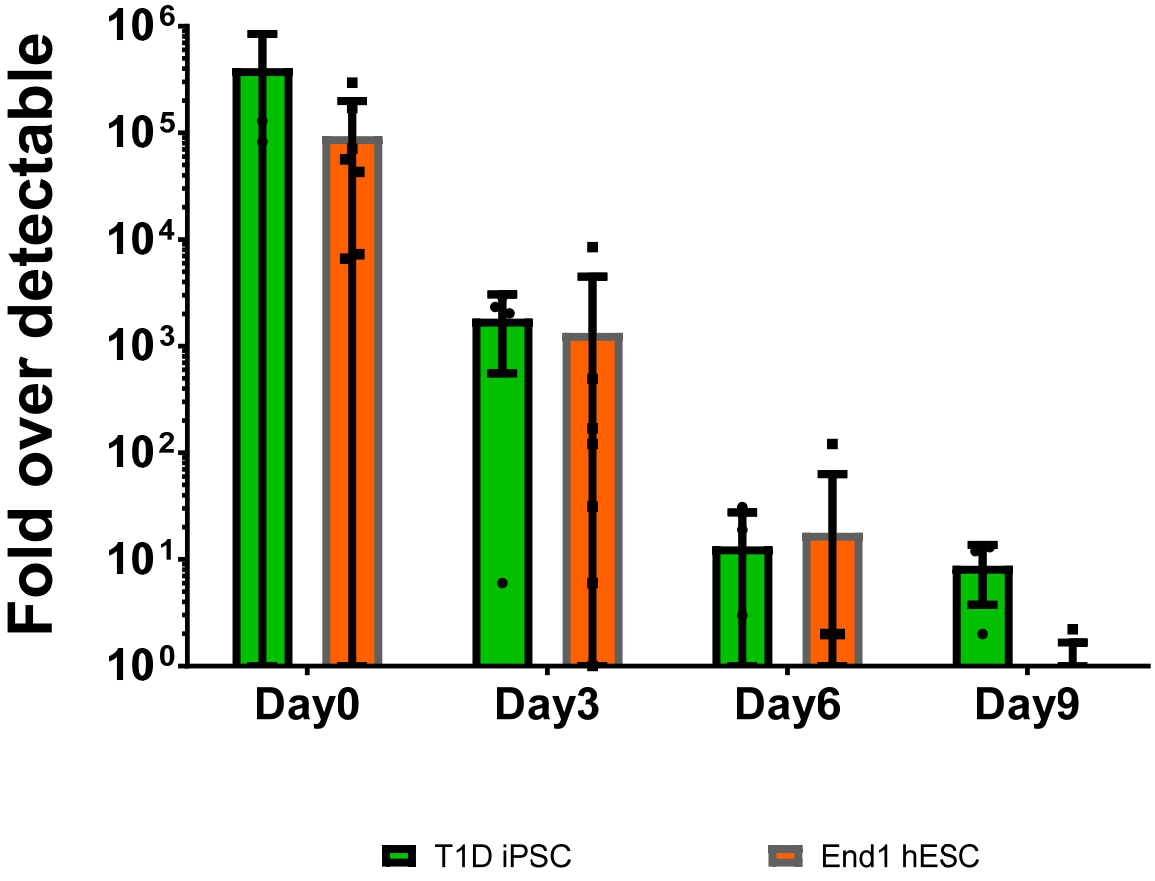

Figure 5.5: *NANOG* transcript expression of encapsulated iPSC compared to encapsulated hESC. Data shown as mean ± SEM, y-axis log10 (fold over detectable), n=4-8/group. Samples which did not reach the detection threshold could not be plotted on a logarithmic graph (n=7 for End1 hESC).

5.4.2.2 Expression of Definitive Endoderm markers *FOXA2* and *SOX17* peaks at day 3 of differentiation.

The expression of definitive endoderm marker *SOX17* was detectable in only one of the iPSC samples at day 0 (Fig. 5.6). At day 3 high levels of *SOX17* transcript were detectable with a mean expression of roughly 10^6 fold over detectable in the iPSC group, which represents almost one order of magnitude greater than the hESC. The expression of *SOX17* in the iPSC group then decreased markedly at day 6 to nearly undetectable levels (Day3 iPSC vs Day6 iPSC $P < 0.05$ ANOVA, Tukey's post-test). However, at day 9, in two out of 4 samples there were increases in *SOX17* expression ($P < 0.05$ ANOVA, Tukey's post-test).

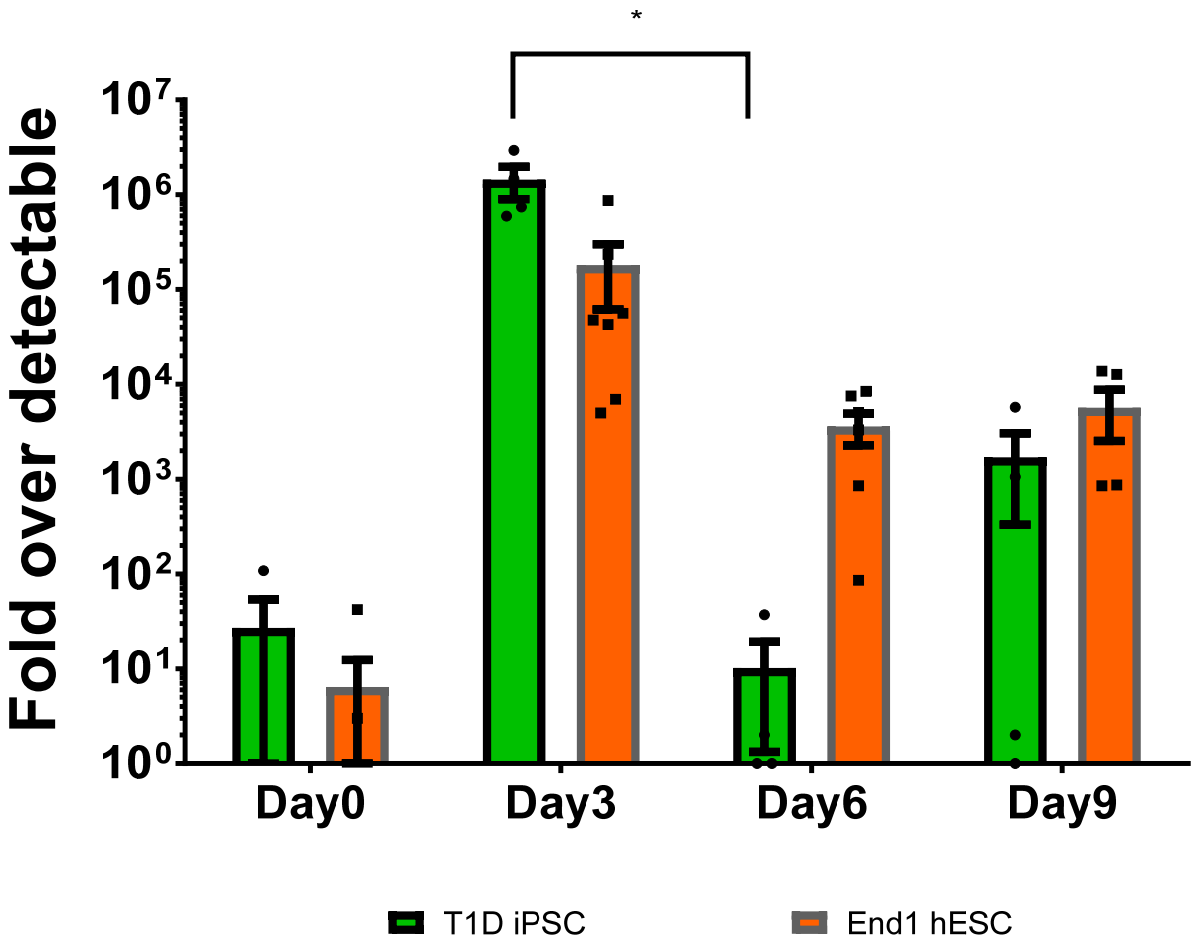

Figure 5.6: *SOX17* transcript expression of encapsulated iPSC compared to encapsulated hESC. Data shown as mean ± SEM, y-axis log10 (fold over detectable), * denotes $P < 0.05$ ANOVA, Tukey's post-test, n=4-8/group. Samples which did not reach detection threshold could not be plotted on a logarithmic graph (n=3 for T1D iPSC and 7 for End1 hESC).

In the iPSC, similar to *SOX17*, definitive endoderm marker *FOXA2* expression was also first detected at day 1. The expression pattern for *FOXA2* was similar to *SOX17* between days 3-9. These results were also significant (Day3 iPSC vs Day6 iPSC $P < 0.05$ ANOVA, Tukey's post-test) (Fig. 5.7).

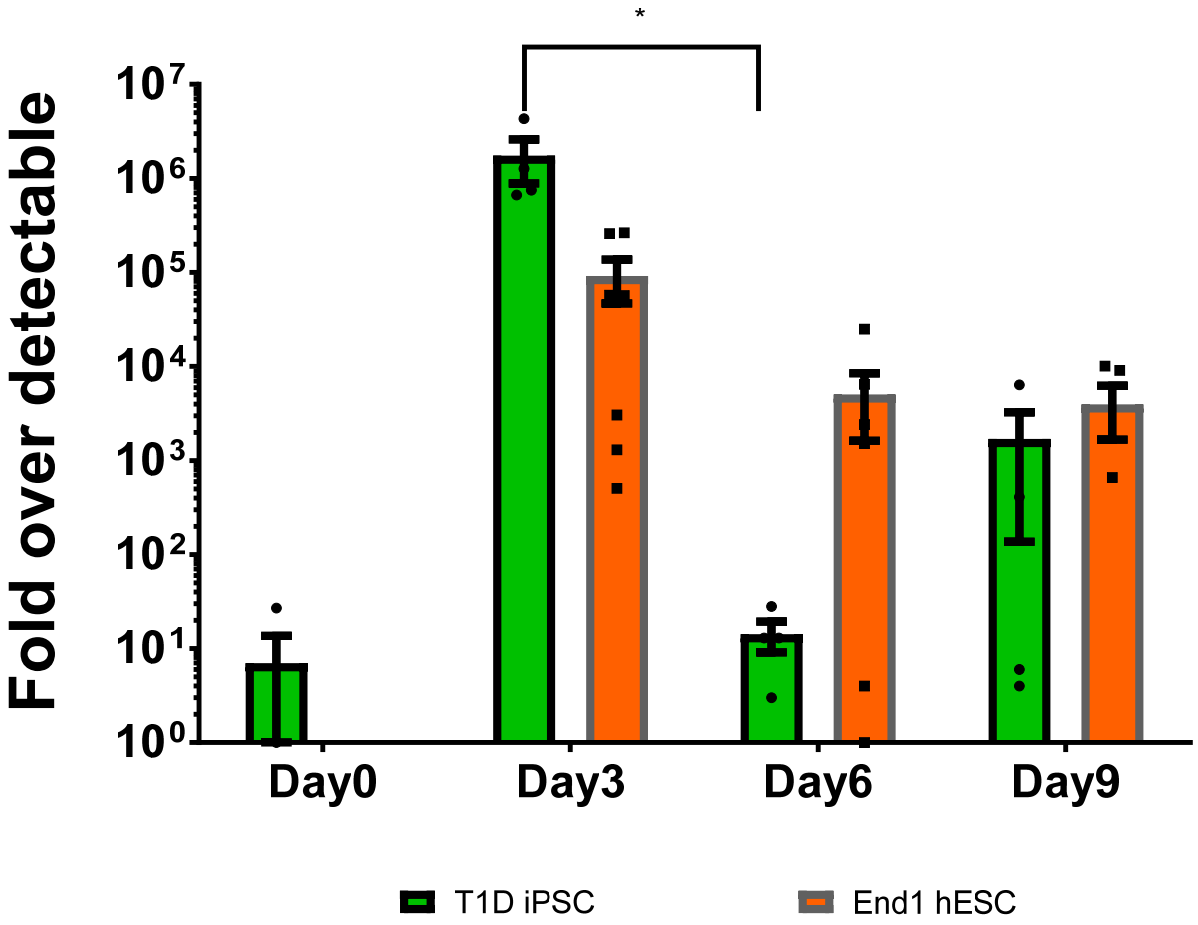

Figure 5.7: *FOXA2* transcript expression of encapsulated iPSC compared to encapsulated hESC. Data shown as mean ± SEM, y-axis log10 (fold over detectable), * denotes $P < 0.05$ ANOVA, Tukey's post-test, n=4-8/group. Samples which did not reach detection threshold could not be plotted on a logarithmic graph (n=2 for T1D iPSC and 7 for End1 hESC).

5.4.2.3 Primitive foregut/pancreatic endoderm markers *HNF4α*, *HNF1β* and *PDX1* expression peaks at day 9 of differentiation.

At day 3 the primitive gut tube markers *HNF4α* and *HNF1β* were first detectable in one of the samples. *HNF4α* increased expression on day 6 to 800x10^3 fold over detectable in the iPSC group. This expression was maintained through to day 9 with a statistical difference between Day 3 and Day 9 iPSC groups $P < 0.05$. There was a great deal of variation of transcript expression between differentiation experiments; this was evident especially in the day 6 and 9 samples (Fig. 5.8).

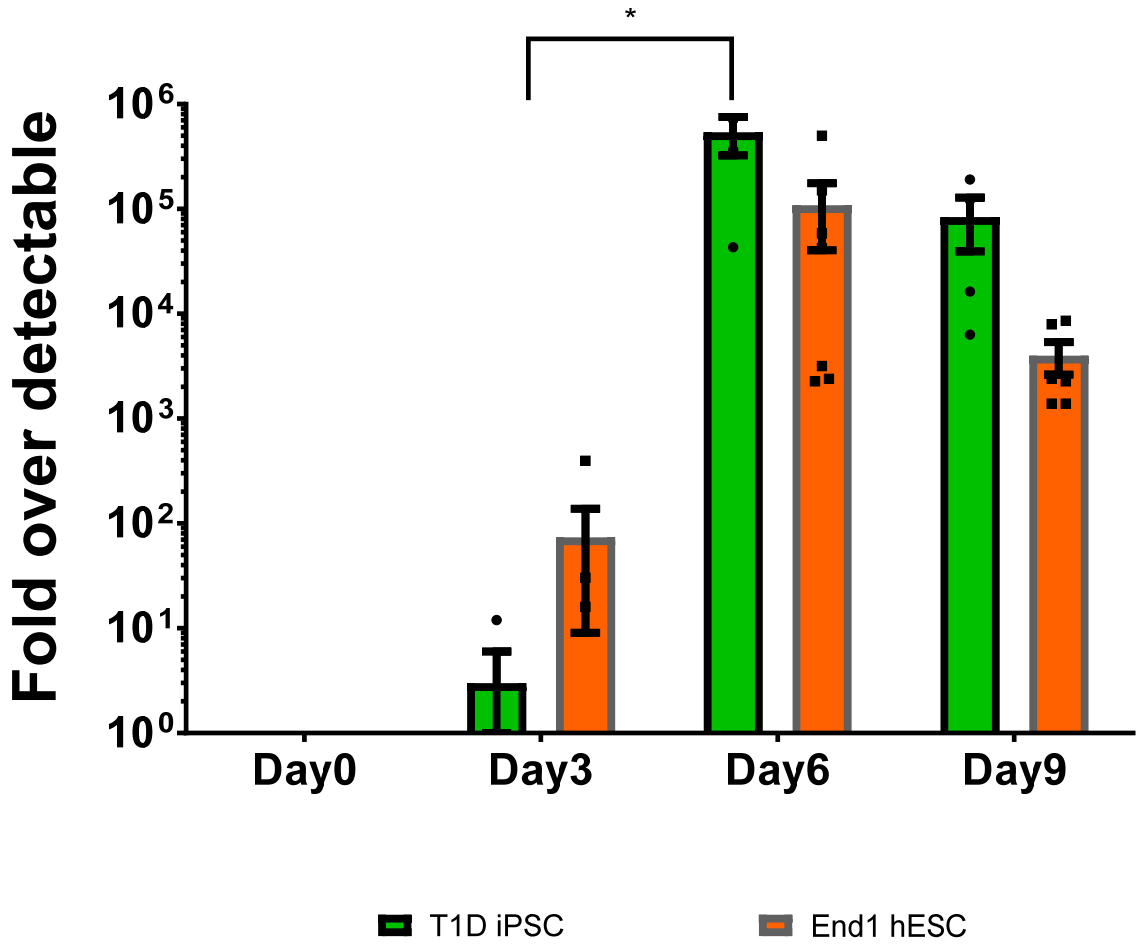

Figure 5.8: *HNF1β* transcript expression of encapsulated iPSC compared to encapsulated hESC. Data shown as mean ± SEM, y-axis log10 (fold over detectable), * denotes $P < 0.05$ ANOVA, Tukey's post-test, n=4-8/group. Samples which did not reach the detection threshold could not be plotted on a logarithmic graph (n=7 for each group).

The *HNF1β* transcript expression pattern was similar to *HNF4α*, first appearing at day 3 with only one sample having detectable levels of expression (Fig. 5.9). The mean expression increased to $700x10^3$ at day 6. A similar level of expression was sustained through to day 9. There was a statistical difference between Day3 iPSC vs Day6 iPSC $P < 0.05$ ANOVA, Tukey's post-test groups.

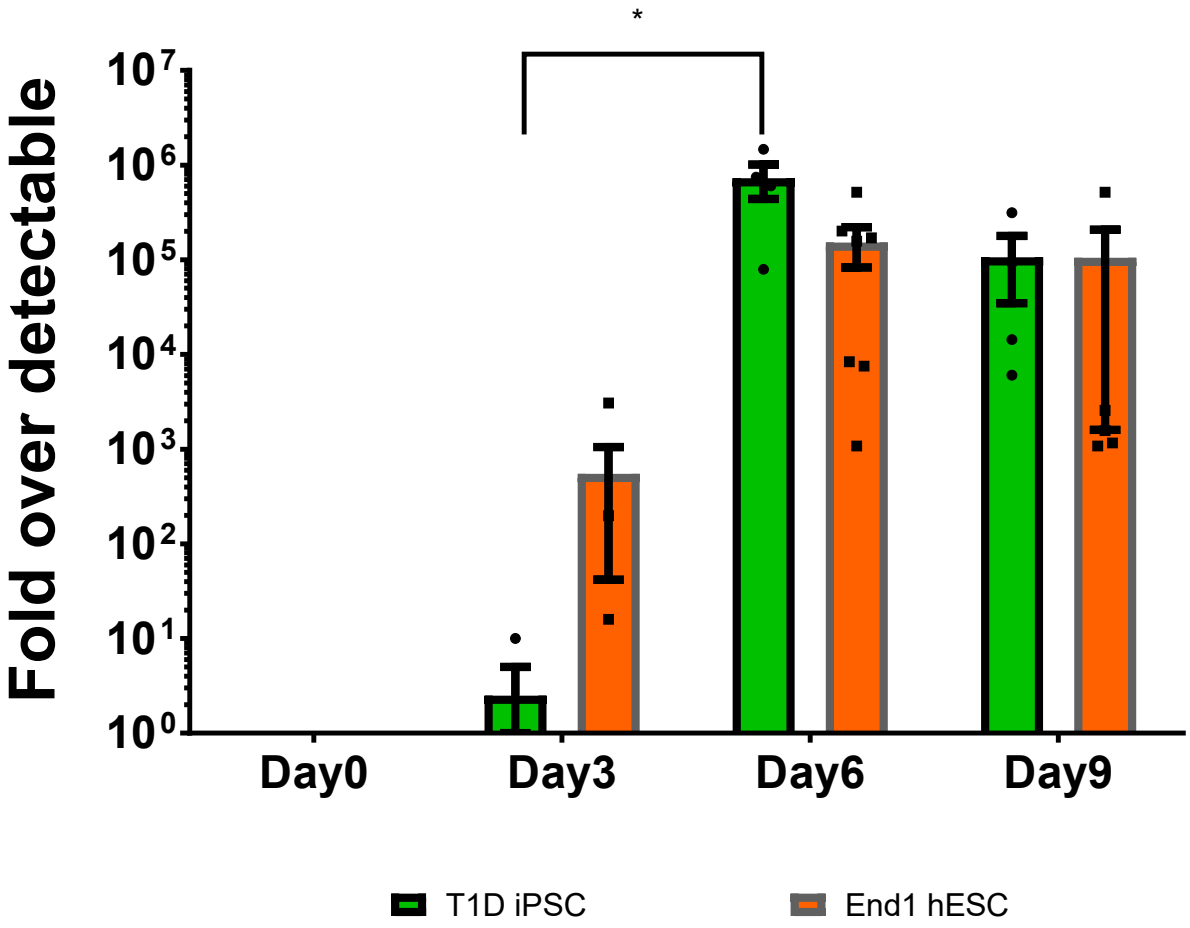

Figure 5.9: *HNF4α* transcript expression of encapsulated iPSC compared to previously shown encapsulated hESC. Data shown as mean ± SEM, y-axis log10 (fold over detectable), * denotes $P < 0.05$ ANOVA, Tukey's post-test, n=4-8/group. Samples which did not reach the detection threshold could not be plotted on a logarithmic graph (n=8 for each group).

At the endpoint of the differentiation process (day 9), *PDX1* expression was at levels comparable to that of the encapsulated differentiated hESC (Fig. 5.10). PDX1 expression was consistent, being detectable in all 4 differentiation experiments taken to day 9. There was no statistical difference in *PDX1* expression between the different cell types while encapsulated in alginate. Expression of *NGN3* and *NKX6-1* transcripts was also

assayed and it was found they were undetectable at all-time points in the differentiation process (data not shown).

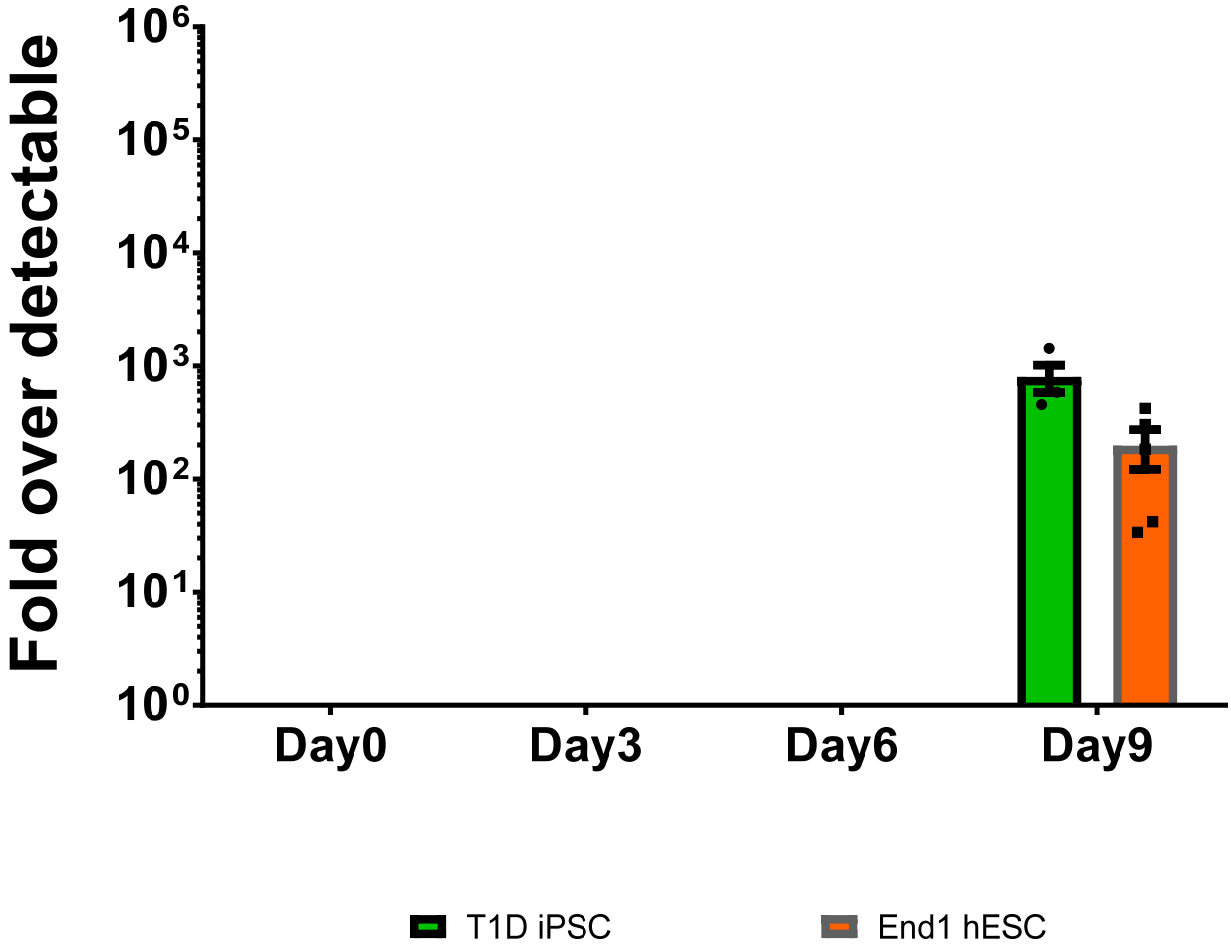

Figure 5.10: *PDX1* transcript expression of encapsulated iPSC compared to encapsulated hESC. Data shown as mean ± SEM, y-axis log10 (fold over detectable), n=4-8/group. Samples which did not reach the detection threshold could not be plotted on a logarithmic graph (n=12 for each group across days 0 to 6).

5.4.2.4 Differentiation of iPSC and hESC on Geltrex® produced similar transcript expression profiles.

Differentiation of the iPSC on Geltrex® showed the same trend in gene expression pattern as the hESC grew on Geltrex®. Both cell types initially expressed extremely high levels of pluripotent markers *OCT4* and *NANOG* of between 490,000 and 130,000 folds over detectable, respectively (day 0). None of the other differentiation markers was detectable at this point. The iPSC progressed through definitive endoderm, with *SOX17* and *FOXA2* expression, which was maintained through to day 9 of the protocol. Primitive foregut markers *HNF1β* and *HNF4α* were expressed highly at day 6 and were not statistically significant compared to expression levels in hESC at this time point. Finally, the expression of PDX1 was detectable at day 9 at higher levels in the iPSC than hESC, $P < 0.05$ Student's *t* test.

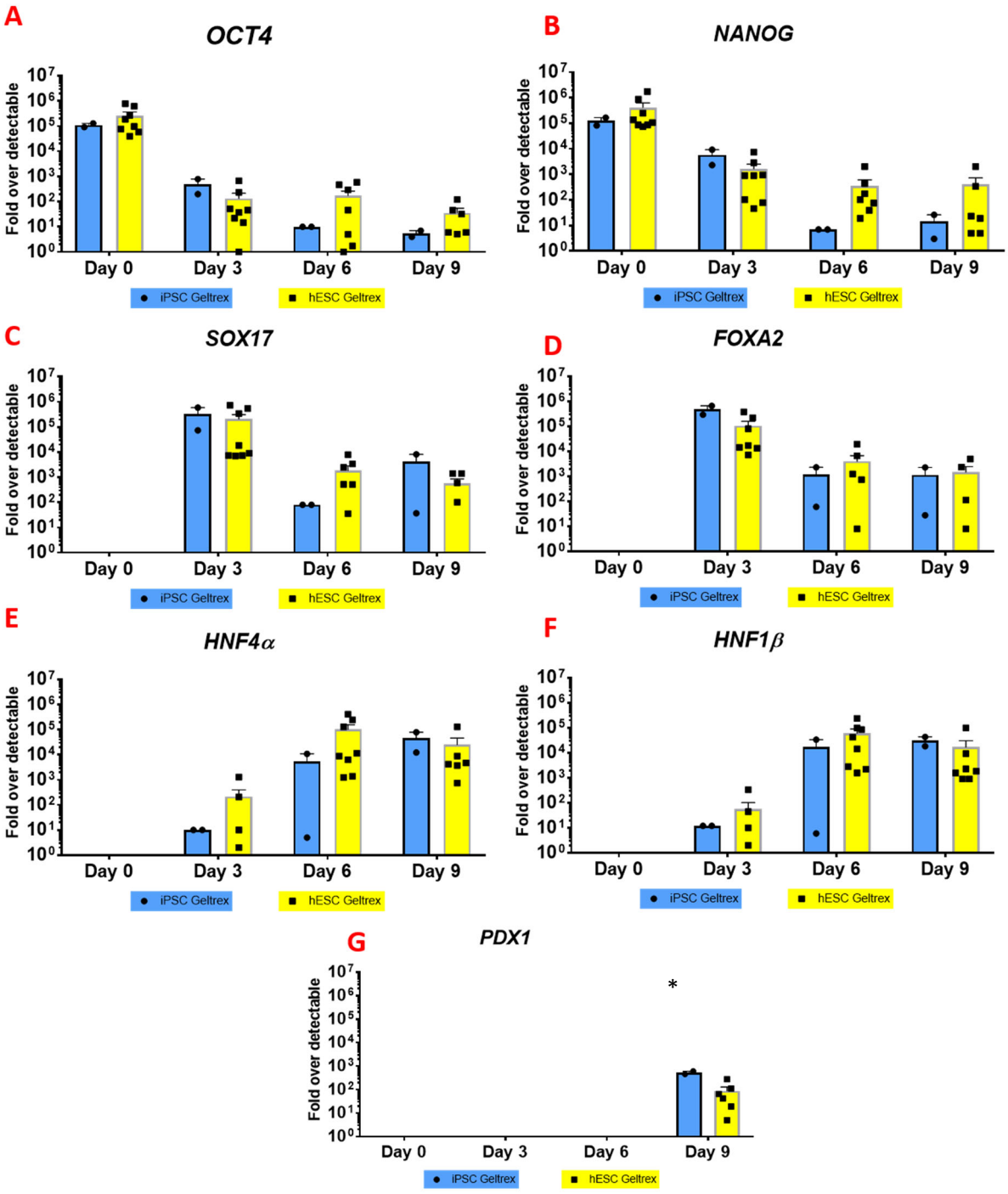

Figure 5.11: Transcript expression of iPSC differentiated on Geltrex® compared to Geltrex® hESC. A) *OCT4*, B) *NANOG*, C) *SOX17*, D) *FOXA2*, E) *HNF4α*, F) *HNF1β,* G) *PDX1*. Data shown as mean ± SEM, y-axis log10 (fold over detectable), n=2-8/group. Samples which did not reach the detection threshold could not be plotted on a logarithmic graph. Significance is denoted by * Student's *t*-test $P < 0.05$.

5.5 Discussion

The use of patient-derived iPSC is one of the proposed methods for overcoming immune destruction of a graft. As the grafted cells originate from the host they should not be recognised as foreign by the host's immune system. However, as the beta-cells in T1D are destroyed by an autoimmune process, even an autologous graft will require isolation from the immune system. It has previously been shown that iPSC can be differentiated in a similar manner to hESC into insulin-producing cells (187). This is the first time iPSC from a person with T1D have been differentiated while encapsulated in an immune-isolative matrix. This chapter aimed to determine if this was possible and if so, whether it was comparable to hESC differentiated in this manner.

First, iPSCs were analysed to test the effect of encapsulation on viability. The alginate is solidified in a bath of $BaCl_2$. Ba^{2+} ions can be cytotoxic, so it is crucial to eliminate residual Ba^{2+} ions by washing the microcapsules in PBS. Viability of iPSC was measured by determining the fraction of 6-CFDA positive cells in the total population, before and after encapsulation. As shown in Fig. 5.3, the viability of non-encapsulated cells at day 0 and the encapsulated cells at day 9 of differentiation was approximately 80%. This result demonstrates there was no effect of encapsulation on the viability of iPSC. This closely resembles the hESC differentiation process and indicates robustness of the encapsulated differentiation protocol (Fig. 4.1). As explained in Chapter 4, it is important to appreciate the absolute quantification of numbers is difficult in these 3D cultures, but assuming the cells were spaced randomly in the capsules, examination of large numbers of cells in a single plane of focus would provide a representative subset of cells to get an accurate estimate of their viability. We have specifically chosen this method of analysis by microscopy compared to other established methods. Viability measurement by flow cytometry analysis (e.g. 7AAD/PI staining) would require the alginate capsules to be dissociated by a high concentration of EDTA, which might reduce the viability of the cells. Our method of focusing on the orthodrome of the alginate capsule ensured that cells with the greatest distance to the surface were examined as well as the greatest number of cells being in focus. If decreased diffusion rate of oxygen and nutrients through the alginate caused

increased cell death, those cells would be located near the core of the capsule. Therefore, this quantification is a conservative estimation of the live cell count and viability.

After ensuring encapsulated cells were viable for 9 days in culture, gene expression of key markers of differentiation was analysed by RT-qPCR. As shown in Figs. 5.2 to 5.10, expressions of *OCT4, NANOG, SOX17, FOXA2, HNF1β, HNF4α and PDX1* were comparable between the encapsulated iPSC and hESC. While unpublished data from the laboratory of, and conducted by, Dr Jun Liu showed the iPSC were pluripotent and could differentiate into the three germ layers (Supplementary figure 5.12), it was important to examine the characteristics of the cells while encapsulated. The successful differentiation of the cells past the definitive endoderm layer was a key success as this has been a previous hurdle for non-encapsulated iPSC obtained from people with T1D (186). Throughout the encapsulated differentiation the iPSC gene expression was comparable to that of the hESC and, as previously discussed (Section 4.4), published hESC and iPSC differentiation (64).

The gene expression data for the iPSC grown on Geltrex® also were comparable to similarly grown hESC (Fig. 5.11). This provides supporting evidence that pluripotent stem cells, regardless of their origin, when exposed to the same differentiation protocol, will produce the same cell type. This has clinical significance if iPSCs are to be considered as part of a cell bank to use as allogenic transplant tissue.

As T1D is an autoimmune condition with an allogenic transplant, the insulin-producing cells would need to be protected from the immune system. This requirement, as well as the protection afforded by alginate capsule during differentiation in a bio-reactor setup, supports the idea that microencapsulation prior to differentiation is an appropriate procedure. This proof of concept would further be of use for allogenic as well as reprogrammed autologous cells in the treatment of T1D.

Previous publications have shown variation in gene expression during and post differentiation on the pancreatic lineage of T1D iPSC (186). As only one iPSC line was available, it was not possible to determine the effect of encapsulation on gene expression variability between iPSC lines or clones. This variability

extended to the point where some clones in previously published work were not able to pass definitive endoderm (186); a problem not observed in our cell line even with a similar induction method.

As the partially differentiated iPSC were not mature beta-cells, assaying them for insulin secretion yielded negative results (data not shown). Taking the cells to a mature stage either through *in vivo* maturation or the greater duration *in vitro* differentiation protocols would enable the investigation of their insulin-producing and glucose-sensing abilities. Future investigation using these cells could focus on the role that differentiation protocol plays in insulin-production and glucose-sensing.

The next stage in understanding the differentiation of iPSC would be two faceted. Firstly, investigate the *in vivo* maturation of these cells via transplantation into an immunodeficient diabetic mouse. This would ideally be comparable to the *in vivo* maturation seen with the hESC. Once this was established, the cells could then be transplanted into an immunocompetent model to enable the investigation of any inherently auto-immunogenic properties of the iPSC. Secondly, a greater number of iPSC lines could be differentiated to understand if there is a difference between T1D-derived lines and potentially T2D lines. This is a natural extension of the project as it is common for T1D treatments to be applied to end-stage T2D patients.

The applications to T2D patients may also inform the application to T1D patients, as late-stage T2D do not have autoimmune destruction of beta-cells, rather a loss of beta-cell mass attributed to overworking the cells. The use of iPSC would not have the autoimmune complication to overcome.

This chapter showed that the iPSC can be successfully differentiated into pancreatic precursor cells while encapsulated in alginate microcapsules. The differentiation gene expression profile is similar both while encapsulated as well as on a 2D substrate. Using iPSC as a pluripotent cell source offers opportunities for both research as well as clinical treatments.

5.6 Supplementary figure

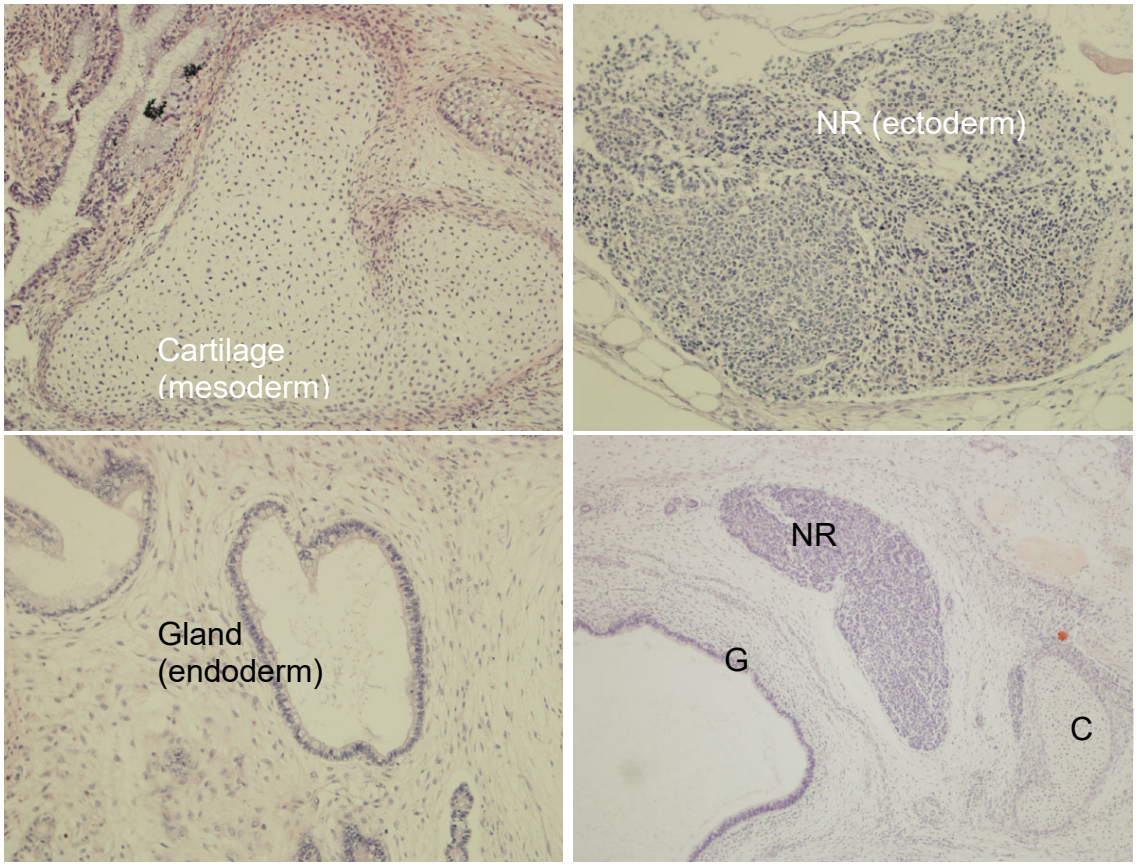

Supplementary Figure 5.12: T1D iPSC cell line developing into the three germ layers when transplanted into an immune deficient mouse. Pictures supplied by Dr Jun Liu, Monash University.

Chapter 6

General discussion and conclusion

6.1 Discussion and conclusion

T1D affects up to 21 million people worldwide, with an increasing incidence. In Australia, for example, it is increasing at the rate of ~3% pa (188) and accounts for 9% of all diabetes cases in that country (189, 190). T1D is an autoimmune disease in which the beta-cells of the pancreas are destroyed. Beta-cells produce and secrete insulin, which is required for the uptake of glucose into muscle and fat cells. Currently, T1D is primarily managed through regular blood glucose measurements followed by multiple daily injections or pump-administered insulin. While these treatment regimens have been improved over time, they remain time-consuming and do not provide the same level of glucose homeostasis as endogenous beta-cells. This can lead to fluctuating glucose levels, macro and microvascular complications such as coronary heart disease, retinopathy and nephropathy (42).

Alternatively, intensive glycaemic control with the use of subcutaneously administered insulin runs the risk of hypoglycaemic episodes due to delayed absorption times and imprecise quantity requirements (42). Individuals who experience these hypoglycaemic episodes without the release of counter-regulatory hormones, including glucagon, adrenaline and growth hormone, are at greatest risk of death (191). As these hormones signal to the liver to convert stored glycogen to glucose and release it. The lack of hypoglycaemic symptoms is termed hypoglycaemia unawareness and is treated by reducing the amount of insulin administered, thereby relaxing glycaemic control. Symptoms of hypoglycaemia may occur thereafter as the body adjusts to the alteration of glycaemic control. An alternative more permanent treatment is by replacing the missing ß cells with a whole pancreas or an islet transplant from a human cadaveric donor.

There are several major limitations to islet transplants. Firstly, the patient is required to undertake lifelong immunosuppression of which at least half will lose insulin independence within 5 years (192). The need for toxic anti-rejection drugs greatly reduces the benefit of the transplant as the recipient is at a greater risk of infections, cancer and nonimmune tissue toxicities from the immunosuppressants (193). Secondly, there is a lack of available transplantable tissue with only 12 islet transplantations taking place in Australia in 2017 (55). To alleviate the need for immunosuppression, the tissue must either be tolerated by the host's

immune system or isolated from the immune system. A reprogrammed autologous source is one option for transplantable tissue. However, T1D is an autoimmune condition, indicating that even an autologous source will be immunoreactive. This leaves immune isolation as the most logical and promising approach for replacement cell therapy transplants.

One option in addressing the lack of transplantable tissue is the use of pluripotent stem cells to generate replacement ß cells. As examined in Chapter 1, a number of companies are currently investigating the use of these cell types in therapies for T1D. While "hybrid closed loop" glucometers and insulin pump combinations have already entered the market, they are yet to respond to changes in blood glucose levels as rapidly or as sensitively as beta-cells (194). In addition, their external nature and costly consumables impact on the quality of life of their users. Therefore, there is still demand for a superior alternative. One such alternative is a cell therapy which does not require immunosuppression. It is likely the combination of immunoisolation device with ß cells derived from stem cells which will replace cadaveric sourced pancreatic islets in the treatment of T1D.

A promising approach to achieving long-term graft survival without immunosuppression is by placing the graft tissue in an immunoisolation device. Though many immunoisolation devices have been developed, none are yet to make it to market. One promising strategy which is being trialled is the use of alginate to provide this immunoisolation. This inert material is permeable to small molecules and can be transformed from a viscous gel into robust microcapsule through brief exposure to a cation solution (usually calcium or barium). Sourced from seaweed, the polysaccharide can be suitably purified to remove immunogenic contaminants so that it will be mostly inert when transplanted *in vivo*. The pluripotent stem cells described in this thesis were encapsulated in high purity barium alginate microcapsules. Many studies have shown these capsules are at least partly immunoprotective to the cells without immunosuppression (195). Similar results have been found with insulin-producing cells differentiated from hESC and encapsulated in surface-modified alginate transplanted in mice (65). The alginate microcapsules are unique from previously published encapsulated differentiation (116), the concentration of the alginate spheres is much higher in

this work (2.2% vs 1.1% Chayosumrit et al, 2010) this increases the structural integrity of the alginate preventing large clusters (and large voids to hold the clusters) from forming. On the 2D geltrex differentiation plates, clusters could be seen as the cells divided moved away and differentiated.

Microencapsulation is a cross-disciplinary area requiring expertise from different fields to overcome the hurdles necessary for the successful clinical translation of this technology. Many physical and chemical properties of the transplantable materials along with their molecular interactions within a biological system must be taken into account when using it for the purpose of cell therapy. While a great deal of work has been undertaken to resolve the requirements for cell growth and immunoisolation, little work has been done to progress the differentiation of cells while encapsulated.

In this thesis, strategies were designed to investigate the differentiation of pluripotent stem cells while encapsulated. This was done to enhance the production and survival of pancreatic progenitors so they may produce a superior outcome after transplantation.

The first limiting factor associated with pancreatic progenitor differentiation was the selection of a differentiation protocol. Although this has been extensively researched progress has been difficult. At the beginning of the project, Rezania *et al.* (67) were the most recent and arguably the most advanced protocol for differentiation of hESCs to pancreatic progenitors. They had shown the differentiation of hESC to poly-hormonal (insulin and glucagon) cells which corrected hyperglycaemia in immunodeficient mice. This was an improvement from the basic protocol published by Kroon *et al* in 2008 (61). Taking these protocols as the foundation, I differentiated cells while they were encapsulated. Compared to differentiation on a 2D surface, previous work on encapsulated differentiation is extremely limited. Chayosumrit *et al.* (116) successfully differentiated alginate encapsulated hESC to the definitive endoderm stage, showing decreasing pluripotency transcripts (*OCT4* and *NANOG*) as well as increasing definitive endoderm transcripts (*FOXA2* and *SOX17*). In this thesis (Chapter 3), it was demonstrated that hESC differentiated while encapsulated in alginate could progress through the developmental stages to pancreatic progenitors. In addition to this, I showed that during this differentiation process viability was not compromised (Fig. 3.3

P > 0.05). The cells expressed developmental stage-specific markers (Fig. 1.4) of the differentiation process in an indistinguishable fashion both from the 2D differentiated hESC (Figs. 3.4 to 3.10 *P* > 0.05 Geltrex® vs Encapsulated) as well as previously published work (61). While there is extensive research being carried out on the differentiation of hESC to pancreatic lineages on 2D matrices, this is the first study to show the similarity of iPSC from a T1D within a 3D matrix.

The second innovation, the maturation of these differentiated cells while encapsulated *in vivo*, was discussed in chapter 4. Previous studies showed the maturation of pancreatic progenitors transplanted under the kidney capsule in diabetic mice (67). The microcapsules cannot be placed under the kidney capsule due to their diameter and the quantity required. The intraperitoneal cavity was selected as an alternative transplantation site. This location has many advantages such as the surgery to place the cells being minimally invasive while maintaining excellent exposure to interstitial fluid and blood supply. The survival of the graft *in vivo* was encouraging (Fig. 4.2; *ex vivo* viability 65%) but the most important measure was the maturation of the cells over this period. As previous work had shown that cells transplanted under the kidney capsule began to correct hyperglycaemia within 50 days (169). In this thesis the encapsulated cells analysed *ex vivo,* were positive for insulin transcript as well as other key maturation markers (Figs. 4.8 to 4.15).

By far, the strongest evidence for continued survival and maturation of the cells *in vivo* was the detection of human C-peptide in the circulatory system of the transplanted mice (Fig. 4.4; *P* < 0.05). Human C-peptide has a short half-life of ~30 min (196). Therefore the source of the human C-peptide found in the transplanted mice would be from the transplant itself. As explained in Chapter 4, the inability of the transplant to correct the hyperglycaemia (Fig. 4.6) is mostly due to lack of enough insulin being produced by the graft to lower circulating glucose levels. As previously discussed, the cells produced 0.54×10^{-4} U/day, an extremely low amount from a transplanted quantity of 2 million cells. This corresponds to 375 pmol (197) of insulin. The insulin content of a beta-cell has previously been reported as 1.1×10^{-14} mol (198) in this content was released in a day, our measurement of 375 pmol in the serum would be coming from

~29455 cells. However, this does not take into account, the degradation of insulin secreted, thereby reducing the serum content. If 29455 cells did secrete insulin from a transplant of 2 million cells this would represent ~1.5% of the transplanted cells secreting insulin. This estimate is contingent on the transplanted cells releasing 100% of their insulin. If the insulin secreting cells are secreting only 5% of their insulin content per day then the number of cells producing insulin may be as high as 30%. Of course, this does not take into account cells death and/or cell proliferation during the differentiation process. Increasing the number of cells transplanted into the mice would be an effective means of trying to increase insulin production. However, increasing the differentiation efficiency (percentage of insulin-producing cells) prior to transplantation might reduce the number of capsules that need to be transplanted and keep the number down to a practicable level. Nonetheless, the survival and maturation of the cells *in vivo* support the potential of this method of stem cell differentiation for transplantation.

Having characterised the differentiation of hESC while encapsulated and shown the continued maturation *in vivo*, the application of this technique to other pluripotent cell sources was discussed in Chapter 5. The survival and differentiation transcripts shown in chapters 3 and 4 indicated that the differentiation down the pancreatic lineage was occurring, the cells were able to reach an insulin-producing stage and therefore induced pluripotent cells from a person with T1D were selected. This has a dual purpose: firstly, as a real-world application as a model for autologous transplant and secondly as a model to understand the immunogenic and developmental components of T1D progression. Successful differentiation of iPSC from a person with T1D into beta-cells has been shown previously (180). Following this example, we characterized the differentiation of iPSC from a person with T1D while the cells were encapsulated in alginate. These cells showed a similar differentiation profile to that of the encapsulated hESC and this is supportive of the techniques applicable across different sources of pluripotent cells.

There are several clear goals which need to be reached for differentiation inside microcapsules to progress and be considered an alternative to encapsulation post differentiation. The foremost is the correction of hyperglycaemia in diabetic mice. As previously mentioned, the current transplantation protocol of 2 million

cells in 2 mL alginate spheres does not provide enough insulin to lower blood glucose levels. Previous publications have shown that as few as 100 clusters of "several hundred cells" was able to correct hyperglycaemia in an immunocompetent mouse model (65). The circulating human C-peptide suggests that there were ~30,000 insulin-producing cells present in the transplant.

This returns us to the original question: why was hyperglycaemia not corrected in the mice? The transplantation site is unlikely to be the cause as previous long term glycaemic control has been achieved using alginate sphere-encapsulated cells in the peritoneum (65). One explanation is the lack of glucose sensitivity of the transplanted cells. If there were as many insulin-producing cells as previously estimated, yet they did not release insulin in response to increased BGL, it would explain the presence of the C-peptide but not the correction of hyperglycaemia. This small consistent release of insulin has been previously reported in immature beta-cell differentiation protocols (73). Future work should focus on the imprecise nature of the maturation, specifically following an extended *in vitro* differentiation protocols to a mature beta-cell (65). As this thesis shows that alginate encapsulation does not seem to inhibit differentiation of pluripotent stem cells towards insulin-producing cells in a shortened, *in vivo* model. It is therefore reasonable to expect that the replication of longer *in vitro* protocols, while encapsulated, would yield the same mature beta-cells.

Experiments undertaking the longer *in vitro* differentiation to a mature beta-cell would also provide the opportunity to understand in greater detail the transplants' first 2 months of maturation while encapsulated. While key outcomes were not observed during this time in my experiments (no correction of hyperglycaemia), the transplanted mice did not require insulin for a month. This period also coincided with a drop in the BGL from beyond the detectable range to 25-30 mmol/L. Assessing the extended *in vitro* differentiation for the insulin-producing capacities of the encapsulated cells during this time could provide an alternative transplantation window.

Finally, this model has been developed in an immunocompromised mouse. While there was no evidence of a foreign-body reaction in our model, current research suggests that alginate alone is not sufficient to

avoid the host's foreign-body response (112). There has been a success with modification of the alginate to avoid this response (65). While modification of the alginate should not inherently affect the outcomes of the differentiation protocol, as the signalling molecules travel through the pores in the alginate structure. However, if the modification changes the mechanical properties of the alginate this may affect cell differentiation. This is another variable which could be explored in the future.

There are several drawbacks of this differentiation procedure which have been highlighted in this thesis. The first is that once the cells are encapsulated any cells which die are retained in the alginate capsule until they break down sufficiently to diffuse out. This combined with the alginate microcapsules rigidity preventing the proliferation of large colonies is a hindrance on the number of insulin-producing cells available. Further investigation of alginate concentration optimization and modification is a clear pathway to correct this. The next limitation is the *in vivo* maturation as a low-efficiency method of maturation. As differentiation protocols have developed, *in vitro* maturation has improved (180). The testing of these longer in vitro maturation protocols on encapsulated cells are likely to yield a more homogeneously mature population. Finally, the model these cells were transplanted into was an immunocompromised mouse model. Without data from an immunocompetent transplant model, specifically one that is a allograft, not xenograft, this work cannot advance past the preclinical stage. This may also involve combining the alginate microcapsules with a larger macroenapsulation device as discussed in Chapter 1.

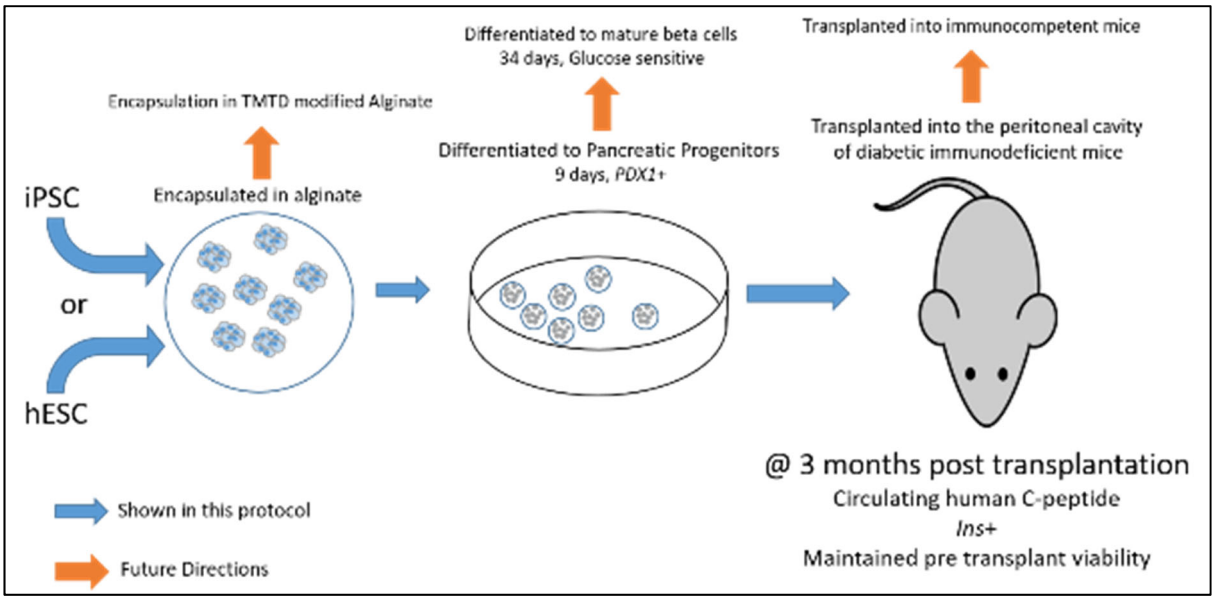

Figure 6.1: Model for differentiation of pluripotent stem cells while encapsulated in alginate.

While not the focus of this body of work, the selection of transplantation sites is important for the success of cell therapies. The transplantation sites in this thesis were selected for their common use in previous research, kidney capsule for non-encapsulated cells and peritoneum for encapsulated. As this field approaches, and is in, clinical testing, alternative sites and retrieval requirements have been trialled. Traditionally, human islets are transplanted into the portal vein; this site is not feasible for microencapsulated cells due to the risk of occlusion. Transplantation of free-floating encapsulated cells into the peritoneal cavity has been the most common location. While the retrieval of these cells *post mortem* is not an issue, in a live patient ensuring the retrieval of any capsules is not feasible. This requirement for the transplant to be retrievable is seen as a safeguard for patients receiving new treatments. Thus the use of macro encapsulation devices around microencapsulation devices may be one method of utilising the strengths of both. In addition to ease of retrievability, these devices may serve to increase angiogenesis or immunoisolation of the transplant. As this thesis has shown that it is possible to differentiate pluripotent stem cells while microencapsulated, it is worth considering if this principle could be extended to cells while both micro and macro encapsulated. In conclusion, this thesis shows that pluripotent stem cells can differentiate whilst encapsulated. Cells remain viable, protected and progress through the expected developmental stages inside alginate microcapsules. Further investigation into the maturation of the cells

to become glucose-sensitive as well as appropriate dosage levels is required before advancement of the therapy to human trials.

Chapter 7

Bibliography

7.1 References

1. Becker AJ, McCulloch EA, Till JE. Cytological demonstration of the clonal nature of spleen colonies derived from transplanted mouse marrow cells. 1963.
2. Phinney DG, Prockop DJ. Concise Review: Mesenchymal Stem/Multipotent Stromal Cells: The State of Transdifferentiation and Modes of Tissue Repair—Current Views. Stem cells. 2007;25(11):2896-902.
3. Jaatinen T, Laine J. Isolation of hematopoietic stem cells from human cord blood. Current protocols in stem cell biology. 2007:2A. .1-2A. .9.
4. Rippon HJ, Bishop AE. Embryonic stem cells. Cell Proliferation. 2004;37(1):23-34.
5. Kitambi SS, Chandrasekar G. Stem cells: a model for screening, discovery and development of drugs. Stem cells and cloning : advances and applications. 2011;4:51-9.
6. De Coppi P, Bartsch G, Siddiqui MM, Xu T, Santos CC, Perin L, et al. Isolation of amniotic stem cell lines with potential for therapy. Nat Biotech. 2007;25(1):100-6.
7. Evaluation of Outcomes With Amniotic Fluid for Musculoskeletal Conditions Musculoskeletal Conditions [Internet]. 2018. Available from: https://clinicaltrials.gov/ct2/show/NCT03390920.
8. I-ACT: Phase I trial of Amnion Cell Therapy for Ischaemic Stroke to establish the maximum tolerable dose [Internet]. 2018. Available from: https://www.anzctr.org.au/Trial/Registration/TrialReview.aspx?id=374260&isReview=true.
9. Asch R, Simerly C, Ord T, Ord V, Schatten G. The stages at which human fertilization arrests: microtubule and chromosome configurations in inseminated oocytes which failed to complete fertilization and development in humans. Molecular Human Reproduction. 1995;1(5):239-48.
10. Hall JG. Twinning. The Lancet. 2003;362(9385):735-43.
11. Thomson JA, Itskovitz-Eldor J, Shapiro SS, Waknitz MA, Swiergiel JJ, Marshall VS, et al. Embryonic stem cell lines derived from human blastocysts. Science. 1998;282(5391):1145-7.
12. Revazova ES, Turovets NA, Kochetkova OD, Kindarova LB, Kuzmichev LN, Janus JD, et al. Patient-specific stem cell lines derived from human parthenogenetic blastocysts. Cloning and stem cells. 2007;9(3):432-49.
13. Munsie MJ, Michalska AE, O'Brien CM, Trounson AO, Pera MF, Mountford PS. Isolation of pluripotent embryonic stem cells from reprogrammed adult mouse somatic cell nuclei. Current biology : CB. 2000;10(16):989-92.
14. Tachibana M, Amato P, Sparman M, Gutierrez NM, Tippner-Hedges R, Ma H, et al. Human embryonic stem cells derived by somatic cell nuclear transfer. Cell. 2013;153(6):1228-38.
15. Hall VJ, Stojkovic P, Stojkovic M. Using therapeutic cloning to fight human disease: a conundrum or reality? Stem cells. 2006;24(7):1628-37.
16. Chung YG, Eum JH, Lee JE, Shim SH, Sepilian V, Hong SW, et al. Human somatic cell nuclear transfer using adult cells. Cell stem cell. 2014;14(6):777-80.
17. FDA. Chapter II: Technology Overview: Somatic Cell Nuclear Transfer and Other Assisted Reproductive Technologies 2014 [updated 07/14/2014. Available from: http://www.fda.gov/AnimalVeterinary/SafetyHealth/AnimalCloning/ucm124765.htm.
18. Wilmut I, Beaujean N, de Sousa PA, Dinnyes A, King TJ, Paterson LA, et al. Somatic cell nuclear transfer. Nature. 2002;419(6709):583-7.
19. Takahashi K, Yamanaka S. Induction of pluripotent stem cells from mouse embryonic and adult fibroblast cultures by defined factors. cell. 2006;126(4):663-76.
20. Wei X, Yang X, Han Z-p, Qu F-f, Shao L, Shi Y-f. Mesenchymal stem cells: a new trend for cell therapy. Acta Pharmacologica Sinica. 2013;34(6):747-54.
21. Rezania A, Bruin JE, Arora P, Rubin A, Batushansky I, Asadi A, et al. Reversal of diabetes with insulin-producing cells derived in vitro from human pluripotent stem cells. Nature biotechnology. 2014;32(11):1121-33.
22. Schwartz SD, Hubschman J-P, Heilwell G, Franco-Cardenas V, Pan CK, Ostrick RM, et al. Embryonic stem cell trials for macular degeneration: a preliminary report. The Lancet. 2012;379(9817):713-20.

23. Passier R, van Laake LW, Mummery CL. Stem-cell-based therapy and lessons from the heart. Nature. 2008;453(7193):322-9.
24. Xia H, Li X, Gao W, Fu X, Fang RH, Zhang L, et al. Tissue repair and regeneration with endogenous stem cells. Nature Reviews Materials. 2018;3(7):174-93.
25. Strauer B-E, Yousef M, Schannwell CM. The acute and long-term effects of intracoronary Stem cell Transplantation in 191 patients with chronic heARt failure: the STAR-heart study. European Journal of Heart Failure. 2010;12(7):721-9.
26. Kang KS, Kim SW, Oh YH, Yu JW, Kim KY, Park HK, et al. A 37-year-old spinal cord-injured female patient, transplanted of multipotent stem cells from human UC blood, with improved sensory perception and mobility, both functionally and morphologically: a case study. Cytotherapy. 2005;7(4):368-73.
27. Mesoblast. Product Pipeline Overview 2015 [Available from: http://www.mesoblast.com/products/overview.
28. Le Blanc K, Samuelsson H, Gustafsson B, Remberger M, Sundberg B, Arvidson J, et al. Transplantation of mesenchymal stem cells to enhance engraftment of hematopoietic stem cells. Leukemia. 2007;21(8):1733-8.
29. Anna Corcione FB, Elisa Ferretti, Debora Giunti, Valentina Cappiello, Francesco Cazzanti, Marco Risso, Francesca Gualandi, Giovanni Luigi Mancardi, Vito Pistoia, Antonio Uccelli. Human mesenchymal stem cells modulate B-cell functions. Corcione A, Benvenuto F, Ferretti E, Giunti D, Cappiello V, Cazzanti F, et al., editors2006 2006-01-01 00:00:00. 367-72 p.
30. Xiao-Xia Jiang YZ, Bing Liu, Shuang-Xi Zhang, Ying Wu, Xiao-Dan Yu, Ning Mao. Human mesenchymal stem cells inhibit differentiation and function of monocyte-derived dendritic cells. Jiang X-X, Zhang Y, Liu B, Zhang S-X, Wu Y, Yu X-D, et al., editors2005 2005-05-15 00:00:00. 4120-6 p.
31. GeneaBiocells. Stem Cell Lines 2015 [Available from: http://www.geneastemcells.com.au/Our-Products/Stem-Cell-Lines.
32. Food, Drug Administration H. International Conference on Harmonisation; guidance on S7A safety pharmacology studies for human pharmaceuticals; availability. Notice. Federal register. 2001;66(135):36791.
33. Mora C, Serzanti M, Consiglio A, Memo M, Dell'Era P. Clinical potentials of human pluripotent stem cells. Cell Biology and Toxicology. 2017;33(4):351-60.
34. Ruiz S, Gore A, Li Z, Panopoulos AD, Montserrat N, Fung H-L, et al. Analysis of protein-coding mutations in hiPSCs and their possible role during somatic cell reprogramming. Nature communications. 2013;4(1):1-8.
35. Turinetto V, Orlando L, Giachino C. Induced pluripotent stem cells: advances in the quest for genetic stability during reprogramming process. International journal of molecular sciences. 2017;18(9):1952.
36. Weissbein U, Benvenisty N, Ben-David U. Genome maintenance in pluripotent stem cells. Journal of Cell Biology. 2014;204(2):153-63.
37. staff Bc. Blausen gallery 2014. Wikiversity Journal of Medicine 2014;1(2):24.
38. Dezaki K, Hosoda H, Kakei M, Hashiguchi S, Watanabe M, Kangawa K, et al. Endogenous ghrelin in pancreatic islets restricts insulin release by attenuating Ca2+ signaling in β-cells implication in the glycemic control in rodents. Diabetes. 2004;53(12):3142-51.
39. Matveyenko AV, Butler PJD, Obesity, Metabolism. Relationship between β-cell mass and diabetes onset. 2008;10:23-31.
40. Davidson MB, Davidson MB. Diabetes mellitus: Diagnosis and treatment: Saunders Philadelphia; 1998.
41. Taplin CE, Barker JMJA. Autoantibodies in type 1 diabetes. 2008;41(1):11-8.
42. Control D, Group CTR. The effect of intensive treatment of diabetes on the development and progression of long-term complications in insulin-dependent diabetes mellitus. New England journal of medicine. 1993;329(14):977-86.
43. Zimmet P, Alberti KGMM, Shaw J. Global and societal implications of the diabetes epidemic. Nature. 2001;414(6865):782-7.

44. Chen L, Magliano DJ, Zimmet PZ. The worldwide epidemiology of type 2 diabetes mellitus present and future perspectives. Nat Rev Endocrinol. 2012;8(4):228-36.
45. Shah SN, Joshi SR, Parmar DV. History of insulin. The Journal of the Association of Physicians of India. 1997;Suppl 1:4-9.
46. Joshi SR, Parikh RM, Das AK. Insulin--history, biochemistry, physiology and pharmacology. The Journal of the Association of Physicians of India. 2007;55 Suppl:19-25.
47. Insulin Administration. Diabetes Care. 2003;26(suppl 1):s121-s4.
48. Kelly WD, Lillehei RC, Merkel FK, Idezuki Y, Goetz FG. Allotransplantation of the pancreas and duodenum along with the kidney in diabetic nephropathy. Surgery.61(6):827-37.
49. Gruessner AC, Sutherland DE. Pancreas transplant outcomes for United States (US) and non-US cases as reported to the United Network for Organ Sharing (UNOS) and the International Pancreas Transplant Registry (IPTR) as of June 2004. Clinical transplantation. 2005;19(4):433-55.
50. Webster AC, Hedley J, Robertson P, Mulley WR, Pilmore HL, Pleass H, et al. Australia and New Zealand Islets and Pancreas Transplant Registry Annual Report 2018-Pancreas Waiting List, Recipients, and Donors. Transplantation direct. 2018;4(10):e390-e.
51. Registry ANZOD. Monthly Report on Deceased Organ Donation in Australia. 2014 Produced 5 December 2014.
52. Shapiro AMJ, Lakey JRT, Ryan EA, Korbutt GS, Toth E, Warnock GL, et al. Islet Transplantation in Seven Patients with Type 1 Diabetes Mellitus Using a Glucocorticoid-Free Immunosuppressive Regimen. New England Journal of Medicine. 2000;343(4):230-8.
53. Shapiro AM, Ricordi C, Hering BJ, Auchincloss H, Lindblad R, Robertson RP, et al. International trial of the Edmonton protocol for islet transplantation. The New England journal of medicine. 2006;355(13):1318-30.
54. Thomas Eggerman M, PhD, Guillermo Arreaza-Rubin M. CITR Tenth Annual Report. The Emmes Corporation; 2017 January 6, 2017.
55. Webster AC, Hedley JA, Anderson PF, Hawthorne WJ, Radford T, Drogemuller C, et al. Australia and New Zealand Islet and Pancreas Transplant Registry Annual Report 2018—Islet Donations, Islet Isolations, and Islet Transplants. Transplantation direct. 2019;5(2).
56. Allan JS. Xenotransplantation at a crossroads: prevention versus progress. Nature Medicine. 1996;2(1):18-21.
57. Klymiuk N, Aigner B, Brem G, Wolf E. Genetic modification of pigs as organ donors for xenotransplantation. Molecular reproduction and development. 2010;77(3):209-21.
58. Grant A. Diabecell Clinical Trial Update 2012 [Available from: http://www.asx.com.au/asxpdf/20120926/pdf/428z0ty9pjdq55.pdf.
59. Wynyard S, Nathu D, Garkavenko O, Denner J, Elliott R. Microbiological safety of the first clinical pig islet xenotransplantation trial in New Zealand. Xenotransplantation. 2014;21(4):309-23.
60. Jiang J, Au M, Lu K, Eshpeter A, Korbutt G, Fisk G, et al. Generation of insulin-producing islet-like clusters from human embryonic stem cells. Stem cells. 2007;25(8):1940-53.
61. Kroon E, Martinson LA, Kadoya K, Bang AG, Kelly OG, Eliazer S, et al. Pancreatic endoderm derived from human embryonic stem cells generates glucose-responsive insulin-secreting cells in vivo. Nature biotechnology. 2008;26(4):443-52.
62. Nostro MC, Sarangi F, Ogawa S, Holtzinger A, Corneo B, Li X, et al. Stage-specific signaling through TGFbeta family members and WNT regulates patterning and pancreatic specification of human pluripotent stem cells. Development (Cambridge, England). 2011;138(5):861-71.
63. Liu H, Yang H, Zhu D, Sui X, Li J, Liang Z, et al. Systematically labeling developmental stage-specific genes for the study of pancreatic beta-cell differentiation from human embryonic stem cells. Cell research. 2014;24(10):1181-200.
64. Pagliuca FW, Millman JR, Gürtler M, Segel M, Van Dervort A, Ryu JH, et al. Generation of functional human pancreatic β cells in vitro. Cell. 2014;159(2):428-39.
65. Vegas AJ, Veiseh O, Gürtler M, Millman JR, Pagliuca FW, Bader AR, et al. Long-term glycemic control using polymer-encapsulated human stem cell-derived beta cells in immune-competent mice. Nature medicine. 2016.

66. Tuch BE, Jones A, Turtle JR. Maturation of the response of human fetal pancreatic explants to glucose. Diabetologia. 1985;28(1):28-31.
67. Rezania A, Bruin JE, Riedel MJ, Mojibian M, Asadi A, Xu J, et al. Maturation of human embryonic stem cell-derived pancreatic progenitors into functional islets capable of treating pre-existing diabetes in mice. Diabetes. 2012;61(8):2016-29.
68. Laikind P. ViaCyte, Inc. Announces FDA Acceptance of IND to Commence Clinical Trial of VC-01™ Candidate Cell Replacement Therapy for Type 1 Diabetes [Webpage]. San Diego, California2014 [updated August 19, 2014. Available from: http://viacyte.com/?press-releases=viacyte-inc-announces-fda-acceptance-of-ind-to-commence-clinical-trial-of-vc-01-candidate-cell-replacement-therapy-for-type-1-diabetes.
69. Lewis SL, Tam PP. Definitive endoderm of the mouse embryo: formation, cell fates, and morphogenetic function. Developmental dynamics. 2006;235(9):2315-29.
70. Bouchi R, Foo KS, Hua H, Tsuchiya K, Ohmura Y, Sandoval PR, et al. FOXO1 inhibition yields functional insulin-producing cells in human gut organoid cultures. Nat Commun. 2014;5.
71. Van Hoof D, D'Amour KA, German MS. Derivation of insulin-producing cells from human embryonic stem cells. Stem cell research. 2009;3(2):73-87.
72. D'Amour KA, Bang AG, Eliazer S, Kelly OG, Agulnick AD, Smart NG, et al. Production of pancreatic hormone–expressing endocrine cells from human embryonic stem cells. Nature biotechnology. 2006;24(11):1392-401.
73. Schulz TC, Young HY, Agulnick AD, Babin MJ, Baetge EE, Bang AG, et al. A scalable system for production of functional pancreatic progenitors from human embryonic stem cells. PloS one. 2012;7(5):e37004.
74. Hughes CS, Postovit LM, Lajoie GA. Matrigel: a complex protein mixture required for optimal growth of cell culture. Proteomics. 2010;10(9):1886-90.
75. Tateishi K, He J, Taranova O, Liang G, D'Alessio AC, Zhang Y. Generation of insulin-secreting islet-like clusters from human skin fibroblasts. Journal of Biological Chemistry. 2008;283(46):31601-7.
76. Kubo A, Shinozaki K, Shannon JM, Kouskoff V, Kennedy M, Woo S, et al. Development of definitive endoderm from embryonic stem cells in culture. Development (Cambridge, England). 2004;131(7):1651-62.
77. Yasunaga M, Tada S, Torikai-Nishikawa S, Nakano Y, Okada M, Jakt LM, et al. Induction and monitoring of definitive and visceral endoderm differentiation of mouse ES cells. Nature biotechnology. 2005;23(12):1542-50.
78. Gouon-Evans V, Boussemart L, Gadue P, Nierhoff D, Koehler CI, Kubo A, et al. BMP-4 is required for hepatic specification of mouse embryonic stem cell–derived definitive endoderm. Nature biotechnology. 2006;24(11):1402-11.
79. Wells JM, Melton DA. Vertebrate endoderm development. Annual review of cell and developmental biology. 1999;15(1):393-410.
80. Murry CE, Keller G. Differentiation of embryonic stem cells to clinically relevant populations: lessons from embryonic development. Cell. 2008;132(4):661-80.
81. Zhang D, Jiang W, Liu M, Sui X, Yin X, Chen S, et al. Highly efficient differentiation of human ES cells and iPS cells into mature pancreatic insulin-producing cells. Cell research. 2009;19(4):429-38.
82. Lardon J, De Breuck S, Rooman I, Van Lommel L, Kruhøffer M, Orntoft T, et al. Plasticity in the adult rat pancreas: transdifferentiation of exocrine to hepatocyte-like cells in primary culture. Hepatology. 2004;39(6):1499-507.
83. Wu SY, Hsieh CC, Wu RR, Susanto J, Liu TT, Shen CR, et al. Differentiation of pancreatic acinar cells to hepatocytes requires an intermediate cell type. Gastroenterology. 2010;138(7):2519-30.
84. Thorel F, Népote V, Avril I, Kohno K, Desgraz R, Chera S, et al. Conversion of adult pancreatic α-cells to β-cells after extreme β-cell loss. Nature. 2010;464(7292):1149.
85. Ye L, Robertson MA, Hesselson D, Stainier DY, Anderson RM. Glucagon is essential for alpha cell transdifferentiation and beta cell neogenesis. Development (Cambridge, England). 2015;142(8):1407-17.

86. Karges B, Durinovic-Belló I, Heinze E, Boehm BO, Debatin K-M, Karges W. Complete long-term recovery of β-cell function in autoimmune type 1 diabetes after insulin treatment. Diabetes care. 2004;27(5):1207-8.
87. Kajiyama H, Hamazaki TS, Tokuhara M, Masui S, Okabayashi K, Ohnuma K, et al. Pdx1-transfected adipose tissue-derived stem cells differentiate into insulin-producing cells in vivo and reduce hyperglycemia in diabetic mice. International Journal of Developmental Biology. 2009;54(4):699-705.
88. Pennarossa G, Maffei S, Campagnol M, Tarantini L, Gandolfi F, Brevini TA. Brief demethylation step allows the conversion of adult human skin fibroblasts into insulin-secreting cells. Proceedings of the National Academy of Sciences. 2013;110(22):8948-53.
89. Pereyra-Bonnet F, Gimeno ML, Argumedo NR, Ielpi M, Cardozo JA, Gimenez CA, et al. Skin fibroblasts from patients with type 1 diabetes (T1D) can be chemically transdifferentiated into insulin-expressing clusters: a transgene-free approach. PloS One. 2014;9(6):e100369.
90. Koblas T, Leontovyc I, Loukotova S, Kosinova L, Saudek F. Reprogramming of pancreatic exocrine cells AR42J into insulin-producing cells using mRNAs for Pdx1, Ngn3, and MafA transcription factors. Molecular therapy-nucleic acids. 2016;5:e320.
91. Monaco AP, Maki T, Ozato H, Carretta M, Sullivan SJ, Borland KM, et al. Transplantation of islet allografts and xenografts in totally pancreatectomized diabetic dogs using the hybrid artificial pancreas. Annals of surgery. 1991;214(3):339-60; discussion 61-2.
92. Sakata N, Sumi S, Yoshimatsu G, Goto M, Egawa S, Unno M. Encapsulated islets transplantation: past, present and future. World journal of gastrointestinal pathophysiology. 2012;3(1):19.
93. Jones KS, Sefton MV, Gorczynski RM. In vivo recognition by the host adaptive immune system of microencapsulated xenogeneic cells. Transplantation. 2004;78(10):1454-62.
94. Aung T, Kogire M, Inoue K, Fujisato T, Gu Y, Burczak K, et al. Insulin release from a bioartificial pancreas using a mesh reinforced polyvinyl alcohol hydrogel tube. An in vitro study. ASAIO journal (American Society for Artificial Internal Organs : 1992). 1993;39(2):93-6.
95. Hayashi H, Inoue K, Aung T, Tun T, Yuanjun G, Wenjing W, et al. Application of a novel B cell line MIN6 to a mesh-reinforced polyvinyl alcohol hydrogel tube and three-layer agarose microcapsules: an in vitro study. Cell transplantation. 1996;5(5 Suppl 1):S65-9.
96. Lee JI, Nishimura R, Sakai H, Sasaki N, Kenmochi T. A newly developed immunoisolated bioartificial pancreas with cell sheet engineering. Cell transplantation. 2008;17(1-2):51-9.
97. Soon-Shiong P, Heintz RE, Merideth N, Yao QX, Yao Z, Zheng T, et al. Insulin independence in a type 1 diabetic patient after encapsulated islet transplantation. The Lancet. 1994;343(8903):950-1.
98. Dufrane D, Goebbels RM, Gianello P. Alginate macroencapsulation of pig islets allows correction of streptozotocin-induced diabetes in primates up to 6 months without immunosuppression. Transplantation. 2010;90(10):1054-62.
99. Matveyenko AV, Georgia S, Bhushan A, Butler PC. Inconsistent formation and nonfunction of insulin-positive cells from pancreatic endoderm derived from human embryonic stem cells in athymic nude rats. American Journal of Physiology - Endocrinology and Metabolism. 2010;299(5):E713-20.
100. Goosen MF, O'Shea GM, Gharapetian HM, Chou S, Sun AM. Optimization of microencapsulation parameters: Semipermeable microcapsules as a bioartificial pancreas. Biotechnology and bioengineering. 1985;27(2):146-50.
101. Godek ML, Duchsherer NL, McElwee Q, Grainger DW. Morphology and growth of murine cell lines on model biomaterials. Biomedical sciences instrumentation. 2004;40:7-12.
102. Klöck G, Frank H, Houben R, Zekorn T, Horcher A, Siebers U, et al. Production of purified alginates suitable for use in immunoisolated transplantation. Appl Microbiol Biotechnol. 1994;40(5):638-43.
103. Zimmermann U, Klöck G, Federlin K, Hannig K, Kowalski M, Bretzel RG, et al. Production of mitogen-contamination free alginates with variable ratios of mannuronic acid to guluronic acid by free flow electrophoresis. ELECTROPHORESIS. 1992;13(1):269-74.
104. Stabler C, Wilks K, Sambanis A, Constantinidis I. The effects of alginate composition on encapsulated βTC3 cells. Biomaterials. 2001;22(11):1301-10.

105. Martinsen A, Skjåk-Bræk G, Smidsrød O. Alginate as immobilization material: I. Correlation between chemical and physical properties of alginate gel beads. Biotechnology and bioengineering. 1989;33(1):79-89.
106. Martinsen A, Storrø I, Skjårk-Bræk G. Alginate as immobilization material: III. Diffusional properties. Biotechnology and bioengineering. 1992;39(2):186-94.
107. Smidsrod O. Molecular basis for some physical properties of alginates in the gel state. Faraday Discussions of the Chemical Society. 1974;57(0):263-74.
108. Smidsrød O, Skja˚k-Br˙lk G. Alginate as immobilization matrix for cells. Trends in Biotechnology. 1990;8(0):71-8.
109. Thu B, Bruheim P, Espevik T, Smidsrød O, Soon-Shiong P, Skjåk-Bræk G. Alginate polycation microcapsules: I. Interaction between alginate and polycation. Biomaterials. 1996;17(10):1031-40.
110. Inger-Lill A, Olav S, Olav SD, Kjetill O, Per Chr H. Some Biological Functions of Matrix Components in Benthic Algae in Relation to Their Chemistry and the Composition of Seawater. Cellulose Chemistry and Technology. ACS Symposium Series. 48: AMERICAN CHEMICAL SOCIETY; 1977. p. 361-81.
111. Martinsen A, Skjåk-Bræk G, Smidsrød O, Zanetti F, Paoletti S. Comparison of different methods for determination of molecular weight and molecular weight distribution of alginates. Carbohydrate Polymers. 1991;15(2):171-93.
112. Veiseh O, Doloff JC, Ma M, Vegas AJ, Tam HH, Bader AR, et al. Size-and shape-dependent foreign body immune response to materials implanted in rodents and non-human primates. Nature materials. 2015;14(6):643-51.
113. M. Ramadas WPKJDMRYACPS. Lipoinsulin encapsulated alginate-chitosan capsules: intestinal delivery in diabetic rats. Journal of Microencapsulation. 2000;17(4):405-11.
114. Damgé C, Maincent P, Ubrich N. Oral delivery of insulin associated to polymeric nanoparticles in diabetic rats. Journal of Controlled Release. 2007;117(2):163-70.
115. Dawson E, Mapili G, Erickson K, Taqvi S, Roy K. Biomaterials for stem cell differentiation. Advanced drug delivery reviews. 2008;60(2):215-28.
116. Chayosumrit M, Tuch B, Sidhu K. Alginate microcapsule for propagation and directed differentiation of hESCs to definitive endoderm. Biomaterials. 2010;31(3):505-14.
117. Dutta D, Heo I, Clevers H. Disease modeling in stem cell-derived 3D organoid systems. Trends in molecular medicine. 2017;23(5):393-410.
118. Wills ES, Drenth JP. Building pancreatic organoids to aid drug development. Gut. 2017;66(3):393-4.
119. Greggio C, De Franceschi F, Figueiredo-Larsen M, Gobaa S, Ranga A, Semb H, et al. Artificial three-dimensional niches deconstruct pancreas development in vitro. Development (Cambridge, England). 2013;140(21):4452-62.
120. Hohwieler M, Illing A, Hermann PC, Mayer T, Stockmann M, Perkhofer L, et al. Human pluripotent stem cell-derived acinar/ductal organoids generate human pancreas upon orthotopic transplantation and allow disease modelling. Gut. 2017;66(3):473-86.
121. Soltanian A, Ghezelayagh Z, Mazidi Z, Halvaei M, Mardpour S, Ashtiani MK, et al. Generation of functional human pancreatic organoids by transplants of embryonic stem cell derivatives in a 3D-printed tissue trapper. Journal of cellular physiology. 2019;234(6):9564-76.
122. Navarro-Tableros V, Gomez Y, Brizzi MF, Camussi G. Generation of Human Stem Cell-Derived Pancreatic Organoids (POs) for Regenerative Medicine. In: Turksen K, editor. Cell Biology and Translational Medicine, Volume 6: Stem Cells: Their Heterogeneity, Niche and Regenerative Potential. Cham: Springer International Publishing; 2020. p. 179-220.
123. Gamble A, Pepper AR, Bruni A, Shapiro AJ. The journey of islet cell transplantation and future development. Islets. 2018;10(2):80-94.
124. Bochenek MA, Veiseh O, Vegas AJ, McGarrigle JJ, Qi M, Marchese E, et al. Alginate encapsulation as long-term immune protection of allogeneic pancreatic islet cells transplanted into the omental bursa of macaques. Nature biomedical engineering. 2018;2(11):810.

125. An D, Chiu A, Flanders JA, Song W, Shou D, Lu Y-C, et al. Designing a retrievable and scalable cell encapsulation device for potential treatment of type 1 diabetes. Proceedings of the National Academy of Sciences. 2018;115(2):E263-E72.
126. Ludwig B, Ludwig S, Steffen A, Knauf Y, Zimerman B, Heinke S, et al. Favorable outcome of experimental islet xenotransplantation without immunosuppression in a nonhuman primate model of diabetes. Proceedings of the National Academy of Sciences. 2017;114(44):11745-50.
127. Song S, Blaha C, Moses W, Park J, Wright N, Groszek J, et al. An intravascular bioartificial pancreas device (iBAP) with silicon nanopore membranes (SNM) for islet encapsulation under convective mass transport. Lab on a Chip. 2017;17(10):1778-92.
128. Sabek OM, Ferrati S, Fraga DW, Sih J, Zabre EV, Fine DH, et al. Characterization of a nanogland for the autotransplantation of human pancreatic islets. Lab on a chip. 2013;13(18):3675-88.
129. ViaCyte. A Safety, Tolerability, and Efficacy Study of VC-02™ Combination Product in Subjects With Type 1 Diabetes Mellitus and Hypoglycemia Unawareness clinicaltrials.gov2017 [updated January 8, 2019. Available from: https://clinicaltrials.gov/ct2/show/NCT03163511?term=ViaCyte&rank=1.
130. Bruin JE, Asadi A, Fox JK, Erener S, Rezania A, Kieffer TJ. Accelerated maturation of human stem cell-derived pancreatic progenitor cells into insulin-secreting cells in immunodeficient rats relative to mice. Stem cell reports. 2015;5(6):1081-96.
131. Southard SM, Kotipatruni RP, Rust WL. Generation and selection of pluripotent stem cells for robust differentiation to insulin-secreting cells capable of reversing diabetes in rodents. PloS one. 2018;13(9):e0203126.
132. ViaCyte. Product Pipeline for Insulin-Requiring Diabetes 2020 [Available from: https://viacyte.com/pipeline/#PEC-Encap-VC-01/.
133. Sernova Confirms Enduring Levels of Fasting C-Peptide in Bloodstream of First Patient in its Phase I/II Clinical Trial for Type-1 Diabetes [press release]. Sernova, October 16, 2019 2019.
134. Veres A, Faust AL, Bushnell HL, Engquist EN, Kenty JH-R, Harb G, et al. Charting cellular identity during human in vitro β-cell differentiation. Nature. 2019;569(7756):368.
135. Carlsson PO, Espes D, Sedigh A, Rotem A, Zimerman B, Grinberg H, et al. Transplantation of macroencapsulated human islets within the bioartificial pancreas βAir to patients with type 1 diabetes mellitus. American Journal of Transplantation. 2018;18(7):1735-44.
136. Cheng STW, Chen L, Li SYT, Mayoux E, Leung PS. The effects of empagliflozin, an SGLT2 inhibitor, on pancreatic β-cell mass and glucose homeostasis in type 1 diabetes. PloS one. 2016;11(1):e0147391.
137. McCrimmon RJ, Henry RR. SGLT inhibitor adjunct therapy in type 1 diabetes. Diabetologia. 2018;61(10):2126-33.
138. Opara EC. Nutrition and diabetes: pathophysiology and management: CRC Press; 2005.
139. Lim F, Sun AM. Microencapsulated islets as bioartificial endocrine pancreas. Science. 1980;210(4472):908-10.
140. Taylor CJ, Peacock S, Chaudhry AN, Bradley JA, Bolton EM. Generating an iPSC bank for HLA-matched tissue transplantation based on known donor and recipient HLA types. Cell stem cell. 2012;11(2):147-52.
141. Deuse T, Hu X, Gravina A, Wang D, Tediashvili G, De C, et al. Hypoimmunogenic derivatives of induced pluripotent stem cells evade immune rejection in fully immunocompetent allogeneic recipients. Nature biotechnology. 2019;37(3):252-8.
142. Xu H, Wang B, Ono M, Kagita A, Fujii K, Sasakawa N, et al. Targeted disruption of HLA genes via CRISPR-Cas9 generates iPSCs with enhanced immune compatibility. Cell Stem Cell. 2019;24(4):566-78. e7.
143. Han X, Wang M, Duan S, Franco PJ, Kenty JH-R, Hedrick P, et al. Generation of hypoimmunogenic human pluripotent stem cells. Proceedings of the National Academy of Sciences. 2019;116(21):10441-6.
144. Sidhu KS, Ryan JP, Tuch BE. Derivation of a new human embryonic stem cell line, endeavour-1, and its clonal propagation. Stem cells and development. 2008;17(1):41-52.
145. Tuch BE VV, Bean P, Lewy D, Evans MDM. Differentiation of human pancreatic progenitors, derived from human embryonic stem cells, into insulin producing cells by transplantation. Aust Diab Soc. 2012;39(146).

146. Takahashi K, Tanabe K, Ohnuki M, Narita M, Ichisaka T, Tomoda K, et al. Induction of pluripotent stem cells from adult human fibroblasts by defined factors. cell. 2007;131(5):861-72.
147. Vaithilingam V. Microencapsulated Human Islets as a Therapy for Type 1 Diabetes: PhD Thesis.: The University of New South Wales; 2010.
148. Hardikar AA, Farr RJ, Joglekar MV. Circulating microRNAs: understanding the limits for quantitative measurement by real-time PCR. Journal of the American Heart Association. 2014;3(1):e000792.
149. Shi G, Jin Y. Role of Oct4 in maintaining and regaining stem cell pluripotency. Stem cell research & therapy. 2010;1(5):39.
150. Baker M. What does Nanog do? Nature Reports Stem Cells. 2009.
151. Qu XB, Pan J, Zhang C, Huang SY. Sox17 facilitates the differentiation of mouse embryonic stem cells into primitive and definitive endoderm in vitro. Development, growth & differentiation. 2008;50(7):585-93.
152. Burtscher I, Lickert H. Foxa2 regulates polarity and epithelialization in the endoderm germ layer of the mouse embryo. Development (Cambridge, England). 2009;136(6):1029-38.
153. Barbacci E, Reber M, Ott M-O, Breillat C, Huetz F, Cereghini S. Variant hepatocyte nuclear factor 1 is required for visceral endoderm specification. Development (Cambridge, England). 1999;126(21):4795-805.
154. Duncan SA, Manova K, Chen WS, Hoodless P, Weinstein DC, Bachvarova RF, et al. Expression of transcription factor HNF-4 in the extraembryonic endoderm, gut, and nephrogenic tissue of the developing mouse embryo: HNF-4 is a marker for primary endoderm in the implanting blastocyst. Proceedings of the National Academy of Sciences. 1994;91(16):7598-602.
155. Bas A, Forsberg G, Hammarström S, Hammarström ML. Utility of the Housekeeping Genes 18S rRNA, β-Actin and Glyceraldehyde-3-Phosphate-Dehydrogenase for Normalization in Real-Time Quantitative Reverse Transcriptase-Polymerase Chain Reaction Analysis of Gene Expression in Human T Lymphocytes. Scandinavian journal of immunology. 2004;59(6):566-73.
156. Segev H, Fishman B, Schulman R, Itskovitz-Eldor J. The expression of the class 1 glucose transporter isoforms in human embryonic stem cells, and the potential use of GLUT2 as a marker for pancreatic progenitor enrichment. Stem cells and development. 2012;21(10):1653-61.
157. Ma F, Chen F, Chi Y, Yang S, Lu S, Han Z. Isolation of pancreatic progenitor cells with the surface marker of hematopoietic stem cells. International journal of endocrinology. 2012;2012.
158. Tseng I-C, Yeh MM, Yang C-Y, Jeng Y-M. NKX6-1 is a novel immunohistochemical marker for pancreatic and duodenal neuroendocrine tumors. The American journal of surgical pathology. 2015;39(6):850-7.
159. Nishimura W, Takahashi S, Yasuda K. MafA is critical for maintenance of the mature beta cell phenotype in mice. Diabetologia. 2015;58(3):566-74.
160. Wang J, Elghazi L, Parker SE, Kizilocak H, Asano M, Sussel L, et al. The concerted activities of Pax4 and Nkx2. 2 are essential to initiate pancreatic β-cell differentiation. Developmental biology. 2004;266(1):178-89.
161. Lee CS, Sund NJ, Vatamaniuk MZ, Matschinsky FM, Stoffers DA, Kaestner KH. Foxa2 controls Pdx1 gene expression in pancreatic β-cells in vivo. Diabetes. 2002;51(8):2546-51.
162. Schmidt RE, Green KG, Feng D, Dorsey DA, Parvin CA, Lee J-M, et al. Erythropoietin and its carbamylated derivative prevent the development of experimental diabetic autonomic neuropathy in STZ-induced diabetic NOD-SCID mice. Experimental neurology. 2008;209(1):161-70.
163. Russ HA, Parent AV, Ringler JJ, Hennings TG, Nair GG, Shveygert M, et al. Controlled induction of human pancreatic progenitors produces functional beta-like cells in vitro. The EMBO journal. 2015;34(13):1759-72.
164. Vaithilingam V, Kollarikova G, Qi M, Lacik I, Oberholzer J, Guillemin GJ, et al. Effect of prolonged gelling time on the intrinsic properties of barium alginate microcapsules and its biocompatibility. Journal of microencapsulation. 2011;28(6):499-507.
165. Riccardi C, Nicoletti I. Analysis of apoptosis by propidium iodide staining and flow cytometry. Nature protocols. 2006;1(3):1458-61.

166. Lumelsky N, Blondel O, Laeng P, Velasco I, Ravin R, McKay R. Differentiation of embryonic stem cells to insulin-secreting structures similar to pancreatic islets. Science. 2001;292(5520):1389-94.
167. Zeineddine D, Hammoud AA, Mortada M, Boeuf H. The Oct4 protein: more than a magic stemness marker. American journal of stem cells. 2014;3(2):74.
168. Vogel C, Marcotte EM. Insights into the regulation of protein abundance from proteomic and transcriptomic analyses. Nature reviews Genetics. 2012;13(4):227.
169. Raikwar SP, Kim E-M, Sivitz WI, Allamargot C, Thedens DR, Zavazava N. Human iPS cell-derived insulin producing cells form vascularized organoids under the kidney capsules of diabetic mice. PloS one. 2015;10(1):e0116582.
170. Wu J, Zhang J, Jiang M, Zhang T, Wang Y, Wang Z, et al. Comparison between nOD/sCiD mice and BalB/c mice for patient-derived tumor xenografts model of non-small-cell lung cancer. Cancer management and research. 2018;10:6695.
171. Grant CW, Duclos SK, Moran-Paul CM, Yahalom B, Tirabassi RS, Arreaza-Rubin G, et al. Development of standardized insulin treatment protocols for spontaneous rodent models of type 1 diabetes. Comparative medicine. 2012;62(5):381-90.
172. Chaparro RJ, Konigshofer Y, Beilhack GF, Shizuru JA, McDevitt HO, Chien Y-h. Nonobese diabetic mice express aspects of both type 1 and type 2 diabetes. Proceedings of the National Academy of Sciences. 2006;103(33):12475-80.
173. Lebowitz MR, Blumenthal SA. The molar ratio of insulin to C-peptide: an aid to the diagnosis of hypoglycemia due to surreptitious (or inadvertent) insulin administration. Archives of internal medicine. 1993;153(5):650-5.
174. NC3Rs. Mouse Decision Tree Blood Sampling https://www.nc3rs.org.uk/mouse-decision-tree-blood-sampling2018 [
175. Nagashima R, Levy G. Effect of perfusion rate and distribution factors on drug elimination kinetics in a perfused organ system. Journal of pharmaceutical sciences. 1968;57(11):1991-3.
176. Su AI, Wiltshire T, Batalov S, Lapp H, Ching KA, Block D, et al. A gene atlas of the mouse and human protein-encoding transcriptomes. Proceedings of the National Academy of Sciences. 2004;101(16):6062-7.
177. Dean SK, Yulyana Y, Williams G, Sidhu KS, Tuch BE. Differentiation of encapsulated embryonic stem cells after transplantation. Transplantation. 2006;82(9):1175-84.
178. Gropp M, Shilo V, Vainer G, Gov M, Gil Y, Khaner H, et al. Standardization of the teratoma assay for analysis of pluripotency of human ES cells and biosafety of their differentiated progeny. PloS one. 2012;7(9):e45532.
179. Shultz LD, Schweitzer PA, Christianson SW, Gott B, Schweitzer IB, Tennent B, et al. Multiple defects in innate and adaptive immunologic function in NOD/LtSz-scid mice. The Journal of Immunology. 1995;154(1):180-91.
180. Millman JR, Xie C, Van Dervort A, Gürtler M, Pagliuca FW, Melton DA. Generation of stem cell-derived β-cells from patients with type 1 diabetes. Nature communications. 2016;7:ncomms11463.
181. Yokoi N, Hayashi C, Fujiwara Y, Wang H-Y, Seino S. Genetic reconstitution of autoimmune type 1 diabetes with two major susceptibility genes in the rat. Diabetes. 2007;56(2):506-12.
182. Kachapati K, Adams D, Bednar K, Ridgway WM. The non-obese diabetic (NOD) mouse as a model of human type 1 diabetes. Animal Models in Diabetes Research: Springer; 2012. p. 3-16.
183. Brons IGM, Smithers LE, Trotter MW, Rugg-Gunn P, Sun B, de Sousa Lopes SMC, et al. Derivation of pluripotent epiblast stem cells from mammalian embryos. Nature. 2007;448(7150):191.
184. Liu J, Ashton MP, Sumer H, O'Bryan MK, Brodnicki TC, Verma PJ. Generation of stable pluripotent stem cells from NOD mouse tail-tip fibroblasts. Diabetes. 2011;60(5):1393-8.
185. Liu J, Ashton MP, O'Bryan MK, Brodnicki TC, Verma PJ. GSK3 inhibition, but not epigenetic remodeling, mediates efficient derivation of germline embryonic stem cells from nonobese diabetic mice. Stem cell research. 2018;31:5-10.
186. Thatava T, Kudva YC, Edukulla R, Squillace K, De Lamo JG, Khan YK, et al. Intrapatient variations in type 1 diabetes-specific iPS cell differentiation into insulin-producing cells. Molecular Therapy. 2013;21(1):228-39.

187. Pellegrini S, Ungaro F, Mercalli A, Melzi R, Sebastiani G, Dotta F, et al. Human induced pluripotent stem cells differentiate into insulin-producing cells able to engraft in vivo. Acta diabetologica. 2015;52(6):1025-35.
188. Prevalence of type 1 diabetes in Australian children. Canberra AIHW, Welfare AIoHa; 2008.
189. Karvonen M, Viik-Kajander M, Moltchanova E, Libman I, LaPorte R, Tuomilehto J. Incidence of childhood type 1 diabetes worldwide. Diabetes Mondiale (DiaMond) Project Group. Diabetes care. 2000;23(10):1516-26.
190. Scheme TNDS. Data Snapshot - Type 1 diabetes (March 2019). 2019.
191. Mokan M, Mitrakou A, Veneman T, Ryan C, Korytkowski M, Cryer P, et al. Hypoglycemia unawareness in IDDM. Diabetes care. 1994;17(12):1397-403.
192. Bellin MD, Barton FB, Heitman A, Harmon J, Kandaswamy R, Balamurugan A, et al. Potent induction immunotherapy promotes long-term insulin independence after islet transplantation in type 1 diabetes. American Journal of Transplantation. 2012;12(6):1576-83.
193. Halloran PF. Immunosuppressive drugs for kidney transplantation. New England Journal of Medicine. 2004;351(26):2715-29.
194. Bekiari E, Kitsios K, Thabit H, Tauschmann M, Athanasiadou E, Karagiannis T, et al. Artificial pancreas treatment for outpatients with type 1 diabetes: systematic review and meta-analysis. bmj. 2018;361:k1310.
195. Silva CM, Ribeiro AJ, Figueiredo IV, Gonçalves AR, Veiga F. Alginate microspheres prepared by internal gelation: Development and effect on insulin stability. International journal of pharmaceutics. 2006;311(1-2):1-10.
196. Matthews D, Rudenski A, Burnett M, Darling P, Turner R. The half-life of endogenous insulin and C-peptide in man assessed by somatostatin suppression. Clinical endocrinology. 1985;23(1):71-9.
197. Takayama M, Yamauchi K, Aizawa T. Quantification of insulin. Diabetic Medicine. 2014;31(3):375-6.
198. Howell S. The mechanism of insulin secretion. Diabetologia. 1984;26(5):319-27.

Appendix 1: Dr Andrew Gal's Pathology report

First Mouse:

The specimen consists of mouse kidney which contains a circumscribed peripheral lesion consisting of a dense infiltrate of cells with a high N/R, small amount of cytoplasm and indistinct cell borders. The nuclei are slightly hyperchromatic, only minimally pleomorphic. There are no nucleoli. Mitoses are not seen. There is an admixture of a small number of karryorhectic nuclei and possibly a small number of polymorphs. There is no discernible background renal or any other type of tissue associated with this infiltrate.

The same cellular infiltrate is also present with a tight perivascular pattern of deposition within the renal parenchyma quite long distances away from the main mass of these cells.

Immune staining was carried out using anti-human antibodies, initially on frozen sections fixed with methanol with no positive reactions. Subsequently the tissue was fixed in formalin, paraffin embedded and further immune stains carried out on sections cut on the processed tissue.

The following results were obtained for the non- murine kidney portion of the specimen on the

Frozen sections:
Positive: SOX10 (cytoplasmic)

Negative: vimentin, CD45, CKBS, OCT4, AFP (there is some staining of the murine kidney and a little background stain is seen within the cellular infiltrate, most likely in underlying murine kidney; the vast majority of the cellular infiltrate does not take up this stain.)

FFPE tissue sections

Positive: CD45 (patchy, minimal staining)

Negative: E-cadherin, vimentin,

These results are difficult to interpret, especially in view of the lack of data on the reactivity of murine tissues with these anti-human antibodies.

The SOX 10 reaction I suspect is an artefact, because this antibody is against an intranuclear antigen.

The lack of clear cut, definite reactivity with any of these antibodies suggests that the cellular infiltrate is not human tissue. I have no experience with murine pathology, but its overall appearance and its presence around renal blood vessels suggests that those cells are of murine origin, representing an inflammatory reaction to the implanted human embryonic tissue. No diagnosable human embryonic tissue has remained in the available sections.

Mouse 124915:

The sections are of poor quality with marked freezing artefact.

There is kidney present with an adjacent latticework-like structure of empty spaces separated by cellular material of uncertain origin, probably kidney, but that is purely an educated guess.
There is a sparse inflammatory cell infiltrate just outside and within the renal capsule and focally within the renal parenchyma.

There is no human/embryonic tissue present.

Mouse 124916

Once again poor quality sections with freezing artefact.

Kidney with a slightly more intense inflammatory cell infiltrate than in Mouse 124915. No human/embryonic tissue.

Mouse 124913

There are two separate pieces of tissue on this slide.

One consists of mouse kidney with inflammatory changes, as previously described.

The second piece appears to consist of an outer cortex surrounding an inner medulla. There is considerable freezing artefact with poor tissue preservation, which makes confident diagnosis difficult.

The overall architecture and its close proximity to the kidney suggests adrenal gland. It also contains a similar, sparse inflammatory cell infiltrate as in the kidney. No human/embryonic tissue is present.

Appendix 2: Supplementary requested figures

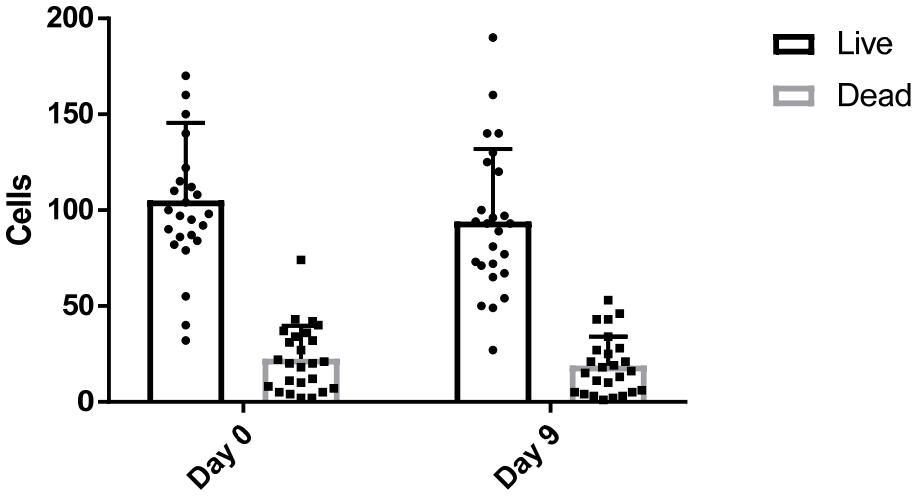

Supplementary Figure 1: Live/dead cell counts from one viability experiment point in figure 3.3.

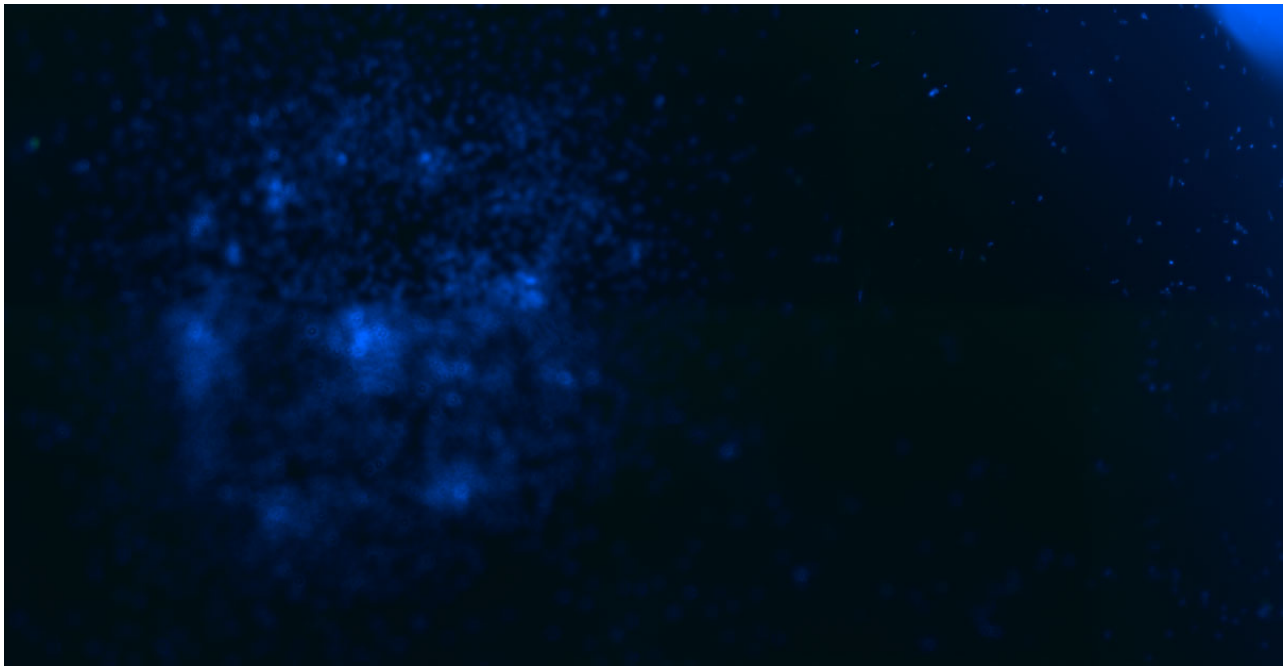

Supplementary Figure 2: Day 3 FOXA2 isotype control (green) with DAPI nuclear stainDue to the shape of the well some sections are out of focus.

Supplementary Figure 3: Day 3 SOX17 isotype control (green) with DAPI nuclear stain. Due to the shape of the well some sections are out of focus.

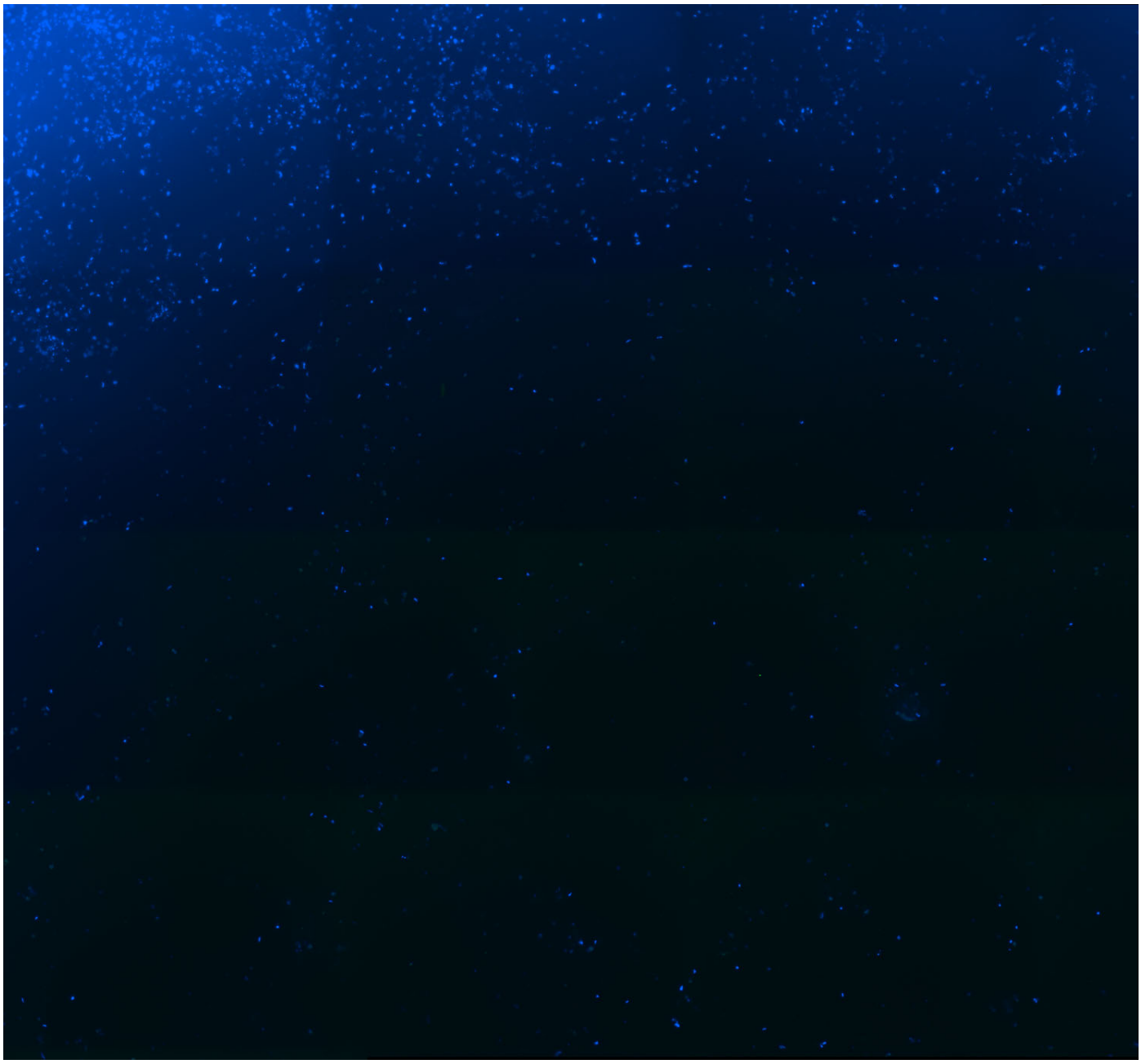

Supplementary Figure 4: Day 6 HNF1β isotype control (green) with DAPI nuclear stainDue to the shape of the well some sections are out of focus.

Supplementary Figure 5: Day 6 HNF4α isotype control (green) with DAPI nuclear stainDue to the shape of the well some sections are out of focus.

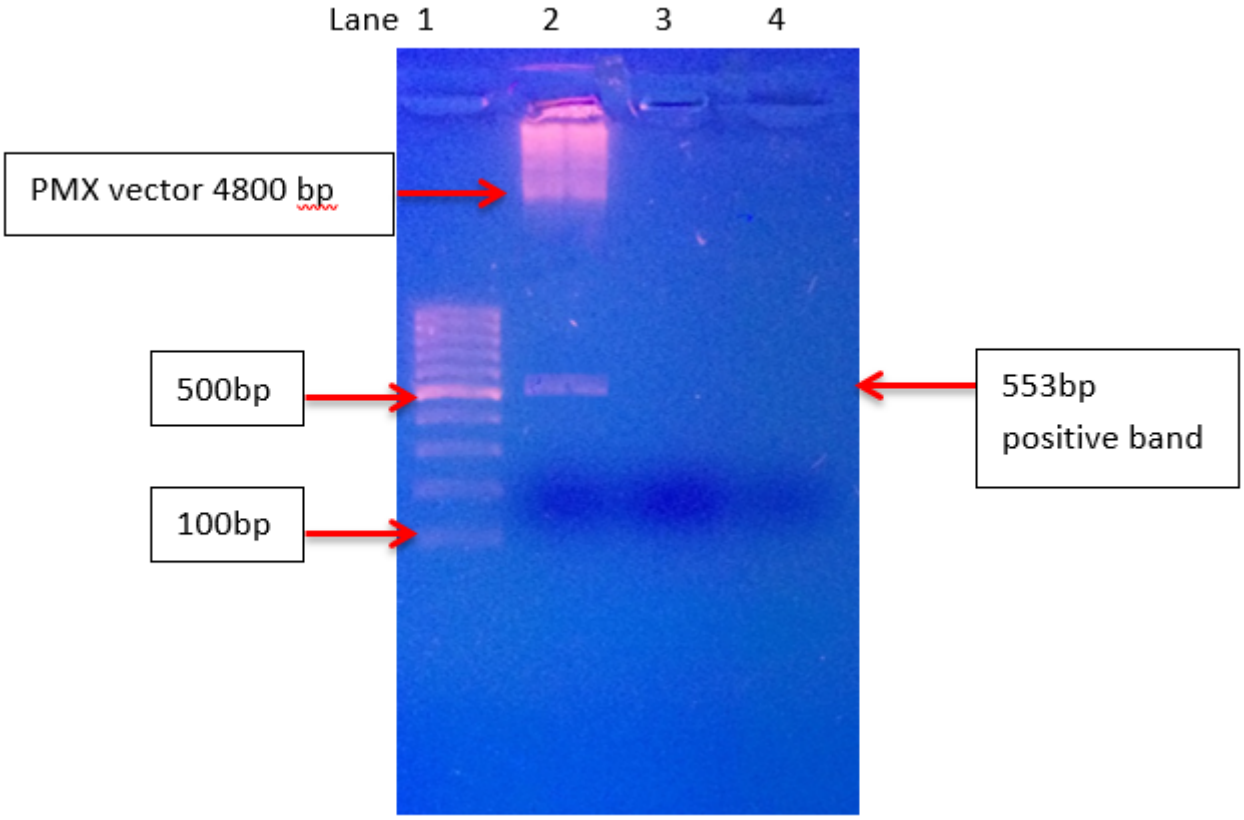

Supplementary Figure 6: Gel of DNA extracted from HEK cells exposed to iPSC mediaLane 1 GeneRuler 100bp DNA Ladder Plus, Lane 2 PMX vector showing the positive band at the expected weight, Lane 3 DNA extracted from HEK cells exposed to IPS media, Lane 4 DNA extracted from unexposed fibroblasts in culture.

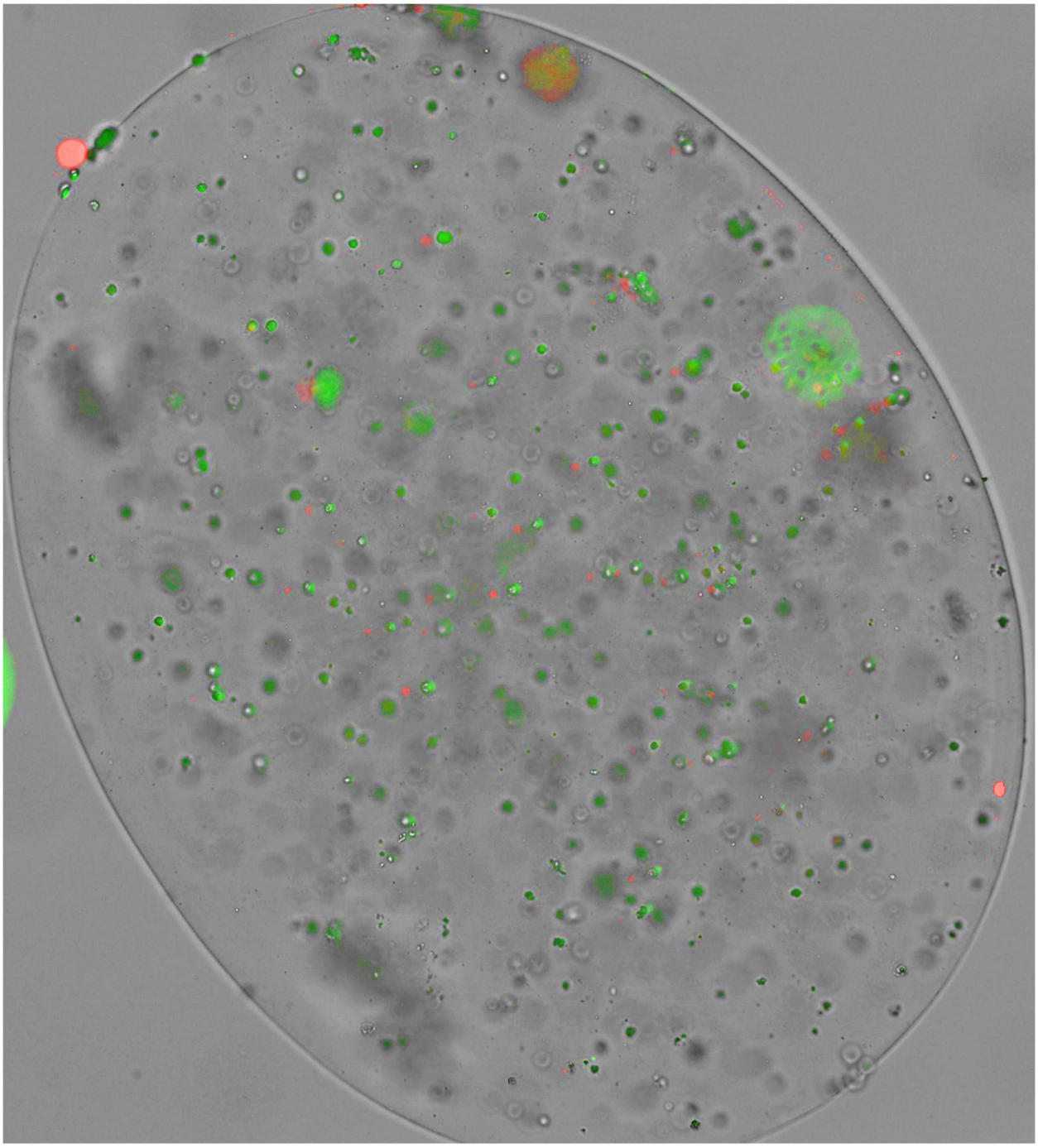

Supplementary Figure 7: Encapsulated pancreatic progenitors ex vivo at day 83 post-transplantation enlarged figure 4.3. Enlarged and contrast adjusted to show clearer CFDA staining.